# EVALUATION OF CHANNELS FOR ANGIOGENIC CELLS INGROWTH IN COLLAGEN SCAFFOLDS *IN VITRO* AND *IN VIVO*

**A THESIS SUBMITTED IN PARTIAL FULFILMENT OF THE REQUIREMENTS FOR THE DEGREE OF DOCTOR OF PHILOSOPHY AT THE UNIVERSITY OF OXFORD**




**BY**

**ASMA YAHYOUCHE**

**WOLFSON COLLEGE**

**AND**

**DEPARTMENT OF MATERIALS**

**UNIVERSITY OF OXFORD**

**TRINITY TERM 2011**

**Evaluation of channels for angiogenic cells ingrowth in collagen scaffolds *in vitro* and *in vivo***

Asma Yahyouche

Department of Materials and Wolfson College

Submitted for the degree of Doctor of Philosophy, Trinity term 2011

## ABSTRACT

Pre-cellularised scaffolds are limited in volume due to the constraints of the time delay required for angiogenic cells ingrowth forming a vascular network and allowing for delivery of nutrients and waste exchange. Channels have the potential to improve the time taken for cellular penetration. The effectiveness of channels in improving angiogenic cells penetration was assessed *in vitro* and *in vivo* in porous 3-D collagen scaffolds. Initial studies conducted *in vitro* demonstrated that the scaffolds supported angiogenic cells ingrowth in culture and the channels improved the depth of penetration of cells into the scaffold. The cells reside mainly around the channels and migrate along the channels. *In vivo*, channels increased cell migration into the scaffolds and in particular angiogenic cells resulting in a clear branched vascular network of micro vessels in the channelled samples which was not apparent in the non-channelled samples. This correlated well with macrophage invasion into scaffolds since angiogenesis *in vivo* is usually accompanied by infiltration of macrophages which participate in organization of angiogenesis, and in regulation of tissue regeneration. Thus, macrophage-mediated biodegradation of collagen scaffolds *in vitro* was also assessed. Furthermore, pre-seeding channelled collagen scaffolds with endothelial cells implantation has potential of speeding up vascularisation of scaffolds compared to human bone marrow stromal cells.

*A mes chers parents*

# AKNOWLEDGMENTS

This research project would not have been possible without the support of many people. I would like to start by expressing my gratitude to my supervisors, Dr Jan Czernuszka and Dr James Clover who were abundantly helpful and offered invaluable assistance, support and guidance throughout the completion of this work.

I owe many thanks to members of the biomaterials group at the Department of Materials especially Robin Walton, Jennifer Tilley, Hao Zhang and Yuan-Tsan Tseng (Gary) for sharing their knowledge and experience and being great lab mates. I would like also to thank everyone who helped me at the Botnar Research Centre. In particular, Dr Zhidao Xia for welcoming me in his lab and allowing me to use his facilities to conduct my *in vitro* experiments as well as providing all assistance, support and help needed. I am equally grateful to his lab members especially Xiao Wang for his help and companionship. I also thank Professor James Triffitt for allowing me to use his animal license to conduct my *in vivo* experiments. I would like to convey thanks to Miss Nolane Chang for her help with *in vivo* experiments by taking my samples to National Institute of Health (NIH) for implantation in mice and carrying out the procedure.

I would thank the Ministry of Higher education and Scientific Research of Algeria for their major contribution towards my tuition fees and living expenses.

Last but not least, I would like to express my deepest gratitude to family and friends without whom this journey would have been hard to bear. A special thank goes to my mum Mrs Bouchina Sacia for her endless love, encouragements, prayers and support without which I could have not got closer and closer to my goal. I thank my sisters, Imene and Hana, for their love, support and being there for me all time. My thoughts go to my friend and sister Lamia Mestek for her companionship in good and bad times. To Ali for all the support and love he gave me.

# TABLE OF CONTENTS

**Abstract** 2

**Acknowledgment** 4

**Table of Contents** 5

**Publications** 10

**List of Figure and Tables** 12

**Chapter 1: Introduction** 20

**Chapter 2: Literature Review** 28

**2.1. Introduction** 28

**2.2. Scaffolds Properties** 29

**2.3. Angiogenesis** 31

**2.4. Collagen** 34

2.4.1. Structure 34

2.4.2. Collagen-Cell Interaction 37

2.4.3. Collagen-Vascular Cells Interaction 38

2.4.4. Collagen Construct Degradation 39

*2.4.4.1. Collagen Degradation in vivo* 40

*2.4.4.2. Collagen degradation in vitro* 41

2.4.5. Reinforcing Collagen scaffolds 42

**2.5. Improving Cell Penetration in Scaffolds** 43

**2.6. Vascularisation of Tissue Engineered Constructs** 44

**2.7. Conclusions** 49

**Chapter 3: Design, Fabrication and Characterisation of Collagen Scaffolds** 51

**3.1. Introduction** **51**

**3.2. Materials and Methods** 55

3.2.1. Scaffolds Design and Fabrication 55

*3.2.1.1. Moulds Fabrication* 55

*3.2.1.2. Collagen Suspension and Freeze Drying* 56

*3.2.1.3. Scaffolds Crosslinking* 57

3.2.1.3.1. Physical Crosslinking (DHT) 57

3.2.1.3.2. Chemical Crosslinking (EDC) 58

3.2.2. Scaffolds Characterisation 59

*3.2.2.1. Microstructural Evaluation Using Electron Scanning Microscopy (SEM)* 59

3.2.2.1.1. Image Analysis and Pore Size Measurements 59

*3.2.2.2. Thermal Properties Using Differential Scanning Calorimetry (DSC)* 59

*3.2.2.3. Mechanical Properties* 60

*3.2.2.4. Swelling Ratio* 61

*3.2.2.5. The Effect of DHT on Collagen Tertiary Structure Using Fourier Transform Infra Red Analysis (FTIR)* 61

**3.3. Results and Discussion** 62

3.3.1. Microstructural Evaluation 62

*3.3.1.1. The Effect of Modifying Freeze Drying Process on Pore Size and Structure* 62

*3.3.1.2. The Effect of Different Crosslinking Methods on Pore Size and Structure* 66

*3.3.1.3. The Microstructure of Channels* 71

3.3.2. The Effect of Crosslinking on Thermal, Mechanical and Swelling Ratio Properties 73

3.3.3. The Effect of DHT on Collagen Tertiary Structure 76

**3.4. Conclusion** 79

**Chapter 4: Angiogenic Cells Growth on Collagen Scaffolds *in Vitro***

**4.1. Introduction** 80

**4.2. Materials and Methods** 80

4.2.1. Cell Culture and Seeding on Scaffolds 81

4.2.2. Assessment of Cellular Viability 82

4.2.3. Assessment of Cellular Attachment and Proliferation 83

4.2.4. Statistics 84

**4.3. Results** 84

**4.4. Discussion and Conclusion** 95

**Chapter 5: Macrophage-mediated Biodegradation of Different Crosslinked Collagen Scaffolds** 99

**5.1. Introduction** 99

**5.2. Materials and Methods** 103

5.2.1. Cell Culture and Seeding on Scaffolds 103

5.2.2. Assessment of Macrophage Attachment, Proliferation and Morphology on Collagen Scaffolds 104

5.2.3. Assessment of Collagen Scaffolds Degradation 105

*5.2.3.1. Assessment of Scaffolds Degradation by Collagenases* 105

*5.2.3.2. Assessment of Scaffolds Degradation by Macrophages* 106

5.2.4. Statistics Correlation Analysis 107

**5.3. Results** 107

5.3.1. Macrophage Attachment, Proliferation and Morphology on Collagen Scaffolds 107

5.3.2. Collagenase and Macrophage-mediated Biodegradation of Collagen Scaffolds 111

5.3.3. Linear Regression and Correlations 113

**5.4. Discussion and Conclusion** 115

**Chapter 6: *In Vivo* Assessment of Vascularisation in Channelled Collagen Scaffolds** 119

**6.1. Introduction** 119

**6.2. Materials and Methods** 120

6.2.1. Samples Preparation Prior to *In Vivo* Implantation 120

*6.2.1.1. Plain (non-cell seeded) Collagen Scaffolds* 120

*6.2.1.2. Cell-seeded Collagen scaffolds* 120

6.2.2. *In Vivo* Implantation 122

*6.2.2.1. Plain (non-cell seeded) Collagen Scaffolds* 122

*6.2.2.2. Cell-seeded Collagen Scaffolds* 123

6.2.3. Light Microscopy Examination of Plain Collagen Scaffolds 123

6.2.4. Haematoxylin/Eosin (H&E) Staining of Plain Collagen Scaffolds 124

6.2.5. Immunohistochemistry 124

*6.2.5.1. F40/F80 Staining* 124

*6.2.5.2. vWF Staining* 125

*6.2.5.3. Alpha Smooth Muscle Actin (α-SMA) Staining* 125

6.2.6. Statistics 126

**6.3. Results** 126

6.3.1. Vascularisation of Implanted Plain Collagen Scaffolds 126

*6.3.1.1. Vascular and Angiogenic Cells Penetration* 126

*6.3.1.2. Macrophage Cells Penetration* 134

6.3.2. Angiogenic Cells Penetration into Cell-seeded Collagen Scaffolds 136

**6.4. Discussion** 139

**6.5. Conclusion** 143

**Chapter 7: Conclusions and Future work** 144

**7.1. Conclusions** 144

**7.2. Future Work** 146

**References** 148

## PUBLICATIONS

**Yahyouche A**, Zhidao X, Czernuszka JT, Clover AJ. **Macrophage-mediated degradation of crosslinked collagen scaffolds.** Acta Biomaterialia Volume 7, Issue 1, January 2011, Pages 278-286.

**Asma Yahyouche**, Jan T. Czernuszka, and A.J.P. Clover. **A True 3-D Channelled Collagen Scaffolds for 3-D Angiogenesis.** Poster presentation at 2nd TERMIS World Congress in conjunction with the 2009 Seoul Stem Cell Symposium, August 31 - September 3, 2009**,** Seoul, *"Science and Technology for Patients!"*.

**A.Yahyouche**, J.M.R.Tilley, J.T. Czernuszka. **Collagen scaffold for tissue engineering: effects of freeze drying and crosslinking on thermal, mechanical enzymatic degradation properties and in vitro-biodegradation**. Poster Presentation at 22nd European Conference on Biomaterials, 07-11th September, 2009, Lausanne.

**Asma Yahyouche**, Xia Zhidao, Jan T. Czernuszka, and A.J.P. Clover. **Improving angiogenesis in tissue engineered scaffolds using microchannels.** Oral Presentation at 1st European Plastic Surgery Research Council, Hamburg, August 2009.

**Asma Yahyouche**, Xia Zhidao, Jan. T. Czernuszka, A.J.P.Clover. **Increase in Cell Migration and Angiogenesis in Channelled Collagen Scaffolds with Channels for Tissue Engineering.** Rapid Fire presentation at TERMIS EU-Meeting -2010, Galway, Ireland, June 2010.

**Asma Yahyouche**, Xia Zhidao, Jan. T. Czernuszka, A.J.P.Clover. **Macrophage-mediated biodegradation of differently crosslinked collagen scaffolds *in vitro***. Poster presentation at TERMIS EU-Meeting -2010, Galway, Ireland, June 2010.

**Unpublished**

**Asma Yahyouche**, Jan. T. Czernuszka, A.J.P. Clover **Angiogenesis in collagen tissue engineered constructs.** Review paper, in writing.

**Asma Yahyouche**, Xia Zhidao, James T. Triffitt, Jan. T. Czernuszka, A.J.P. Clover. **Improved Angiogenic Cell penetration *In Vitro* and *In Vivo* in Collagen Scaffolds with Internal Channels** (submitted to Journal of Materials Science: Materials in Medicine)

# List of Figures

**Figure 2.1:** The process of angiogenesis. **A-** Initiation of angiogenic response. **B-** Migration and proliferation of endothelial cell. **C-** Lumen and tube-like structure formation. **D-** Maturation of the new vessel.

**Figure 2.2:** Schematic drawing showing: **A-** Primary amino acids. **B-** The collagen triple helix. The individual α chains are left-handed helices with approximately three residues per turn. The alpha chains are in turn coiled around each other following a right-handed twist. **C-** Staggered quaternary structure

**Figure 3.1**: Picture of: **A-** the mould with caps for sample with and without channels, and **B-** assembled moulds with and without channels.

**Figure 3.2:** 1% collagen dry scaffolds. **A-** The 5 cm collagen scaffold rods as taken out of the moulds. **B-** 0.5-0.6 cm slides of non-channelled, 3-channels and 9 channels collagen scaffolds.

**Figure 3.3:** pore size distribution graph and mean pore size of different collagen samples measured with ImageJ. Image J considers the scale of images which allows the use of images of different scales. 1 and 0.5% is collagen content, -20 and -80 °C is freezing temperature. The lower the collagen content is, the bigger the pore size is. Conversely, the higher the freezing temperature is, the lower the pore size is.

**Figure 3.4**: SEM cross section images of: **A-** 1% collagen scaffold, -80°C scale bar-right = 1mm & left = 400μm. **B-** 1% collagen scaffold, -20°C, scale bar = 600μm. **C-** 0.5% collagen scaffold, -20°C, scale bar = 600μm. SEM illustrates low-density, open-cell foam and porous structure with an interconnected network of struts freeze-dried scaffolds.

**Figure 3.5:** SEM images of cross-sectional view of the interior of differently cross linked collagen scaffolds. EDC samples had more elongated pores, non-homogenous structure,

fewer fibres in between the pores and more sheet-like structures with condensed walls compared to DHT and non cross linked samples. EDC: carbodiimide DHT: dehydrothermal treatment.

**Figure 3.6:** Pore size distribution graph of differently cross linked collagen scaffolds measured with ImageJ. * compared to non cross linked, $p < 0.05$. # compared to 33mM EDC, $p< 0.05$. Cross linked samples presented higher amount of pores over 300µm compared to non cross linked samples that did not have any pores over 400µm. All samples had higher percentage of pores between 50-200µm. EDC: carbodiimide, DHT: dehydrothermal treatment

**Figure 3.7:** Pore size distribution graph of EDC cross linked collagen scaffolds at concentration 10mM & 50mM freeze dried once or twice measured with ImageJ. EDC cross linking through ethanol defrost and single freeze dried step did not affect pore size distribution. EDC: carbodiimide DHT: dehydrothermal treatment

**Figure 3.8:** Scanning Electron micrographs illustrating cross-sectional view of collagen scaffolds. **A-** Sample with 3 channels, average channel diameter measured at 2.02 ± 0.15mm, average distance between channels measured at 3.52 ± 0.31mm. **B-** View of single channel in 3-channels sample. **C-** View of cross section through channels. **D-** Sample with 9 channels, average channel diameter measured at 1.17 ± 0.14mm, average distance between side channels measured at 2.39 ± 0.22mm and distance to central channel measured at 3.20 ± 0.52mm. **E-** View of single channel in 9-channels sample. **F-** View of cross section through one channel.

**Figure 4.1**: Assessment of Cell proliferation on scaffolds made of different collagen concentrations over time using Alamar Blue assays. RFU: Relative Fluorescence Unit. * Statistically significant, $p < 0.05$. All scaffolds supported the growth of three

types of culture to similar extent. HUV-EC: endothelial cells. HAV.SMC: smooth muscle cells.

**Figure 4.2:** Live/Dead Staining of scaffolds made of 1% and 0.5% collagen, with and without channels. Scale bar = 200μm. HUV-EC: endothelial cells. HAV.SMC: smooth muscle cells.

**Figure 4.3-A:** Attachment ratio of HUV-EC-C (endothelial cells), HA-VSMC (smooth muscle cells) and co-culture cells on collagen scaffolds at day 1 after 24 hours incubation examined by Alamar Blue™ Assay. HUV-EC-C and co-culture had higher attachment ratio to scaffolds. Addition of channels improved cellular attachment as compared to scaffolds without channels. Co-culture 9 channels seeded scaffolds had the highest attachment ratio. * Significant difference, $p<0.05$.

**Figure 4.3-B** Proliferation of HUV-EC-C (endothelial cells), HA-VSMC (smooth muscle cells) and co-culture cells on collagen scaffolds from day 1 to day 7. At day 1, no significant difference in cell number between different scaffolds or different cell cultures. From day 1 to day 7, different cell cultures proliferated significantly on all scaffolds. At day 7, there was significant difference in cell number between scaffolds with and without channels for HA-VSMC and co-culture cells but not for HUV-EC-C. 9 and 0 channels, but not 3 channels scaffolds, had higher cell number of HA-VSMC than HUV-EC-C which is turn higher than co-culture cells. * compared with same type of scaffolds and cell culture at day 1. Φ comparison of same scaffold type seeded with different cells. + Comparison between different scaffolds seeded with same type of cells. $p<0.05$

**Figure 4.4:** Live/Dead staining of HUV-EC-C (endothelial cells) seeded scaffolds (green colour for live cells). The cells reside mainly around the channels and migrate along the channels. For 9 channels scaffolds, there are more cells between channels

compared to 3 channels ones due to smallest distance between channels (B3 vs. D3). Scale bar= 500μm for A, B, C-2 and C-3 and =1mm for C-1, D.

**Figure 4.5:** Live/Dead staining of HA-VSMC (smooth muscle cells) and co-culture seeded scaffolds (green colour for live cells). The cells reside mainly around the channels. For 9 channels scaffolds, there are more cells between channels compared to 3 channels ones due to smaller distance between channels (B3 vs. D1 for HA-VSMC). Scale bar =1mm

**Figure 4.6:** DAPI staining of HUV-EC-C (endothelial cells) seeded collagen scaffolds *in vitro*. **A-** Scaffold with no channels. **B-** Sample with 3 channels, view of cross section through 1 channel. **C-** Sample with 3 channels, view area far from channel. The cells appear as bright galaxy along the channel with fewer cells far away from channel.

**Figure 5.1-A:** Attachment ratio of RAW264.7 macrophages on collagen scaffolds at day 1 after 24 hours incubation examined by Alamar Blue$^{TM}$ Assay. Cross linking improves macrophages attachment compared to non cross linked samples. Physical treatment of collagen scaffolds (DHT: dehydrothermal treatment) significantly improved attachment compared to chemical treatment (EDC: carbodiimide). The optimum condition for macrophage attachment on these collagen scaffolds is 3 days DHT with an attachment ratio of 79%. * compared with non cross linked samples $p<0.05$

**Figure 5.1-B:** Proliferation of RAW264.7 macrophages on collagen scaffolds from day 1 to day 7. At day 1, more macrophages were observed on crosslinked samples. From day 1 to day 7, macrophages proliferated on all samples. At day 7, cell number was significantly more on crosslinked samples compared to non-crosslinked samples except 50mM EDC (carbodiimide). * compared with non crosslinked at day 1. #

compared with non crosslinked at day 7. + compared to day 1 within groups. $p<0.05$. DHT: dehydrothermal treatment

**Figure 5.2.** Scanning Electron micrographs illustrating RAW264.7 macrophages attaching to collagen scaffolds *in vitro*. **A-** Murine 264.7 macrophages attached and proliferated on collagen scaffolds, scale bar = 200μm. **B-** Cells firmly attached to the collagen surface via Podosome-like structure, scale bar = 6μm. **C-** Macrophages aggregation and fusion to form Giant cells, scale bar = 30μm. **D-** Note the formations of giant cells, scale bar = 40μm.

**Figure 5.3-A:** Collagen degradation by macrophages measured by Sircol$^{TM}$ soluble collagen assay. The amount of collagen released decreases with increasing crosslinking. * compared with non-crosslinked samples $p<0.05$. EDC: carbodiimide. DHT: dehydrothermal treatment.

**Figure 5.3-B:** Enzymatic degradation of 1% collagen scaffolds after different crosslinking using 50Units bacterial clostridial type I collagenase at 37°C for 1 hour. Increasing crosslinking increases resistance to enzymatic degradation. * compared with non-crosslinked samples $p<0.05$. EDC: carbodiimide, DHT: dehydrothermal treatment.

**Figure 5.4:** Linear regressions of enzymatic degradation against macrophage degradation, Young's modulus ($E$) and denaturation temperature ($T_d$). Enzymatic degradation correlated with **A-** denaturation temperature, **B-** Young's modulus and **C-** swelling ratio and **D-** macrophage activity. Enzymatic activity is the amount of collagen degraded by Clostridial Bacterial Type I Collagenase. Macrophage activity is the amount of collagen degraded by macrophages and released in the culture medium.

**Figure 6.1:** Scanning Electron micrographs illustrating cross-sectional view of channelled collagen scaffold implanted in mice, **A-** sample with one channel, average

channel diameter measured at 2.02 ± 0.15mm, **B-** sample with two channels, average channel diameter measured at 1.17 ± 0.14mm. **C-** Photograph of the implanted collagen scaffolds just before retrieval. 3 samples were implanted each side subcutaneously.

**Figure 6.2:** Photographs of scaffolds taken at time of explantation. The presence of channels in the scaffolds allows for the development of a more rapid and more mature vasculature**,** scale bar A, B, C (left) and D (left) = 1mm and C & D (right), 500μm.

**Figure 6.3: Vascular penetration in plain collagen scaffolds.** Mean total area of collagen invaded by granulation tissue/blood vessels after 2 weeks implantation. Channels increase the rate of blood vessel development. * compared to sample without channel at the same time point. # compared to same type of sample at week 1 ($P < 0.001$).

**Figure 6.4:** H&E staining of plain collagen scaffolds explants. **A-** Week 1 without channel, scale bar = 100 and 50μm. **B-** Week 1 with channels, scale bar = 100 and 50μm. **C-** Week 2 without channels, scale bar = 200 and 50μm. **D-** Week 2 with channels, scale bar = 200μm.

**Figure 6.5:** Angiogenic Cell penetration in plain collagen scaffolds. **A-** Total cell number invasion into collagen scaffolds with or without channels. The total cell number was significantly higher in channelled samples compared to non-channelled samples at week 1 & 2, * statistically significant, $p<0.05$. **B-** The vWF particle count as measure of angiogenic cells invasion into collagen scaffolds. At either week 1 or 2, the presence of channels increased significantly vWF count, * statistically significant, $p<0.05$.

**Figure 6.6: A-** DAPI staining of collagen scaffolds after explantation, scale bar = 100μm. **B-** vWF staining of collagen scaffolds after explantation.

**Figure 6.7: A-** F4/80 staining scale bar = 20μm. **B-** Macrophage invasion into collagen scaffolds with or without channels. * compared to week 1 without channels $p<0.05$. The presence of channels increased macrophage invasion into scaffolds.

**Figure 6.8:** The area fraction of α-SMA staining in cell-seeded collagen scaffolds after implantation in mice. * Statistically significant $p < 0.05$. 4 weeks after implantation, the area fraction of α-SMA increased in EC (endothelial cells)- seeded samples in channeled same but significantly in samples with 2 small channels whilst hBMSC (mesenchymal stem cells)- seeded samples had a significant increase of α-SMA area fraction in sample with 1 large channel. At week 8, hBMSC-seeded samples had more or less the same area fraction cross all samples compared to EC-seeded samples where the staining area fraction increased significantly in sample with 2 small channels compared to the other samples.

**Figure 6.9:** α-SMA staining of cell HUV-EC (endothelial cells) and hBMSC (mesenchymal stem cells) pre-seeded collagen scaffolds after explantation.

## List of Tables

**Table 3.1:** Denaturation temperature ($T_d$), Young's modulus ($E$) and Swelling ratio (Q) of collagen samples. EDC causes a significant improvement in $T_d$ and $E$. Though DHT improved $E$, it did cause a decrease in $T_d$. Both treatments reduced swelling ratio. * compared with non-crosslinked samples $p<0.05$. $^{+}$ compared to 1 day DHT $p<0.05$. $^{\#}$ compared to 10mM EDC samples $p<0.05$. EDC: carbodiimide, DHT: dehydrothermal treatment

**Table 3.2**: Observed band frequencies from IR spectra of collagen samples and their associated molecular vibrations. The assignment of band frequencies to particular

bands is decided by using reference tables from literature. DHT: dehydrothermal treatment

**Table 3.3**: IR characteristics of processing on collagen with freeze drying and DHT comparing to non-crosslinked samples. $A_{1659/1643}$ is the internal amide I absorbance ratio; $A_A$, $A_{I,}$ $A_{II}$ and $A_{CH3}$ are the absorbance intensity of the amide A, amide I, amide II and $CH_3$ bands respectively. * Statistically significant compared to control sample, $p < 0.05$. DHT: dehydrothermal treatment

## List of Diagrams

**Diagram 3.1.** EDC (carbodiimide) crosslinking reaction scheme. Carboxyl-to-amine crosslinking with EDC. Molecules (1) and (2) are chemicals that have respective carboxylate and primary amine groups.

# CHAPTER 1: INTRODUCTION

Tissue engineering aims to provide therapies to replace such damaged and diseased tissues by guiding and controlling tissue growth, either *in vitro* or *in vivo*, using a combination of biomaterials, cells and growth factors [1]. One common tissue engineering strategy utilizes tissue-specific cells that are isolated from a small tissue biopsy from the patient and harvested *in vitro*. The cells are subsequently incorporated into three-dimensional polymer scaffolds that act as analogues to the natural extracellular matrices found in tissues. These scaffolds deliver the cells to the desired site in the patient's body, provide a space for new tissue formation, and potentially control the structure and function of the engineered tissue [2].

Yet, a critical obstacle in tissue engineering is the inability to maintain large masses of living cells upon transfer from the *in vitro* culture conditions into the host *in vivo*. *In vivo*, most cells do not survive more than a few hundred micrometres from the nearest capillary, due to diffusion limitations [3]. Capillaries and the vascular systems are required to supply essential nutrients including oxygen, remove waste products and provide a biochemical communication highway [4].

For cell adhesion and migration, it is important for the scaffold to have specific parameters that influence cell motility. For cell proliferation and differentiation, it is necessary to provide cells with sufficient nutrients and especially oxygen to regulate cellular activity. *In vitro* culturing of cells provides such nutrient through standard culture media by diffusion of ions into the cell membrane[5]. However as they start to migrate within the scaffold and produce extracellular matrix, diffusion is limited to critical distance.

Therefore, although many scientists have reported good cell seeding efficiency and cell viability within a scaffold *in vitro*, new tissue has been generated in only small amounts. *In vitro* tissue engineering has demonstrated maximum thickness of 5.0, 0.5, and 0.18 mm for cartilaginous, bone-like, and cardiac like tissues respectively[6]. However when larger scaffolds have been used cells found difficulties in migrating and surviving for long time periods within the centre core of a scaffold. In order to improve the cell culture media exposure to cells, different cell culturing methods have been used. This aims to provide mechanical stimuli and increase culture media exposure to cells throughout scaffold [6, 7]. However these techniques do not readily lend themselves to getting nutrients deep into scaffold when vascularisation would be essential. Therefore, this thesis aims to explore a different approach to allowing nutrient ingress into scaffolds by introduction of channels that would improve nutrient exchange leading to improved cellular infiltration.

All tissues and organs (with the exception of possibly cartilage) need to be vascularised to be able to survive. Generating a vascular supply to thick tissue-engineered constructs remains a major challenge [8]. To date , there are no tissue-engineered constructs presently available which have an inherent vasculature such as capillary bed ready to be connected to the host vascular system[9]. Angiogenesis is the sprouting of blood vessel which is a principal mechanism of blood vessel formation [10]. It is defined as formation of new capillaries from pre-existing blood vessels and represents a complex dynamic process characterised by a coordinated sequence of humoral cellular interactions [11, 12].

There are six basic steps in angiogenesis: 1- vasodilatation of the parental vessel, reducing contact between adjacent endothelial cells (EC) 2- degradation of the basement membrane of a parental vessel by the secretion and activation of a wide range of proteolytic enzymes 3- EC migration and proliferation resulting in the formation of a leading edge of a new capillary 4- generation of capillary lumen and formation of tube-like structure 5- basement membrane synthesis 6- recruitment of pericytes and vascular smooth muscle cells. The smallest microvessels are the capillaries with an inner diameter of 4-10um and a very thin wall of EC. The immature lined tubes that arise during angiogenesis subsequently differentiate into capillaries[12].

Currently, approaches to vascularise tissue engineered constructs are under investigation. The vascularisation of new tissue can be accomplished in two separate ways or a combination of both approaches. Vessels from the surrounding tissue can be stimulated to infiltrate the implanted construct. This process can be induced by the release of angiogenic growth factors. These factors diffuse into the local environment, where they encourage existing blood vessels to grow into the implanted construct. Alternatively, a capillary network may theoretically be prefabricated within the engineered organ before the transplantation. After incorporation of endothelial cells into the three dimensional scaffold, these cells will become blood vessels within the matrix and form a capillary network. These networks can develop connections to vessels from surrounding tissue. Both approaches are associated with time delay before vascular perfusion can occur [13, 14]. Both approaches adopted various ways in order to increase vascularisation o tissue-engineered constructs. For instance, pore size has been varied in attempt to achieve optimal scaffold’s pore size for cellular

adhesion and migration. Furthermore, endothelial cells and fibroblasts have incorporated to initiate angiogenesis *in vitro.* Various extracellular components such glycosaminoglycans and growth factors were incorporated as well into scaffolds to promote angiogenesis *in vivo*. However, it still takes 4 weeks to achieve mature vasculature [15-17].

The ideal matrix should be biocompatible, readily available, permeable to incoming vessels or chemicals, non immunogenic, biodegradable, inert, have a slow-release mechanism, and lastly be easily administered. Tissue engineered constructs act as temporary scaffolds, which maintain cells in situ and induce neovascularisation[18]. Endothelial lining of blood capillaries consists of single layer of flattened cells whose basal surface interacts with extracellular matrix. Since blood capillaries *in vivo* entirely surrounded by extracellular matrix containing collagen as a major component, collagen could be material of choice for the scaffold [19]. Collagen gels provide a more physiological, isotropic environment that has been shown to promote the organisation of different cells into three dimensional, tissue-like structures. As well, collagen has been also reported to promote cell migration and this could contribute to tubular network formation [20].

Endothelial cells are the key regulator of this process, by forming endothelial tubules. However, these neovessels are dependant on growth factor concentration. The neovessel becomes independent of these growth factors once a smooth muscle or pericyte coat has been achieved. Consequently, co-culture of endothelial and smooth muscle cells is vital if stable vessels are to be produced [14]. Therefore, it was hypothesised that the addition of endothelial cells or endothelial cells and perivascular

support cells could potentially improve angiogenic cell penetration into scaffolds prior to implantation.

Despite success with small (thin) tissue-engineered constructs such as bladder wall [21, 22] and dermal substitutes [23, 24], the biggest roadblock in scaffold-guided tissue engineering is engineering large tissue volumes. This challenge arises due to the lack of rapid vascularisation (angiogenesis) of large three-dimensional (3-D) scaffold constructs. Accordingly, angiogenesis is a pre-requisite for scaffold-guided tissue engineering of large tissue volumes. Hence there is a strong need for developing strategies that can promote angiogenesis in 3-D scaffold constructs of biodegradable polymeric scaffolds. A cellularized tissue engineered scaffold could have a host of clinical applications such as rapidly vascularised constructs for use for cutaneous resurfacing as well as incorporation of task specific cells for thick-tissue engineering such as bone. There would be a particular advantage to plastic and reconstructive surgeons. Applications could include body resurfacing for injuries caused by burns and trauma. Therefore, once the initial strategy of improving cell penetration within the scaffolds with the introduction of channels is explored, initial *in vivo* studies are explored to see the efficacy of introduction of channels and cellularised scaffolds to promote angiogenesis within the scaffold. This particular need forms the basis of the proposed project. In this work, our aim was to develop a scaffold that would allow rapid angiogenic cells ingress. Introduction of channels as a way of circulating medium within centre of scaffold could be useful. Channels have been developed in scaffolds as a method for increasing the in growth of angiogenic cells into the scaffolds in attempt to overcome the diffusion constraint. These channels were

assessed *in vitro* to assess the depth of penetration of angiogenic cells and *in vivo* to assess the influence of channels on scaffold cellularization and vascularisation. The thesis is organised in the following manner:

**Chapter 1:** this chapter presents an introduction to thesis.

**Chapter 2:** this chapter presents a literature review focusing on the use of collagen in the aid of angiogenesis. Initially, the vascularisation problem is elucidated. Since body supplies its tissues with sufficient amounts of oxygen and nutrients via blood vessels, scientists have progressed to understanding the angiogenesis process and trying to mimic this within a tissue engineered construct. Thus, this review includes the capillary formation and maturation in the natural state. This will be followed by a summary of scaffolds available for angiogenesis. Collagen is a key material used in modern tissue engineering as it biocompatible, biodegradable, and has low antigenicity. It affects the adhesion, morphology and migration of cells in particular vascular cells. So a review of collagen is presented, focusing mainly on its properties and interaction with cells in the context of angiogenesis. Finally, the review summarises the main work done so far in order to achieve blood vessel formation on a collagen tissue engineered constructs using various approaches.

**Chapter 3:** this chapter summarises scaffolds production and characterisation. Freeze drying is the chosen process to make up collagen scaffolds. In order to explore strategies for improving cell penetration in scaffolds *in vitro*, initially, attempts were made to alter scaffold design to improve the ingress of nutrients and hence cell survival. The hypothesis was that by introducing channels into scaffolds, nutrients

exchange would be improved leading to improved cellular infiltration. Different scaffold designs were constructed to assess this hypothesis through the introduction of 1, 3 or 9 channels into the scaffold, in order to decrease the distance for nutrients diffusion. As the biodegradability of different scaffold constructs is essential in their biocompatibility, it was also important to assess the effects of ways of improving the potential survival *in vivo* to allow the scaffolds to be useful. Hence different methods of crosslinking were assessed in order to determine their potential compatibility for angiogenic cell survival. Physical and chemical cross linking methods were assessed and their intrinsic property assessed by modalities such as swelling ratio, young's modulus and degradation rate. Altogether, this shed light on the potential scaffold for this study.

**Chapter 4:** in this chapter, it was evaluated whether the potential scaffold would attract angiogenic cells, Human aortic normal smooth muscle cells (HA-VSMCs) and human umbilical vein endothelial cells (HUVECs), to attach and remain viable *in vitro* then support proliferation as well as whether the presence of channels will promote a better attachment, proliferation and penetration deeper into scaffolds. This aimed to select the optimum approach for angiogenic cell penetration in the scaffolds *in vitro* to allow for evaluation of this construct in vivo.

**Chapter 5:** Correlation between enzymatic degradation of collagen *in vitro* and *in vivo* in the presence of crosslinking is long established. However, there is no previously published data confirming the correlation between enzymatic collagen degradation and an *in vitro* model of macrophage degradation. Therefore, the cell-mediated biodegradation of different collagen scaffolds *in vitro* and the correlation of

the chemical degradation of scaffolds with an *in vitro* model of scaffold degradation using RAW264.7, a murine monocyte/macrophage cell line were evaluated in this chapter.

**Chapter 6:** this chapter presents the *in vivo* evaluation of the optimised scaffold design. It is equally important for a scaffold to support cellular attachment and proliferation *in vitro* and to allow rapid vascularisation and cellularisation *in vivo*. Thus, the *in vivo* studies investigated whether the presence of channels would allow faster blood vessels infiltration into scaffolds. The first study evaluated the presence of channels only on plain scaffolds. There has been some preliminary *in vivo* success with implanted cell-seeded constructs. Pre-cellularized scaffolds can enhance angiogenesis through hypoxia. Scaffolds containing embedded cells experience decreased oxygen tension, and the resulting hypoxia is a powerful angiogenesis stimulant and can improve the rate of scaffold vascularisation *in vivo* [25, 26]. Therefore, the second study investigated pre-seeded scaffolds with human bone marrow stromal cells (hBMSCs) and human umbilical vein endothelial cells (HUVECs).

**Chapter 7:** conclusions of the study and recommendations for future work and research are described in this chapter.

# CHAPTER 2: LITERATURE REVIEW

## 2.1. INTRODUCTION

All tissues and organs need to be vascularised to be able to survive. *In vivo*, most cells do not survive more than a few hundred micrometres from the nearest capillary due to diffusion limitations [3]. A vascular network is required to supply essential nutrients including oxygen, remove waste products and provide a biochemical communication highway [4]. Generating a vascular network in thick tissue-engineered constructs remains a major challenge [8, 9]. If tissue engineering is to develop beyond inert matrices for tissue engineering and create constructs containing task specific cells, there is a need to produce scaffolds that allow for rapid neovascularisation. Artificial vascular systems with inbuilt micro channels have been developed [27], and these have improved cellular penetration deep within a scaffold [28]. For example, vascular cells can be isolated from a tissue biopsy, cultured *in vitro* before incorporation into scaffolds that act as analogues to the natural extracellular matrices found in specific tissues. These scaffolds can deliver the cells to the desired site providing a space for new tissue formation and controlling the structure and function of the engineered tissue [2] .

These approaches seem increasingly important as despite good success in engineering thin and relatively avascular tissues [21-24]; the inability to produce rapid vascularisation limits the size of cellularised scaffolds that can be used. *In vivo*, tissue engineering has demonstrated maximum thickness of 5.0, 0.5, and 0.18 mm for cartilaginous, bone-like, and cardiac-like tissues respectively [6]. When larger

scaffolds have been used, cells did not migrate nor survive beyond 2mm beneath the scaffold surface [8]. *In vitro*, scaffold prefabrication has used dynamic seeding in order to overcome the diffusion limit, providing mechanical stimuli and increased culture media exposure to cells throughout scaffold [6, 7].

Collagen is the most abundant protein in mammalian tissues accounting for approximately 25% of human body proteins and is a main component of the extra cellular matrix (ECM) [29-32]. Various collagens (type I, III and IV) are widely distributed in all blood vessels forming a large part of the basement membrane (along with glycosaminoglycans, elastin and laminin), media and adventitia [33] . Vascular endothelial cells secrete various ECM proteins including collagen type I, collagen type IV, and fibronectin [34], with these proteins contributing to vessel wall stability and resisting tension created by pulsatile blood flow [35-37].

## 2.2. SCAFFOLDS PROPERTIES

Properties of the scaffold itself influence cell motility for cell adhesion and migration, possibly creating an internal structure that allows for diffusion of nutrients and oxygen. [5]. Scaffolds should act to mimic the 3D form of the ECM to guide cell function and direct cell migration [38]. A 3D collagen framework has a superior biological acceptability for cell permeation [39-41].

Ideally scaffolds should be biocompatible, porous, mechanically stable, but eventually biodegradable [42-46] . Collagen had these elements with good biocompatibility and low antigenicity due to absence of tyrosine proteins [47]. It interacts with cells in

connective tissues, transducing signals for the regulation of cell anchorage, migration, proliferation, differentiation, and survival [48] and promotes the organisation of different cells into 3D tissue like structure [20]. The physical mechanical properties and porosity of the scaffold can be controlled by altering processing methods and parameters. The pore size in collagen can dramatically affect cell behaviour encouraging cell migration and penetration into the scaffold [49]. Collagen, *in vivo*, activates a complex cellular response resulting in release of collagenases responsible for the degradation and replacement of scaffold. This can be controlled by cross linking [50-52] either chemically (glutaraldehyde [53, 54], carbodiimide [55]) or physically (Ultra Violet irradiation [56] and dehydrothermal treatments [57]) or blending it with other polymers[31]. Furthermore processing methods allow for growth factor incorporation allowing for manipulation of the biological activities [15, 58-60].

Collagen is positively charged and hydrophilic and may be attractive to cell adhesion since cells have negatively charged membranes and prefer positive charge and hydrophilic surfaces for adhesion and mobilisation [61]. Collagen substrates affect the adhesion, migration and morphology of cells in particularly vascular cells. Extracellular attachment of glycoproteins, such as fibronectin, chondronectin and laminin bind uniquely to collagens and play important roles in cell-collagen interactions [62]. In addition to structural and mechanical functions, collagens play an important role in determining cell attachment and spreading that consequently influence cell differentiation and movement [63].

A number of biodegradable synthetic polymers have been successfully adapted to have the exact mechanical properties and degradation kinetics needed to suit the application, including adapting the shape and pore size [64]. Several have always been approved by Food and Drug Administration (FDA) including PLA (poly lactic acid), PLGA (poly lactic-co-glycolic acid), PLLA(poly-L-lactide) [65]. However, they lack cell recognition signals and the surfaces are typically hydrophobic [66], their degradation products are acidic, and in abundance can cause damage to both native tissue and implanted tissue [67]. These are reviewed elsewhere [68].

## 2.3. ANGIOGENESIS

Angiogenesis has several key steps; initiation, endothelial migration and proliferation, lumen formation and vessel stabilisation [Figure 1.1].

Endothelial cells (EC) are activated in response to hypoxia or ischemia [Figure 1.1-A]. Vascular relaxation occurs in response to cytokines including nitric oxide (NO) [69]. Vascular Endothelial Growth Factor (VEGF) induces NO production and increases endothelial cells permeability [70]. Increased vascular permeability allows extravasations of plasma proteins that lay down a provisional scaffold, rich in fibronectin and vitronectin, which promotes further migration and proliferation of endothelial cells [71-73].

The ECM needs to be digested to allow endothelial cells to migrate [Figure 1.1-B]. This action is mediated by a matrix metalloproteinases (MMPs), mainly MMP-2, MMP-9, and membrane type MT1-MMP, which selectively degrade ECM

components [74]. In addition to MMPs, proteinases of the plasminogen activator, chymase or heparanase families contribute to ECM degradation and activate or liberate growth factors including basic Fibroblast Growth Factor (bFGF), VEGF and Insulin Growth Factor-1 (IGF-1), sequestered within the extracellular matrix [72].

Endothelial cells invasion is accompanied by cellular proliferation [Figure 1.1-C], regulated by growth factors [75], including Fibroblast growth factor-2 (FGF-2) and VEGF[38]. Assembly of endothelial cells in solid cords is followed by lumen formation regulated by VEGF, integrins and Angiopoietin -1 (Ang-1) [Figure 1.1-D].

Initially new vessels are VEGF dependant with vessels becoming stabilised by acquiring a mesenchymal support cells inhibiting endothelial cells proliferation and stimulating extracellular matrix formation [76]. Platelet Derived Growth Factor (PDGF) released by endothelial cells acts as a chemoattractant for mural cells [77]. This contact stimulates release of the Transforming Growth Factor Beta (TGF-β), contributing to the formation of quiescent vessel and ECM production [78].

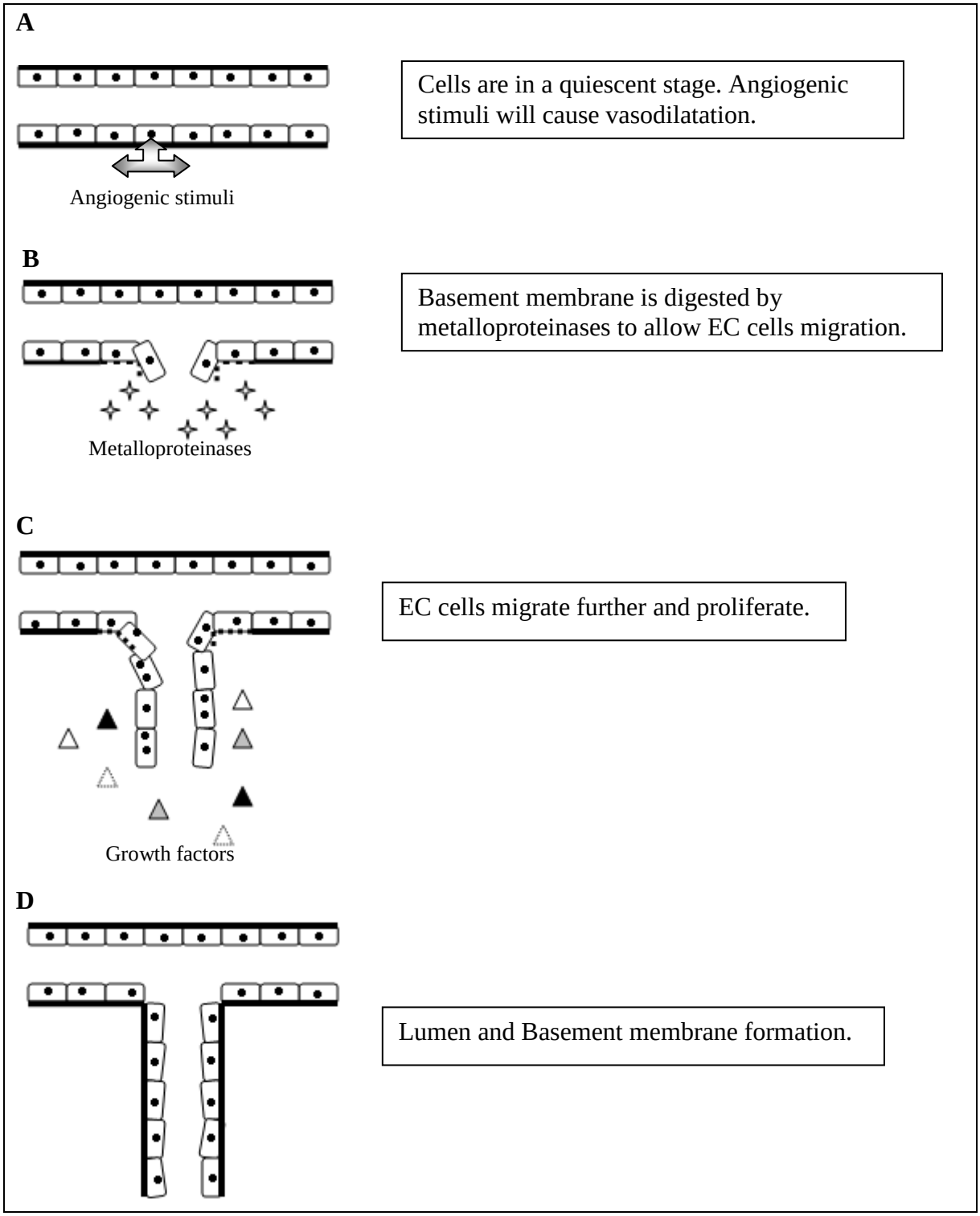



**Figure 2.1:** The process of angiogenesis. **A-** Initiation of angiogenic response. **B-** Migration and proliferation of endothelial cell. **C-** Lumen and tube-like structure formation. **D-** Maturation of the new vessel.

## 2.4. COLLAGEN

Collagen fibrils and their networks contribute to ECM in most hard and soft tissues (bone, blood vessels, cartilage, tendon, cornea and skin). Collagen plays a key role in maintaining the structural, biological and physiological function of ECM [79], a dynamic and flexible structure that helps define cell behavior [80].

Collagen gels provide a physiological, isotropic environment that has been shown to promote the organisation of different cells including epithelial cells [81], pancreatic endocrine cells [82] and endothelial cells into 3D tissues like structure [19].

Collagen provides the tensile strength in tissues which makes it an attractive material to use to make substitutes for those tissues [83]. Collagen can contract as it is populated with cells due to cell traction, however endothelial cells (EC) can distract collagen during angiogenesis facilitating further EC invasion [84]. Collagen causes little tissue reaction [47]. Any reaction is confined to a transient local mild inflammation with an increase in local macrophages that resolves quickly [85-87], in contrast to polylactide scaffolds where there can be longer lasting inflammation [64].

### 2.4.1. Structure

The collagen molecule is essentially a triple helix with non-helical structures that are present at both ends of the chains [30]. Up to 2009, 30 unique types of collagen have been reported [88]. These are reviewed elsewhere [29, 30, 89]. All forms of collagen are made of three left handed polypeptide chains. These chains are coiled in a right

handed direction about a common axis to form the rope like molecule “supercoil” with a pitch of 8.6nm [30, 32, 90]. This is stabilised mainly by hydrogen bonds on the NH ….O=C type as well as covalent bonds [Figure 1.2] [32, 91].

The main feature of the collagen triple helix is the high glycine (Gly) and amino acid residues and, the repeating residues Gly-X-Y where X and Y are most likely to be proline and hydroxyproline respectively [30, 32, 92]. Since glycine has no side chains, its presence at every third residue allows for a shallow helix in the centre of the superhelical structure [93] characterising the primary structure of collagen. The extended spiral structure of the single peptide chains forms the secondary structure, whereas the tertiary structure is due to the triple peptide chain tuning around a central axis [91].

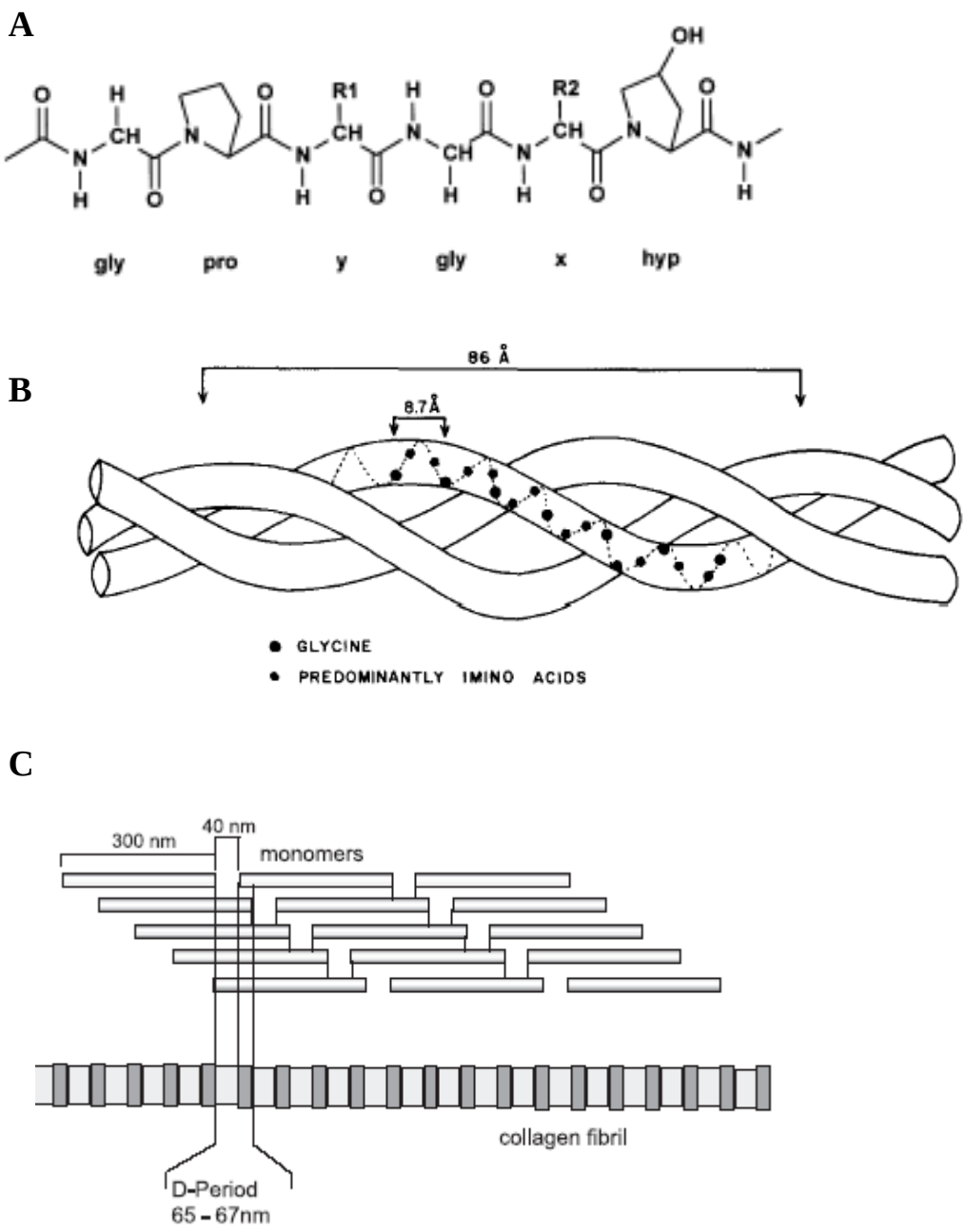



**Figure 2.2:** Schematic drawing showing: **A-** Primary amino acids, **B-** The collagen triple helix. The individual α chains are left-handed helices with approximately three residues per turn. The alpha chains are in turn coiled around each other following a right-handed twist. **C**- Staggered quaternary structure [modified from [7], [2], and [64]**.**

### 2.4.2. Collagen-Cell interactions

Ccollagen substrates affect the adhesion, migration and morphology of cells in particularly vascular cells which are discussed below. Extracellular attachment of glycoproteins, such as fibronectin, chondronectin and laminin bind uniquely to collagens and play important roles in cell-collagen interactions [62]. In addition to structural and mechanical functions, collagens play an important role in determining cell attachment and spreading that consequently influence cell differentiation and movement [63].

Most cells require an appropriate substratum for growth in culture. A variety of cells use fibronectin, a glycoprotein composed of two protein chains linked together by disulfide bridges at their carboxyterminal ends [94]. Fibronectin binds to collagen providing a substratum for cell growth by containing a collagen-like region that binds to relatively small portions of amino acid chains on native and denatured collagens (type I to type V). Cells, in the presence of $Ca^{2+}$ or $Mg^{2+}$, adhere to the fibronectin-collagen complex [95, 96]. The triple helical nature of collagen regulates integrin-mediated cellular interactions [97] by recognizing a specific amino acid side chains in collagen resulting in a conformational change that triggers signalling [98].

The collagen binding site is less tightly coiled due to the absence of hydroxyproline, proline and carbohydrates and involves an octapepetide of the α1 (I) chain as well as the collagenase cleavage site that is necessary for binding [99]. This facilitates the uncoiling of collagen for the purpose of binding to fibronectin on cells.

### 2.4.3. Collagen-vascular cells interaction

Cell-Matrix interaction is of central importance in tissue engineering. Vascular cells-matrix namely collagen is of particular interest in this review.

Under both normal and pathologic conditions, ECs are in constant communication with the ECM. This interaction plays an important part in many ECs functions, including adhesion and migration [34, 100-102], proliferation [34, 102, 103], differentiation [104], signal transduction [34, 102, 105], and morphogenesis[34, 102, 106].

Collagen type 1 induces tubule formation in a variety of endothelial cells [19] [107-109]. This is in contrast to other ECM substrates such as laminin, type IV collagen, and fibronectin. This unique property might involve RGD-dependant attachment with its fibrillar structure acting as a 3D template for tubule formation [110]. Collagen also promotes EC migration[106] which could contribute to tubule formation, since cells need to be in close contact to form tubule, probably by interacting with the entire surface of EC inducing the formation of new apical faces segregated from the collagen matrix and encircling newly formed lumina [19].

Cell-cell contact is important in ECM production. Smooth muscle cell (SMC) production of type I collagen is reduced when co-cultured with EC. Some matrix proteins that usually reside in EC basement membrane can inhibit SMC matrix synthesis. EC inhibit SMC synthesis of collagen type 1 in an *in vitro* culture model,

not through changes in active TGF-β1 levels but possibly through secreted matrix proteins [111].

In the initial stages of angiogenesis, fibrillar collagens promote rapid and invasive EC growth. Moreover, collagen type I along with other ECM component is capable of supporting chemotactic migration [34]. Type I collagen-induced angiogenesis requires ligation of GFPGER (502–507), a key sequence on type I collagen, to the endothelial cell α 2β1 integrin. The inhibition of integrin β subunit A-domain disrupts endothelial cell-collagen interactions and collagen-induced capillary morphogenesis [112]. The integrins are a group of sequence-related proteins that are involved in cell-ECM and cell-cell adhesion. The ECM receptor integrins are heterodimers composed of variable α and β subunits. At least three kinds of integrin receptors have been identified in endothelial cells: $\alpha_2\beta_1$ (laminin and collagen receptor), $\alpha_5\beta_1$ (fibronectin receptor), and $\alpha_V\beta_3$ (vitronectin and thrombospondin receptor) [113].Collagen fibrils are a key determinant of SMC function. Vascular SMCs use $\alpha_2\beta_1$ integrin to crawl on type I collagen and that this motility can be enhanced through localized proteolysis of the collagen substrate [114].

### 2.4.4. Collagen construct degradation

The degradation of porous scaffolds affects the cell viability and growth as well as host response. Once a scaffold is implanted, it should maintain its mechanical properties until the cells lay down enough ECM, before preferably becoming completely adsorbed [115]. *In vivo* degradation of collagen matrix is a complex mechanism where the collagen matrix is infiltrated by fibroblasts, macrophages and

neutrophils which contract the implant and release collagen degrading enzymes [52, 116, 117]. The infiltration and thus the rate of degradation depend on the properties of the biomaterial including porosity and pore size, degree of cross-linking and enzyme levels [118]. The formation of cross-links between the triple helical regions of adjacent molecules would restrict access to the degradative enzymes as well as the formation of bonds during cross-linking reduces the number of specific cleavage sites [118]. Therefore, this can be useful in tissue engineering to achieve tissue formation-implant degradation match.

#### 2.4.4.1. Collagen degradation *in vivo*

Collagen turnover occurs physiologically and in scaffolds [119]. MMPs are involved in collagen turnover in addition to their role in endothelial migration. 24 MMPs have been characterized and are divided according to their primary structure and substrate specificity into five subclasses, including collagenases and gelatinases [120]. Collagenases cleave tropocollagen (TC) at one single site, producing two fragments: $TC_1$ at about ¾ and $TC_2$ at about ¼ of the original molecule as a result of the hydrolysis of a single Gly-Ile/Leu bond in each α chain of the collagen molecule before further digested by other MMPs [50, 121]. Apart from collagenases, gelatinases play an important role in degrading rapidly denatured collagen and collagen fragments [50]. Apart from collagenases, gelatinases play an important role in degrading rapidly denatured collagen and collagen fragments [50].

#### 2.4.4.2. Collagen degradation *in vitro*

Collagen degradation requires water and enzyme penetration as well as digestion of linkages. Though collagen swells to a certain extent upon exposure to water, it can only be digested completely when collagenases take part. Whilst tissue collagenases cleave one time cross all three chains as described above, collagenases from clostridium histolyticum (CHC) make multiple scissions per chain [122]. Those enzymes cleave undenatured helical regions at physiological pH and temperature [123]. Other non-specific proteinases, like pepsin, can only attack telopeptides or denatured helical regions. This makes them responsible for further degradation down to amino acids [124].

Generally, CHC is used for *in vitro* experiments due to its abundant availability in purified forms and broad spectrum of action cleaving all types of collagen [125]. Furthermore, its specifity is similar to human neutrophil and fibroblast collagenase making *in vivo/in vitro* correlation possible[126]. The enzyme preferentially hydrolyzes the X-Gly bond in a sequence R-Pro- X-Gly-Pro. This sequence is found almost exclusively in collagen and susceptibility to the enzyme is often used as a criterion for collagen [127, 128]. Collagenase is too big to penetrate into fibrils of collagen and thus digestion occurs at the fibril surface. Thus, within the molecular architecture of the polymeric collagen fibrils, the tropocollagen is inaccessible by the enzyme resulting in reduced degradation rate. This could explain the very low turnover of mature collagen *in vivo* [129].

### 2.4.5. Reinforcing collagen scaffolds

The material properties of collagen scaffolds can be reinforced by cross linking either by physical or by chemical techniques in order to develop materials with a high degree of mechanical integrity and stability during implantation [130]. The extent and method of cross linking influences the swelling ratio [131], thermal properties [118], stress-strain characteristics [132] and resistance to collagenases digestion [133]. Without cross linking, a collagen sponge collapses in contact with fluids and forms a gel at the fluid boundary. Cross linking is an effective method to control the resorption/degradation rate of collagen [134]. Determining the degradation rate by bacterial collagenases is often used to predict the rate of resorption.

A number of chemical agents have been investigated to cross link collagen for use in scaffolds including glutaraldehyde [133], formaldehyde [135], polyepoxy compounds [136], acyl azide [137], carbodiimides [138] and hexamethylene diisocyanate [54, 139]. Glutaraldehyde is widely used as it is cheap, readily available and is highly soluble in aqueous solution. However, it is potentially cytotoxic and can cause calcification in host tissue due to incomplete removal of toxic residues. Aldehydes and other metabolites can be found which in turn compromise the biocompatibility of the scaffolds [140]. Carbodiimides (CDA or EDC) are a promising alternative as they contain no potentially cytotoxic residuals and do not remain active. The non toxic urea derivative released when the cross link is generated is easily rinsed from the collagen, leaving no residual chemicals [141]. However, it is a time consuming technique.

Physical cross linking can be achieved by; heat, dehydrothermal treatment (DHT),

unltraviolet (UV), and γ-irradiation. Physical cross linking has the advantage that it does not introduce potentially cytotoxic chemicals [134]. In DHT, cross linking is induced by heat drying collagen under vacuum to 100°C [118]. This can denaturate the collagen [142]. It has been reported that the process of UV irradiation can induce cross links into collagen fibrils. However, this is complicated by peptide bond scission events that may also occur through free radical mechanisms. The fine tuning of irradiation processes may therefore allow either the degradative processes or cross linking processes to be enhanced [143].

## 2.5. IMPROVING CELL PENETRATION IN SCAFFOLDS

Creating internal channels to permit the flow of nutrient-rich medium throughout the scaffold is one strategy proposed for maintaining cell survival deep within the scaffold. 3-D printing can be used to create micro channels to overcome the diffusion limitations of current foam scaffolds [144]. Solid freeform fabrication (SFF) can produce scaffolds with predefined and reproducible internal morphology to act as an artificial vascular system [145]. The traditional SFF technique has made scaffolds from synthetic polymers [146-148] and ceramics [149]. This technique has drawbacks as they are processed at high temperatures limiting the choice of materials and preventing the incorporation of biological molecules. A novel SFF technique has been developed producing collagen scaffolds with complex internal morphology using a sacrificial mould and critical point drying technique. The moulds can contain predefined and reproducible features as small as 200μm [27]. These channelled

collagen scaffolds have been successfully used in chondrogenesis using bone marrow derived stem cells resulting in good matrix synthesis within the channels and not in the periphery [28, 150].

## 2.6. VASCULARISATION OF TISSUE ENGINEERED SCAFFOLDS

Vascularisation of tissue engineered construct could be achieved either by *in vitro* prevascularisation or *in vivo* pre vascularisation. The latter involves vessels from the surrounding tissue that can be stimulated to infiltrate an implanted construct by the release of angiogenic growth factors diffusing from the scaffold encouraging existing blood vessels to grow into the implanted construct [151, 152]. *In vitro* prevascularisation involves culturing endothelial cells *in vitro* on scaffolds with the objective of building a 3-D prevascularised system which is then implanted into the ischemic area. The aim is to build a natural connection with the existing vasculature in the surrounding vessel supplied tissue. Both approaches are associated with time delay before vascular perfusion can occur [13, 14, 153, 154]. Microvascular network constructed *in vitro* within a 3 D construct has shown not only to develop functional anastomoses with the host's blood supply but also to promote rapid, complete and optimal vascularisation of the implanted tissues [155] .

In *in vitro* prevascularisation approach, there has been success in pre-forming capillaries prior to implantation. ECs were co-cultured with fibroblast in a fibrin gel. The fibrin based tissues were prevascularised with capillaries then implanted

subcutaneously in mice. Prevascularizing a fibrin-based tissue with well-formed capillaries accelerated anastomosis with the host vasculature, and promoted cellular activity consistent with tissue remodelling [154]. Endothelial cells demonstrated the ability to organise into tube-like structure *in vitro* when cultured on collagen type-1 substrate. Cloned capillary endothelial cells from bovine adrenal cortex plated either in plastic culture dishes or on the top of collagen gels formed typical monolayers. In contrast, the monolayers formed on collagen gels underwent dramatic reorganisation when covered with a second layer of collagen which within 2 days formed a network of branching and anastomising tubes resembling capillary beds *in vivo*. This shows clearly that endothelial cells grown inside 3 dimensional collagen matrices even after repeated passage in culture have the ability to form vessel-like structures if provided with an adequate environment. Moreover, it demonstrated the fact that collagen promoted cell migration which contributed to tubular networks[19]. In another study, endothelialized reconstructed skin was developed based on collagen sponge cultured with endothelial cells, keratinocytes and fibroblasts. A network of human capillary-like structures was spontaneously formed in the dermal part. After transplantation of the construct into nude mice, the connection of the prevascularized construct to the host tissue required 4 days. In comparison, a 14-day period was necessary to achieve a similar result with non-endothelialized control transplants [156].

Although *in vitro* prevascularisation saves time as the host blood supply does not need to perfuse all the way into the core centre of the scaffold as it connects with the prevascular network at the marginal area, the tissue lacks microsurgical connections with host vasculature leading to a slower perfusion.

In *in vivo* prevascularisation approach, porous collagen type I scaffolds were implanted in the palatal mucosa of male Wistar rats in a study of their potential for future applications in cleft palate surgery. Angiogenesis started after 1 week indicated by collagen type IV staining and showed a peak after 4 weeks, slowly declining afterward. Studies using injectable bovine dermal collagen in human skin showed no vascularization up to 13 weeks after implantation. This difference might be caused by the porous structure of the collagen scaffolds [157]. The potential of collagen scaffolds for attracting angiogenesis/arteriogenesis was studied *in vivo* by implantation on healthy or cryoinjured left ventricle of rats up to 60 days post-injury times. The scaffolds were seeded by EC and SMC individually before implantation. The collagen cardiac patches were almost completely absorbed in 60 days and became populated by new arterioles and capillaries in both intact and cryoinjured[158].

Progenitor endothelial cells (EPC) show some of the same properties as EC. Human umbilical cord blood EPC have an inherent ability to assemble into a microvascular-like network when seeded on PGA-PLLA (poly-L-lactide) woven scaffold with SMC suggesting that they could be used to introduce a microvascular network into tissue engineered organs and tissues that might readily anastomoses with existing vessels in the host. EC in absence of SMC still adhered to PGA-PLLA scaffold and remained viable but little tissue was formed. Seeding with SMC dramatically enhanced assembly of EC into microvessel like structure [159] . The implantation of EPC with SMC combined in matrigel in the back of mouse resulted in the formation of extensive blood vessel network, after one week, with those new vessels linked functionally to the host vasculature with the vessel lumen [160].

Attempts have been made to incorporate growth factors such as VEGF, Ang-1 and bFGF into collagen based scaffolds to enhance the vessel growth [161], [163]. Human umbilical endothelial cells proliferate quicker on collagen scaffolds loaded with VEGF [162] .VEGF has been used successfully to enhance the angiogenic potential of scaffolds both in chorioallantoic membrane models and when implanted in animals [163], [164]. A number of different methods were used to incorporate these growth factors; Heparin has been incorporated by EDC cross linking and used as a binding site for growth factor incorporation. Surprisingly, the angiogenic capability of the scaffolds was increased just by the addition of the cross linked heparin, before being further augmented by VEGF incorporation [163]. Combining VEGF to the scaffolds is important, as simply adding growth factor to the medium, does not stimulate nearly the same level of EC proliferation. Other growth factors are potentially useful, such as Ang-1, which has induced sprouting of EC and more importantly recruits mural cells to developing vessel [165]. Ang-1 has been mobilized alone and co-immobilized with VEGF on collagen scaffolds. Scaffolds with immobilized VEGF and/or Ang-1 increased EC proliferation and infiltration in the chorioallantoic membrane compared to unmodified scaffolds and soluble growth factor controls [166]. Further strategies are likely to incorporate multiple growth factors into the scaffolds to enhance vascularisation. Collagen scaffolds dually loaded with VEGF and FGF2 enhanced angiogenesis, epidermilization and led to improved wound healing compared to wounds treated with bare collagen scaffolds [167]. Covalently linking both VEGF and FGF2 to acellular collagen scaffold displayed the highest blood vessel density and more mature vasculature compared to non loaded scaffold or single growth factor loaded scaffold, when subcutaneously implanted in rats [15]. Collagen has the

advantage of possessing active functional groups that allow immobilization of growth factors [168-170] and being processed at low temperatures preventing growth factors denaturation.

The reuse of biological structures is another approach to overcome the vascularisation problem. By decellularizing mammalian sections, a naturally-derived 3D structure supplying microvascular networks can be obtained. The repopulation of the matrix with desirable human primary cells introduces the possibility, to build perfusable constructs [171]. The decellularizing process reveals a matrix of collagen and elastin fibres traversed by arteries and veins. Biological, vascularised matrices can be used for appropriate nourishment of the engineered tissue and ensure better transplantation efficiency [172]. However, the availability of such structures for wider use hinders its popularity.

Large blood vessels have been constructed *in vitro*. Weinberg and Bell developed a model of blood vessel *in vitro* constructed from collagen and cultured bovine aortic smooth muscle cells, with an intima, media and adventia, cast in a modular mould. Adventitial fibroblasts were cast on top to make the adventia. Bovine aortic endothelial cells were seeded in the lumen producing a model blood vessel that met many of the physiological and biological criteria of mammalian artery [173]. In 1998, l'Heureux's group created a large blood vessel that meets three fundamental qualities: mechanical strength, blood biocompatibility and suturability. This model has features that make it a good model for *in vitro* vascular cells studies, but there are still technical problems to be overcome before its clinical use, such as cell sourcing, upscaling this model and time needed for production [174].

## 2.7. CONCLUSION

The development of an inherent capillary bed *in vitro* is crucial for ensuring the viability and function of tissue-engineered tissues, as is the ability to connect with the host vasculature once implanted. Current strategies are an accumulation of materials engineering and both *in vivo* and *in vitro* angiogenesis. These include scaffold design and cell seeding.

The main issues in scaffold design are the strength acquired by cross linking, the structure and the size of any channels and the ability to integrate growth factors. These parameters need to be optimized in order to achieve a viable pre vascularised scaffold for use in tissue engineering.

Collagen may be an ideal scaffold for tissue engineering since it acts as a native surface for cell attachment and migration compared to synthetic materials and is a major ECM component. To date, collagen scaffolds with a foam design structure has not allowed cell migration deep into the structure [175, 176]. Collagen scaffolds with predefined and reproducible internal structure, like channels running across the scaffold, could be a great benefit to tissue engineering. The channels could increase mass transport of nutrients and oxygen deep into the scaffold until tubule formation is achieved. A 3D porous channelled collagen scaffolds increasing the ingrowth of angiogenic cells into the scaffold mass might provide a solution.

Though co-culture is used to mimic the beneficial and complex interaction of cells, the optimal combination of cells, their ratios and conditions to maximise

celluarisation are still unknown. EC are a pre-requisite, although it is not yet established whether precursor cells pre-seeded into the scaffold might increase tubules. Co-culture could include mesenchymal perivascular support cell. Smooth muscle cells have traditionally been used although it could well be that other pericyte type cells could be beneficial in production of tissue specific microvessels [14].

Growth factors appear to be beneficial and cocktails may be advantageous. This specific need needs to be established, particularly with a view to effect over time, initially inducing tubule formation and lately inducing vessel stabilization. In order to do this controlled release systems may need to be developed.

Scaffold properties need to be developed further to achieve fast enough occurring neovascularisation. Unless these difficulties of creating an intrinsic circulation can be overcome, tissue engineering of complex pre cellularized products will be restricted.

# CHAPTER 3: DESIGN, FABRICATION AND CHARACTERISATION OF COLLAGEN SCAFFOLDS

## 3.1. INTRODUCTION

The aim is to develop a collagen scaffold that would support angiogenic cells ingress and consequently allows more rapid vascularisation *in vivo*. Pore size in one of the main key parameters that is crucial for scaffold development in tissue engineering. The pore size should be big enough to allow cells to migrate into the scaffold where they become bound to ligands expressed on the scaffold, but small enough to establish a sufficiently high specific surface for a minimal ligand density required for efficient binding of a critical number of cells to the scaffold [17, 177, 178].

It is been reported that collagen scaffold pore size ranging from 50 to 200μm is suitable for endothelial and smooth muscle cells infiltration *in vitro* and *in vivo* and angiogenesis [17, 162, 179-181]. If pores are too small cells can not migrate towards the centre of the construct limiting the diffusion of nutrients and removal of waste products. Conversely, if pores are too large there is a decrease in specific surface area available limiting cell attachment [17]. Thus, we attempted to make a scaffold with such pore size. In addition to trying to achieve the optimal pore size for angiogenic cells ingrowth, channels were introduced into collagen scaffolds to alter the internal

structure in attempt to improve nutrients exchange into scaffold and thereby lead to an improved rate of angiogenic cell penetration [27, 28, 150].

Collagen scaffolds can be manufactured by precipitation, critical point drying and freeze drying [175]. Freeze drying, or otherwise known as lyophilisation, is method of making porous foam-like scaffolds with the advantage that the pore size could be effectively controlled by altering the process parameters. Freeze-drying involves the removal of water or other solvent from a frozen product by a sublimation process. Upon freezing the collagen suspension, ice crystals form thereby forcing and aggregating collagen molecules to the interstitial spaces and when removed by sublimation, they leave a porous structure that mirrors the sublimated ice crystals [178]. Modifications of freeze drying process are the key to producing scaffolds with various pore sizes and structures. Since the scaffolds pore structure mirrors the ice crystals structure formed, pore structure can effectively be controlled by changing the freezing process [182, 183]. Altering the freezing temperature and collagen suspension concentration could affect the pore size of scaffolds [150, 175, 184]. Thus, collagen scaffolds were made using different collagen concentrations and frozen at different temperatures in order to achieve the optimal pore size suitable for culturing angiogenic cells.

Mechanical properties are another crucial factor in developing a scaffold for tissue engineering. Untreated collagen has low mechanical properties and is degraded rapidly *in vivo* which is another factor that limits its use. Scaffolds should be strong enough to allow *in vivo* implantation and be mechanically functional once implanted until the cells lay down enough extracellular matrix [185, 186] . This can be altered by

cross linking achieved through either chemical or physical cross linking. The extent and method of cross linking influences aspects of the scaffolds such as the thermal properties, swelling ratio, stress-strain characteristics and resistance to collagenases digestion [54, 133, 187]. Two methods of cross linking were explored: dehydrothermal treatment (DHT), a physical method, and 1-ethyl-3-(3-dimethylaminopropyl) carbodiimide hydrochloride (EDC), a chemical method. DHT is a simple method where cross linking is induced by simply heating dry collagen under vacuum to approximately 100°C [118]. This removes water from the collagen molecules, resulting in the formation of intermolecular cross links through condensation reactions either by esterification or amide formation [188]. It does not involve the use of cytotoxic reagents. Due to exposure to high temperature, it provides sterilisation in addition to cross linking. However, the high temperature rearranges the triple helix structure of collagen into random-chain configuration leading to denaturation [57]. EDC activates the carboxylic acid side groups of proteins, usually aspartic and glutamic acid residues in the case of collagen, which then react with the amine groups of other polypeptide chains to create amide bonds [Diagram 3.1]. It shows promise as it contains no potentially cytotoxic residuals and do not remain active. The nontoxic urea derivative released when the crosslink is generated is easily rinsed from the collagen [141].

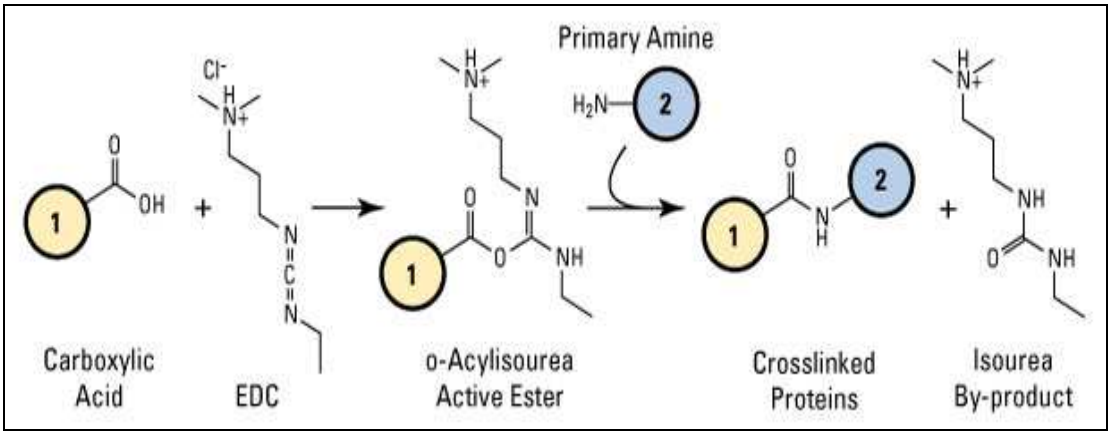



**Diagram 3.1.** EDC (carbodiimide) crosslinking reaction scheme. Carboxyl-to-amine crosslinking with EDC. Molecules (1) and (2) are chemicals that have respective carboxylate and primary amine groups.

In conclusion, this chapter presents work on the control of collagen scaffolds processing. It will illustrate how altering processing method parameters can affect collagen characteristics and scaffolds properties and how internal structures such as channels can be inserted into scaffolds using pins. The optimal processing conditions will be determined to use for scaffold production for further studies.

# 3.2. MATERIALS AND METHODS

## 3.2.1. Scaffolds Design and Fabrication

### 3.2.1.1. Moulds Fabrication

Moulds and caps were made for casting the scaffolds in the mechanical workshop of Department of Materials, University of Oxford. These poly (tetrafluoroethylene) (PTFE, biocompatible) cylinders had 15mm internal diameter and 6.5cm height. Caps were used to cover the two extremities of the mould with diameter of 20mm in order to obtain flat surface (Figure 3.1). The caps were attached to the mould by cello tape during the freezing of the sample. To introduce some vertical channels in the scaffolds, caps were drilled and pins were put through the caps resulting in samples with 3 channels (made of laboratory tubes, biocompatible, 2.4mm) and samples with 9 channels (made of titanium tubes, biocompatible, 1mm) (Figure 3.1).

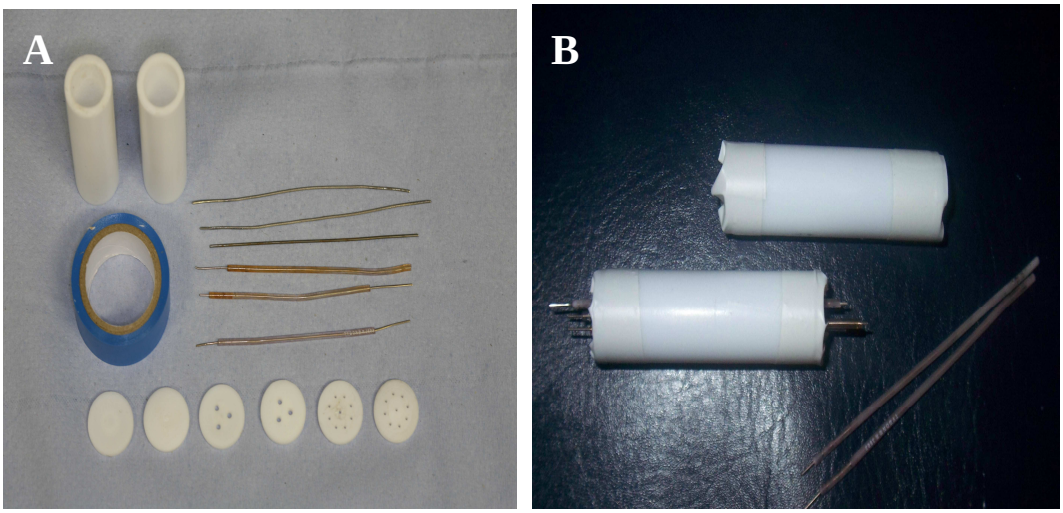



**Figure 3.1**: Picture of: **A-** the mould with caps for sample with and without channels, and **B-** assembled moulds with and without channels.

### 3.2.1.2. Collagen Suspension and Freeze Drying

A polymeric type I tropocollagen from the mature bovine Achilles tendon (Devro (Scotland) Ltd, UK) dispersions were prepared by placing dried insoluble collagen fibres in 0.05M acetic acid (Sigma–Aldrich) solution with pH adjusted to 3.2 by the drop-wise addition of 0.5M sodium hydroxide. The dispersions were homogenised for 90 seconds on ice using conventional blender (Braun 400W). The dispersions were then de-aired at a pressure of approximately 0.1kPa at room temperature under vacuum till no more air bubbles were present. They were then stored at 4 °C (ER7610C, Electrolux refrigerator) until further use [27]. During freezing, collagen suspensions are frozen at specific temperature. The ice crystals were formed during freezing overnight; then, the frozen suspensions within the moulds were dried using freeze dryer (MicroModulyo, EC Apparatus Inc., USA) at -50°C and less than $1x10^{-2}$ mbar for 48 hours to bring them into solid state. Lastly, scaffolds are released from the moulds.

In attempt to control the pore size by varying freezing temperature, collagen scaffolds were made using a bovine type 1 collagen dispersion of 1% weight to volume frozen at either -20°C or - 80°C. Alternatively, pore size can be controlled by varying the concentration (volume fraction) of collagen during dispersion preparation [184]. Thus, A bovine type 1 collagen dispersion of 1% weight to volume (1g collagen in 100ml yields a 1% w/v dispersion) and 0.5% w/v were prepared and frozen at -20°C. It is

expected that higher freezing temperature and lower content of collagen during the freeze drying process yields a higher pore size scaffolds.

For scaffolds with channels, the pins used to create channels were removed before freeze drying. After freezing, the moulds were dipped in water for few seconds to loosen the pins which were removed by a gripper then scaffolds were immediately freeze dried (Figure 3.2).

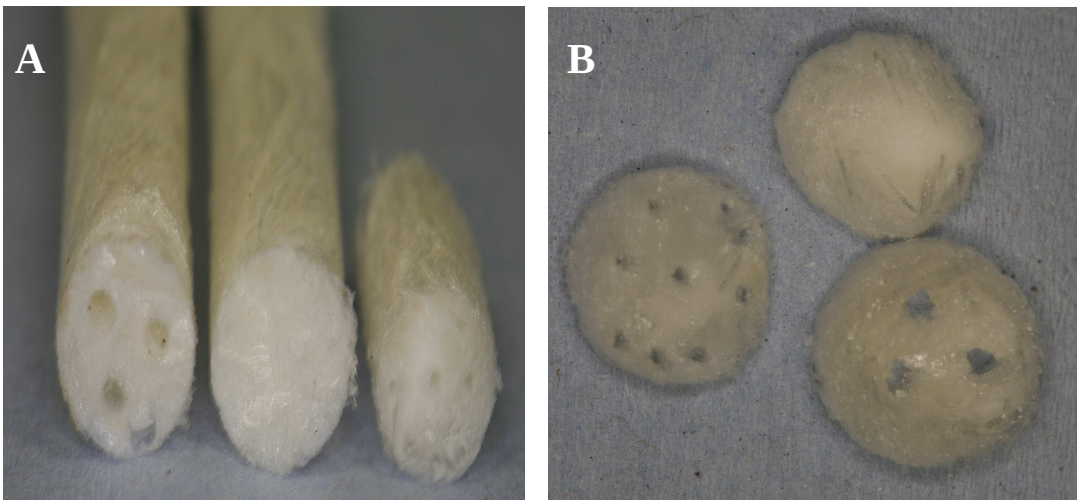



**Figure 3.2:** 1% collagen dry scaffolds. **A-** The 5 cm collagen scaffold rods as taken out of the moulds. **B-** 0.5-0.6 cm slides of non-channelled, 3-channels and 9 channels collagen scaffolds.

### 3.2.1.3. Scaffolds Crosslinking

#### 3.2.1.3.1. Physical Crosslinking (DHT)

Scaffolds made of 1% collagen and frozen at -20°C were subjected to heat dehydration at 110°C under a $10^{-2}$ mbar vacuum (1Pa) (Heraeus Vacutherm vacuum

drying oven 6000) for one day, three days and five days. The temperature was allowed to return to 20°C before removing the vacuum [134].

#### 3.2.1.3.2. Chemical Crosslinking (EDC)

Chemical cross linking with EDC is well documented in literature. Generally, collagen scaffolds are made out of collagen suspension, freeze dried then cross linked before freeze drying again. In this study, we suggested ethanol defrost step, an alternative time-efficient method, avoiding second step of freeze drying. Frozen 1% collagen scaffolds at -20°C were defrosted in ethanol then incubated for 30 minutes at room temperature in 50mM 2-morpholinoethane sulfonic acid (MES) (pH 5.0) solution. Subsequently, matrices were incubated in solution containing 50 mM MES (pH 5.0) and variable *N*-Ethyl-*N*′-(3-dimethylaminopropyl) carbodiimide (EDC) (Sigma- Aldrich, UK) (10mM, 33mM and 50mM) concentrations for 4 hours at room temperature. N-hydroxy-succinimide (NHS) was added in an EDC: NHS ratio of 3:1. Excess EDC was rinsed from the matrix using 0.1M $Na_2HPO_4$ (pH 9.1) twice for one hour followed by washing with distilled water four times, each time for 30 minutes [131, 189]. Samples were frozen again then freeze dried as described. To investigate whether our method would affect pore structure and morphology, 10mM and 50mM EDC samples were cross linked as well using two steps freeze drying to compare their properties with similar samples cross linked using single step of freeze drying.

## 3.2.2. Scaffolds Characterisation

### 3.2.2.1. Microstructural Evaluation Using Scanning Electron Microscopy

Dry collagen scaffolds were cross-sectioned with a razor blade and sputter coated with Platinum using a Polaron SC502 Sputter Coater (Fison Instruments, UK), and examined using JEOL JSM-840F Scanning Electron Microscope (SEM) (Peabody, MA) at 3-5kV.

#### 3.2.2.1.1. Image Analysis and Pore Size Measurement

Image analysis software (ImageJ, Wayne Rasband) was then used to determine the mean pore diameter and distribution within the scaffold. The pore diameter for each sample was determined using equation (1) where D is the pore diameter and A is the pore area, assuming circular pores. The pore area is determined by Image J. The total number of pores analyzed for each sample was greater than 500. The values were expressed as the mean ± standard deviation.

$$D = [(4 \times A)/\Pi)]^{1/2} \quad (1)$$

### 3.2.2.2. Thermal Properties Using Differential Scanning Calorimetry (DSC)

Differential Scanning Calorimetry (DSC) measures the amount of energy (absorbed or released heat) required to heat or cool a specimen at a controlled rate, keeping the specimen at nearly zero temperature difference from an inert reference material. It is

an important tool for measuring thermal properties and transition temperatures of various substances, primarily used in polymer science[190].

The thermal stability of different collagen samples were measured with a thermal analyser module (METTLER TOLEDO DSC-182e) and its thermal analysis software (STARe). The system is based on the heat flux principle (Boersma principle), cooled with a water cooling system and calibrated to an indium standard. 5mg of sample with 15µl of distilled water was placed in an aluminium pan and sealed. An important contact area between the sample and the pan was encouraged. After a soaking time of 20min at 4°C, five samples of each condition were heated between 10-80°C at 10°C/min rate against an empty reference pan in an Aragon atmosphere. The thermal analysis software was used to calculate the denaturation temperature ($T_d$).

#### 3.2.2.3. Mechanical Properties

The tensile properties of scaffolds were measured using Dynamic Mechanical Analyser (DMA7e, Perkin-Elmer) both dry and wet. Prior to testing the cross-sectional area of the individual scaffolds was measured using a handheld micrometer. Bar-shaped dry samples were mounted and subjected to an increasing load at a rate of 60mN/min until failure. For wet testing, similar samples were immersed in room temperature water and subjected to an increasing load at a rate of 20mN $min^{-1}$ The ultimate tensile strength (UTS) and strain to failure ($\varepsilon_f$) were recorded and Young's modulus ($E$) was calculated from the slope of the steepest portion of the stress–strain curve. An average of three runs was used to determine the Young's modulus.

### 3.2.2.4. Swelling Ratio

The relative cross link densities of the scaffolds were determined indirectly by ascertaining their swelling ratio [191]. Samples were boiled for 120 seconds, and then pressed for 20 seconds between dry filter paper with 10N load to remove excess water remaining in the pores. They were then weighed to determine wet weight (WW). The samples were dried at 110 °C overnight and reweighed to determine the dry weight (DW). The swelling ratio ($Q = 1/V_f$) is then calculated using the equation (2) where density $_{collagen}$ = 1.32 g/cm$^3$ and density $_{water}$ = 1.00 g/cm$^3$.

$$Q = 1/V_f = \frac{DW/Density_{collagen}}{WW/Density_{collagen}} + \frac{WW - DW}{Density_{water}} \quad (2)$$

### 3.2.2.5. The Effect of DHT on Collagen Tertiary Structure Using Fourier Transform Infrared Analysis (FTIR)

Fourier Transform infrared analysis (FTIR) analysis is a method of determining the chemical bonds present in a material and their state of vibration (bending, stretching, and contracting). An infrared beam is passed through a thin specimen and the absorbance of the infra red light absorbance by specific bonds at specific wavelengths (wavenumbers) is measured against a background spectrum. Potassium bromide (KBr) is a common material used for the preparation of organic samples as it is transparent to infrared light between 4000cm$^{-1}$ and 400cm$^{-1}$ wavenumber [192]. FTIR provides an effective tool in determining structural changes before and after processing of collagen scaffolds. It was used to investigate the cross linking and

collagen denaturation of 1% collagen scaffolds, frozen at -20°C after 3 days DHT treatment.

Collagen scaffolds were mixed and ground with KBr powders (1:10 weight ratio) in a pestle and mortar before being pressed into a disc using a 10mm diameter stainless steel die to a compaction force of 100kN. The discs were placed in a FTIR spectrometer (Spectrum 2000, Perkin Elmer) in transmission mode and fifty scans were averaged at a $2cm^{-1}$ resolution over the range $400cm^{-1}$ to $4000cm^{-1}$, with the background scan removed.

## 3.3. RESULTS AND DISCUSSION

### 3.3.1. Microstructural Evaluation

#### 3.3.1.1. The Effect of Modifying Freeze Drying Process on Pore Size and Structure

The freezing temperature and collagen concentration affected the pore size which correlates well with the pore size values presented in figure 3.3. The pore size increased significantly by increasing freezing temperature from 94.83μm ± 1.11 for samples frozen at -80°C to 130.65μm ± 2.71 for samples frozen at -20°C, which is reflected in the images (Figure 3.4-A & B). Figure 3.4 shows a cross section view of different scaffolds visualised under SEM. It illustrates low-density, open-cell foam and porous structure with an interconnected network of struts freeze-dried scaffolds.

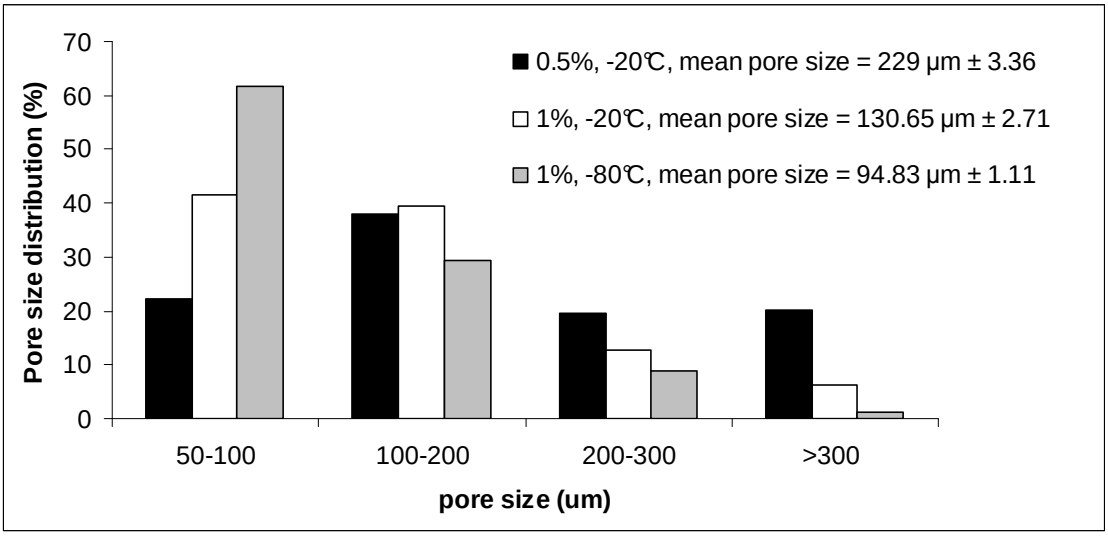



**Figure 3.3:** pore size distribution graph and mean pore size of different collagen samples measured with ImageJ. Image J considers the scale of images which allows the use of images of different scales.1 and 0.5% is collagen content, -20 and -80 °C is freezing temperature The lower the collagen content is, the bigger the pore size is. Conversely, the higher the freezing temperature is, the lower the pore size is.

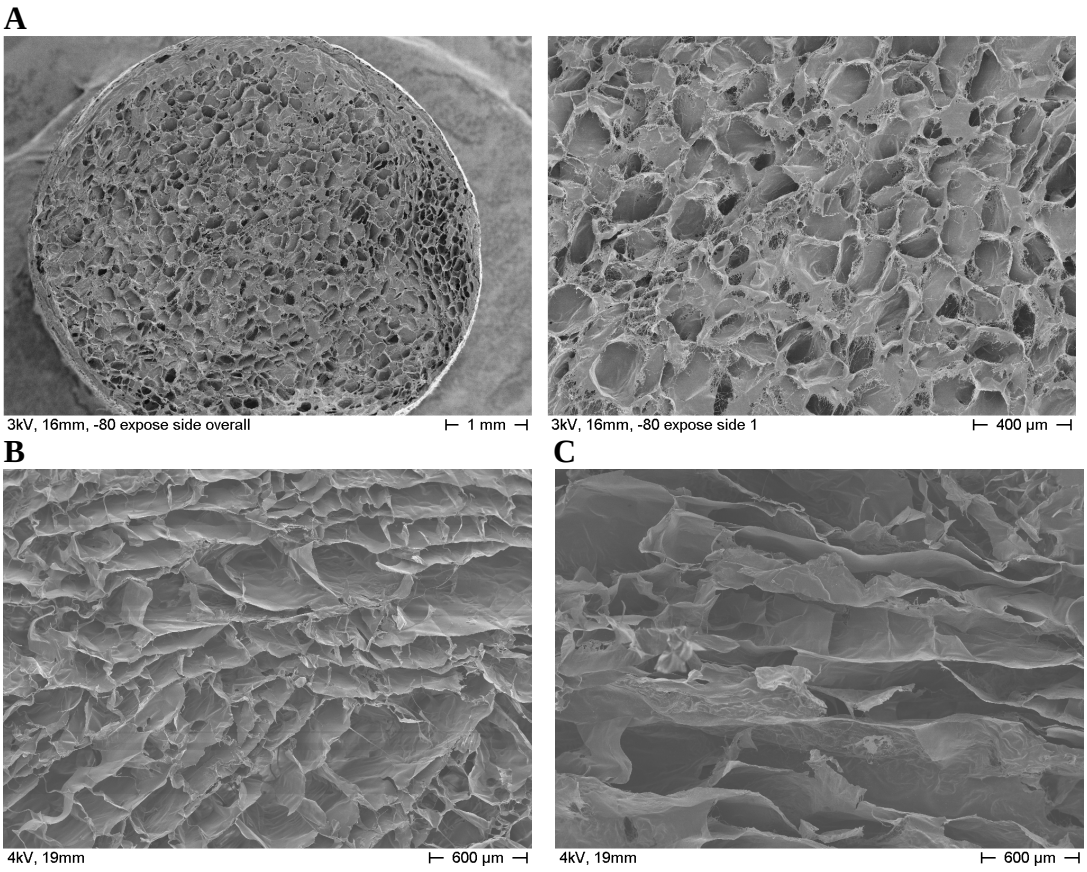



**Figure 3.4**: SEM cross section images of: **A-** 1% collagen scaffold, -80°C scale bar-right = 1mm & left = 400µm. **B-** 1% collagen scaffold, -20°C, scale bar = 600µm. **C-** 0.5% collagen scaffold, -20°C, scale bar = 600µm. SEM illustrates low-density, open-cell foam and porous structure with an interconnected network of struts freeze-dried scaffolds.

Similarly, the pore size increased significantly when collagen suspension concentration was lowered, where pore size increased from130.65µm ± 2.71 for samples made using 1% collagen suspension to 229µm ± 3.36 for samples made using 0.5% collagen suspension. Figure 2.3-B&C clearly shows the bigger pore size on 0.5% collagen compared to 1% collagen scaffold.

This agrees well with literature where it had been reported that higher freezing temperature and lower content of collagen during the freeze drying process yields a higher pore size scaffolds. The pore structure of the freeze-dried scaffolds mirrors the ice-crystal morphology after freezing. Slow freezing at high temperature ( such as -20°C ) leads to a larger ice crystal growth through nucleation forming larger pores with sheet like structure of aggregated collagen fibres [184]. Increasing collagen concentration results in highly interconnected porous structure but smaller pore size [150].

Due to rapid quench freezing during the freeze drying process, the ice crystal nucleation and growth is non-uniform leading to heterogeneity of scaffolds as result of time and space variable transfer of heat through the suspensions. Therefore, the full pore size distribution analysis of different samples was conducted and results are shown in figure 3.3. The majority of pores of samples frozen at -80°C were within the range 50-100μm (60%) and hardly any pores over 300μm (1%) compared to similar sample frozen at -20°C where most pores were in the range 50-200μm (80% with 41% in range 50-100μm and 39% in range 100-200μm) with fewer pores over 300μm (6%). In contract to 1% collagen scaffolds, the 0.5% ones had higher amount of pores in the range 100-200μm (38%) and a considerable amount over 300μm (20%).

Collagen scaffold pore size ranging from 50 to 200μm is suitable for endothelial and smooth muscle cells infiltration *in vitro* and *in vivo* and angiogenesis [17, 162, 179-181]. Collagen scaffolds made using 1% collagen, frozen at -20 °C exhibits such pore size characteristics where the mean pore size recorded was 130.65μm ± 2.71 and 80% of pore ranged between 50-200μm (figure 3.3). The 0.5% collagen scaffold resulted in

bigger pore size which may not be suitable for endothelial and smooth muscle cells growth. In addition, the scaffolds were mechanically weak and difficult to handle. Though no mechanical testing was done on this sample, it is well documented in literature that increased pore size affect scaffold structural integrity lowering its mechanical properties. Lower collagen content result in less dense scaffolds with reduced stiffness [150, 193].

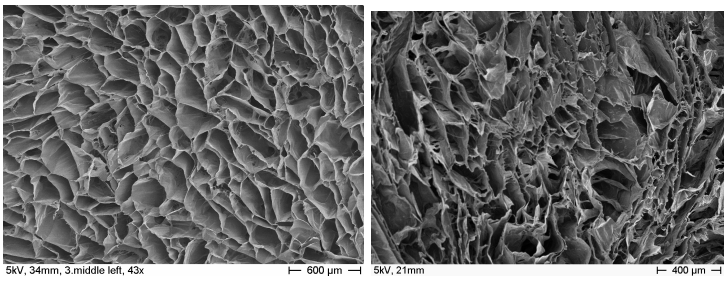
#### 3.3.1.2. The Effect of Different Cross linking Methods on Pore size and Structure

The interconnected 3D porous structure is retained after cross linking either physically or chemically however some changes occurred to pore size and morphology. EDC samples had more elongated pores and non-homogenous structure compared to DHT samples. Fewer fibres in between the pores and more sheet-like structures with condensed walls appeared in EDC samples compared to non cross linked samples. Cross linking samples with EDC through ethanol defrost and single step freeze drying does not damage pore shape compared to samples freeze dried twice. Figure 3.5 illustrates cross sectional view of collagen scaffolds made of 1% collagen suspension, frozen at -20°C and crosslinked differently, showing porosity and interconnectivity.

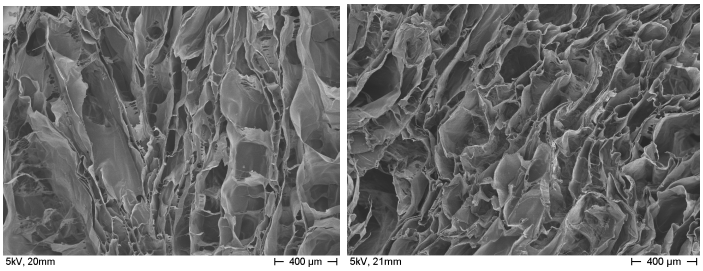
For DHT, pore size increased slightly though not significantly compared to non crosslinked (Figure 3.6, non-crosslinked =110± 0.79μm, 1day DHT = 113 ± 3.51μm, 3 days DHT = 121 ± 4.5μm and 5 days DHT = 120 ± 6.19μm, $p<0.05$). In contrast, EDC reduced pore size which was significant for 50mM EDC samples (10mM = 111 ± 10.19μm, 33mM = 103 ± 9.20μm and 50mM = 81 ± 4.10μm, $p<0.05$). EDC cross linked samples with a single step of freeze drying did not affect pore size at the lowest

EDC concentration (Figure 3.7, 10mM = 111 ± 10.19μm vs. 10mM 2xFD =100 ± 43.06μm); however, it significantly increased pore size for the highest EDC concentration (50mM = 81 ± 4.10μm vs. 50mM 2xFD = 54 ± 15.21μm).

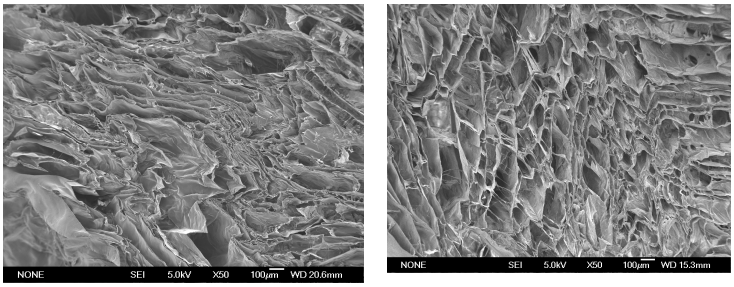
From SEM images, a pore size distribution analysis was applied (Figures 3.6 & 3.7). Cross linked samples presented higher amount of pores over 300μm compared to non cross linked samples that did not have any pores over 400μm. All samples had higher percentage of pores between 50-200μm. EDC cross linking through ethanol defrost and single freeze dried step did not affect pore size distribution.



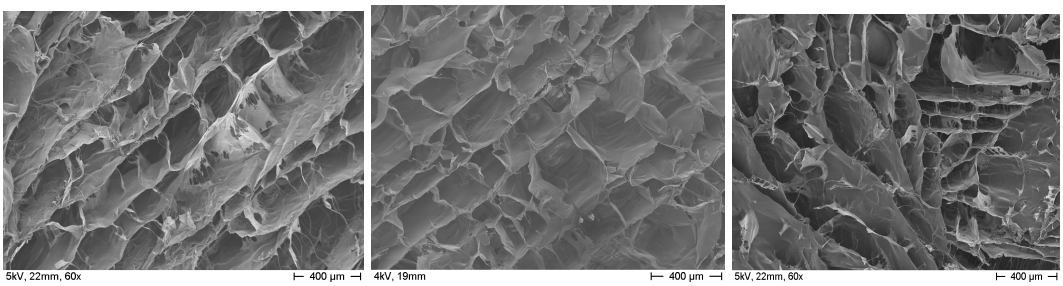

**Non cross linked** **33mM EDC**




**10mM EDC 2xFD** **10mM EDC 1xFD**




**50mM EDC 2xFD** **50mM EDC 1xFD**




**1 day DHT** **3 days DHT** **5 days DHT**

**Figure 3.5:** SEM images of cross-sectional view of the interior of differently cross linked collagen scaffolds. EDC samples had more elongated pores, non-homogenous structure, fewer fibres in between the pores and more sheet-like structures with condensed walls compared to DHT and non cross linked samples. EDC: carbodiimide, DHT: dehydrothermal treatment

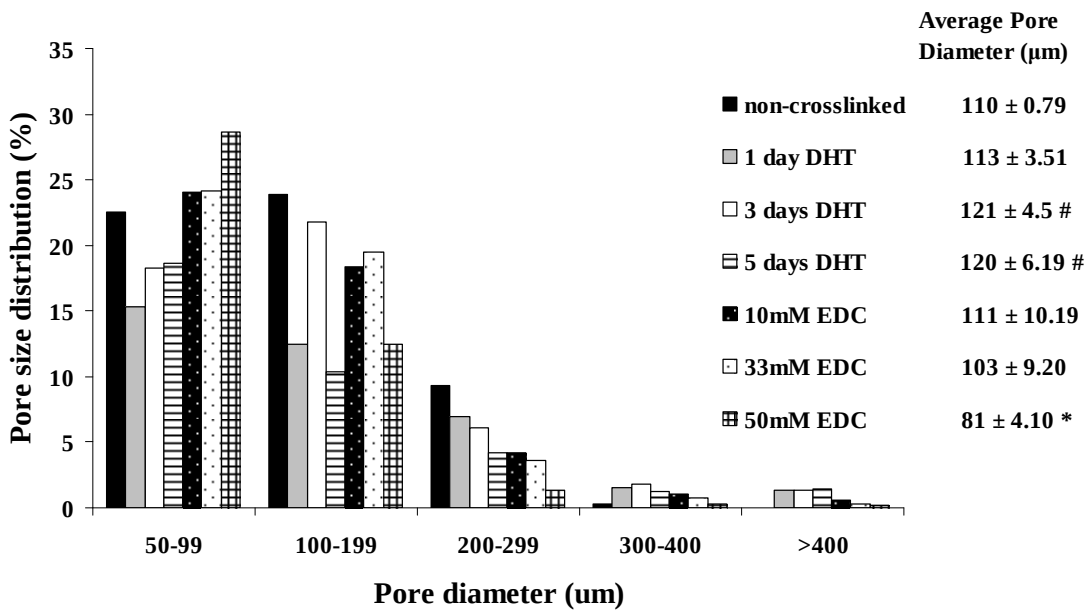



**Figure 3.6:** Pore size distribution graph of differently cross linked collagen scaffolds measured with ImageJ. * compared to non cross linked, $p < 0.05$. # compared to 33mM EDC, $p < 0.05$. Cross linked samples presented higher amount of pores over 300µm compared to non cross linked samples that did not have any pores over 400µm. All samples had higher percentage of pores between 50-200µm. EDC: carbodiimide, DHT: dehydrothermal treatment

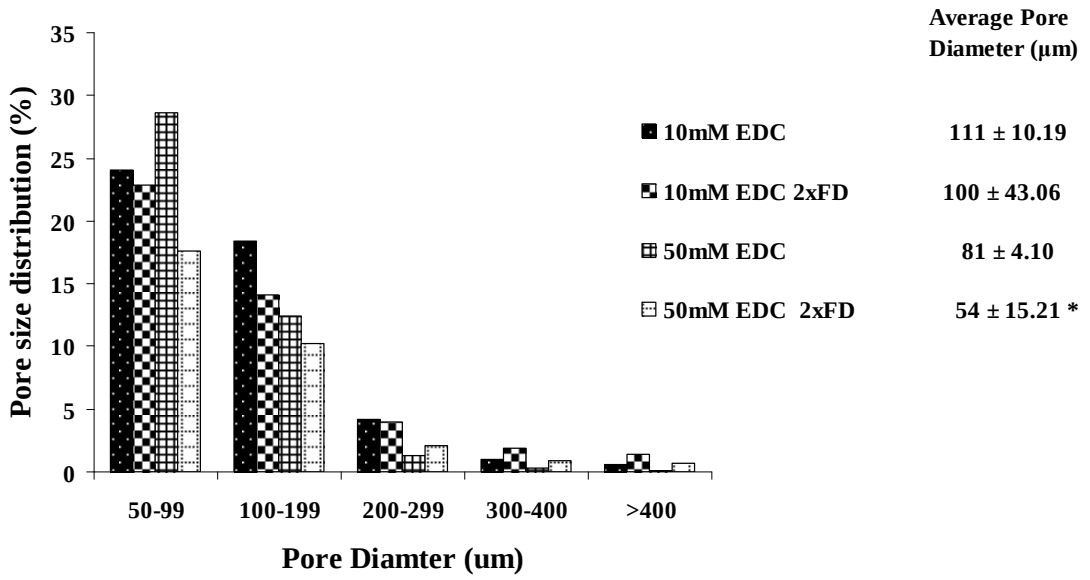



**Figure 3.7:** Pore size distribution graph of EDC cross linked collagen scaffolds at concentration 10mM & 50mM freeze dried once or twice measured with ImageJ. EDC cross linking through ethanol defrost and single freeze dried step did not affect pore size distribution. EDC: carbodiimide, DHT: dehydrothermal treatment

The more organized pore structure and slightly bigger pores during DHT could be attributed to the further dehydration which removes more water molecules causing overall shrinkage in sample size but increases the pore size. The results suggest that the changes in morphology of EDC crosslinked samples are due to the rehydration and refreezing process in the EDC cross linking treatment before freeze drying. Pore formation occurs as result of ice crystals formation during the freezing of the collagen suspension that is removed by freeze drying leaving a void that forms the pores. This additional refreezing can induce the collagen fibres to be combined again to form sheets, leading to the fusion of some smaller pores as well as possible secondary larger ice crystals formation that could affect original structure. Refreezing can also lead to the collapse of the scaffold which can oppose small pores fusion [55, 194].

Hence, the collapse effect is more prominent than the fusion resulting in overall smaller pores especially at higher EDC concentration. Furthermore, if the collapse is not homogenous can lead to longer pores and overall non-homogenous structure which is apparent in figure 3.5.

To sum up, as far as pore size and morphology is considered, DHT crosslinked samples deems to be more suitable for angiogenic cells ingrowth.

#### 3.3.1.3. The Microstructure of Channels

The channels could be easily viewed and the structure in between still porous and interconnected (Figure 3.8). Samples with 3 channels had an average channel size of approximately 2.02 ± 0.15mm and the average distance between channels measured at 3.52 ± 0.31mm whilst 9 channel samples had a smaller channel size of approximately 1.17 ± 0.14mm and the average distance between side channels measured at 2.39 ± 0.22mm and distance to central channel measured at 3.20 ± 0.52mm.

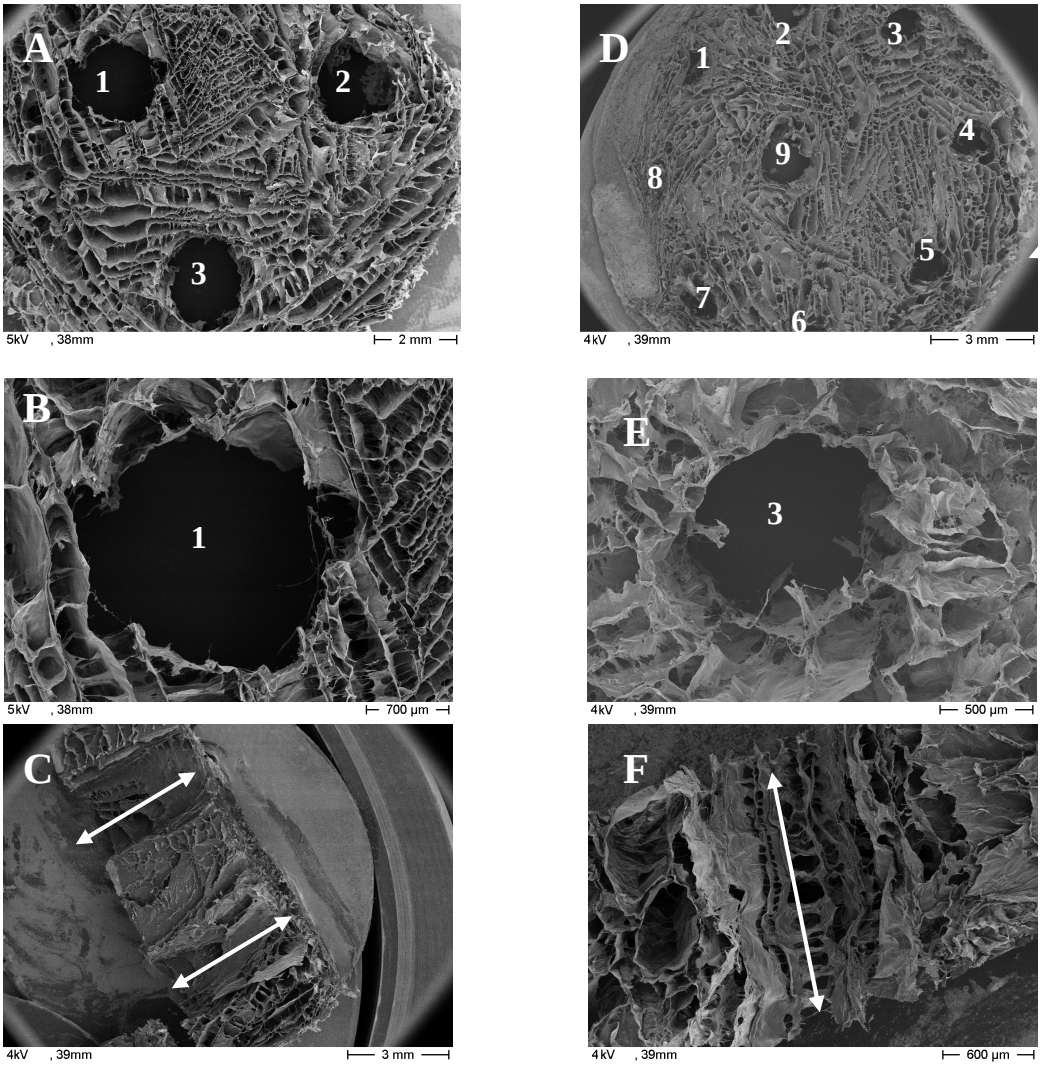



**Figure 3.8:** Scanning Electron micrographs illustrating cross-sectional view of collagen scaffolds. **A-** Sample with 3 channels, average channel diameter measured at 2.02 ± 0.15mm, average distance between channels measured at 3.52 ± 0.31mm. **B-** View of single channel in 3-channels sample. **C-** View of cross section through channels. **D-** Sample with 9 channels, average channel diameter measured at 1.17 ± 0.14mm, average distance between side channels measured at 2.39 ± 0.22mm and distance to central channel measured at 3.20 ± 0.52mm. **E-** View of single channel in 9-channels sample. **F-** View of cross section through one channel. ⟷ Along channel.

### 3.3.2. The Effect of Crosslinking on Thermal, Mechanical and Swelling Ratio Properties

The degree of crosslinking was calculated by determining both the denaturation temperature and the mechanical properties of scaffolds (Table 3.1). Formation of cross links in the EDC cross linked collagen matrices significantly increased the denaturation temperature ($T_d$) of the samples. The $T_d$ increased significantly ($p<0.05$) with increased cross linking from 61°C for non cross linked samples to 77, 89 and 91°C for 10mM, 33mM and 50mM EDC respectively. Similarly, EDC cross linking improved the mechanical properties of samples. The Young's modulus of dry samples increased from $2x10^3$ kPa for non cross linked samples to $4x10^3$ kPa for 10mM EDC samples and significantly ($p<0.05$) to $7x10^3$ kPa and $12x10^3$ kPa for 33mM and 50mM EDC respectively. As for wet samples, the non cross linked samples were too weak to test. As expected, the wet sate exhibited a much lower Young's modulus. Treating samples with EDC significantly ($p<0.05$) increased wet samples Young's modulus with increased concentration from $0.08x10^3$ kPa for 10mM EDC samples to $0.18x10^3$ kPa and $0.19x10^3$ kPa for 33mM and 50mM EDC respectively.

Treating the scaffolds with thermal cross linking reduced the denaturation temperature. This behaviour has been observed elsewhere [186, 195]. This drop was significant for samples treated for 5 days ($p<0.05$) where $T_d$ dropped to 54°C compared to 58°C and 56°C for 1 day and 3 days DHT respectively. While generally considered undesirable as it disrupts the native collagen conformation, denaturation may reduce the inflammation response and increase cellular infiltration *in vivo* [196].

However, DHT increased Young's modulus of dry samples to $4.60x10^3$ kPa, $3.15x10^3$ kPa and $5.46x10^3$ kPa for 1 day, 3 days and 5 days DHT respectively. In contrast to dry samples, the Young's modulus of wet samples increased significantly ($p<0.05$) by increasing days of treatment from $0.02x10^3$ kPa for 1 day DHT to $0.06x10^3$ kPa and $0.11x10^3$ kPa for 3 days and 5 days DHT respectively.

The swelling ratio decreased significantly after both types of cross linking treatments compared to non cross linked samples. The cross linking density was more pronounced in EDC treated samples where swelling ratio decreased from 5.34 for non cross linked samples to 3.15, 2.43 and 2.27 for 10mM, 33mM and 50mM EDC respectively compared to DHT where swelling ratio dropped to 4.22, 3.67 and 3.17 for 1 day, 3 days and 5 days DHT respectively. Increasing the cross linking density reduces the freedom of collagen chain movement. This increases the resistance to network expansion resulting in a decreased swelling ratio [197]. Both treatments decreased swelling ratio due to increased cross linking. The swelling ratio also suggests that the degree of cross linking was higher in EDC cross linked samples compared to DHT.

To conclude, EDC cross linking resulted in increased cross linking degree and density compared to DHT as confirmed by increased denaturation temperature, Young's modulus and swelling ratio.

| **Cross linking Method** | | **Non cross linked** | **DHT** | | | **EDC** | | |
|---|---|---|---|---|---|---|---|---|
| **Details** | | **Control** | **1 day DHT** | **3 days DHT** | **5 days DHT** | **10mM EDC** | **33mM EDC** | **50mM EDC** |
| **Denaturation temperature ($T_d$) ($^o$C) ± SD** | | 61.89 ± 1.21 | 58.26 ± 2.57 | 56.18 ± 0.21 | 54.42 ± 0.24* | 77.72 ± 1.26* | 89.16 ± 8.17* $^{\#}$ | 91.64 ± 7.18* $^{\#}$ |
| **Young's modulus ($E$) (x$10^3$ kPa) ± SD** | **Dry samples** | 2.32 ± 0.78 | 4.60 ± 0.83 | 3.15 ± 0.30 | 5.43 ± 2.25* | 4.30 ± 1.38 | 7.75 ± 0.48* $^{\#}$ | 12.5 ± 2.63* $^{\#}$ |
| | **Wet samples** | - | 0.02 ± 0.004 | 0.06 ± 0.02$^{+}$ | 0.11 ± 0.001$^{+}$ | 0.08 ± 0.005 | 0.18 ± 0.01$^{\#}$ | 0.19 ± 0.005$^{\#}$ |
| **Swelling ratio (Q) ± SD** | | 5.34 ± 0.21 | 4.22 ± 0.21$^{*}$ | 3.67 ± 0.16$^{* +}$ | 3.17 ± 0.22$^{* +}$ | 3.15 ± 0.10$^{*}$ | 2.43 ± 0.003$^{* \#}$ | 2.27 ± 0.33$^{* \#}$ |

**Table 3.1:** Denaturation temperature ($T_d$), Young's modulus ($E$) and Swelling ratio (Q) of collagen samples. EDC causes a significant improvement in $T_d$ and $E$. Though DHT improved $E$, it did cause a decrease in $T_d$. Both treatments reduced swelling ratio. * compared with non cross linked samples $p<0.05$. $^{+}$ compared to 1 day DHT $p<0.05$. $^{\#}$ compared to 10mM EDC samples $p<0.05$. EDC: carbodiimide, DHT: dehydrothermal treatment

### 3.3.3. The Effect of DHT on Collagen Tertiary Structure

FTIR was used to determine cross linking and denaturation of DHT treated collagen samples. Table 3.2 demonstrates that all samples showed the characteristic peaks of collagen (Amide A, B, I, II and III). It summarises the observed band frequencies and their associated molecular vibrations taken from the literature [192, 198]. Amide A indicates N-H stretching along the tropocollagen. Amide I refers to the stretching vibrations of peptide carbonyl group (C=O bond) and provides information on the hydrogen bonding state of the triple helix of collagen. The Amide II and III peaks correspond to vibration modes of C-N bond which is the backbone of amino acid sequence. The amide II bands (1553 $cm^{-1}$) arise from the N–H bending vibrations coupled to C–N stretching vibrations. [199]. The presence of these bands in IR spectrum confirms that the primary structure of collagen has not been modified. All structural changes that occurred during processing of collagen affected a higher level of collagen structure. Since the amide II band absorbance peak at 1553 $cm^{-1}$ is proportional to the amount of $NH_2$, it could be analyzed to show formation of cross links through DHT. As the $NH_2$ is converted to NH during cross linking formation through condensation reaction [188], a decrease in the absorbance at 1553 $cm^{-1}$ corresponds to an increase in cross linking [200]. The absorbance ratio of amide II when normalised to $CH_3$ (which is unaffected by the formation of cross links or denaturation) (Table 3.3) significantly decreased with DHT treatment from 1.99 ± 0.22 for non cross linked sample to 1.37 ± 0.05 for DHT treated collagen samples meaning increased cross linking in the DHT treated scaffolds which agrees with swelling ratio and Young's modulus results.

All samples had more or less the same amide A peak (~3226 $cm^{-1}$) which suggests no significant triple helix degradation which is in agreement with the similar internal amide I absorbance ratios (Table 3.2). The internal amide I absorbance ratio has been used to qualitatively compare the amount of intact triple helix within a collagen sample [201]. As well, there was no considerable shift in Amide I peak (Table 3.2). The higher wavenumber of amide B for non cross linked samples (2959 $cm^{-1}$) compared to DHT treated samples (2934 $cm^{-1}$) could be explained by the fact that a change in the C-H stretching occurred around collagen molecules after processing. The hydrogen bonds formed between side chains stabilise the secondary structure of alpha helices and tertiary structure of tropocollagen. Thus, in according to the shift of Amide B peaks occurring after processing, conformation of the collagen triple helix changes and tend to shift toward that of gelatine (Amide B: 2925$cm^{-1}$) because of dehydration process (increase in temperature in DHT). There were no significant shifts to be reported for amide II and III. It is clear from table 3.3 that there was a significant decrease in Amide A and Amide II bands intensity ($A_{A/CH3}$ and $A_{II/CH3}$) between non cross linked samples and DHT treated scaffolds. This could be explained by the fact that DHT reinforces collagen by creation of intermolecular cross links (between COOH groups of an acidic residue and $NH_2$ groups of a basic residue from neighbouring chain), which could lead to some denaturation as result of chain fragmentation and bond cleavages [202].

| Peak Assignment | Wavenumber ($cm^{-1}$) | |
|---|---|---|
| | **Collagen scaffolds 1%, 3 days DHT** | **Collagen scaffold 1% non-crosslinked** |
| **N-H stretch (amide A)** | 3326 | 3327 |
| **C-H stretch *asymmetrical* (Amide B)** | 2934 | 2959 |
| **C-H stretch *symmetrical*** | 2958 | - |
| **C=O stretch coupled with H boning (amide I)** | 1643-1659 | 1647-1659 |
| **C=O stretch coupled with N-H bending (amide II)** | 1549 | 1553 |
| **$CH_3$ bending *asymmetrical*** | 1452 | 1455 |
| **C-N stretch plus N-H in-plane deformation (amide III)** | 1239 | 1240 |
| **C-C stretch** | 1082 | 1082 |

**Table 3.2**: Observed band frequencies from IR spectra of collagen samples and their associated molecular vibrations. The assignment of band frequencies to particular bands is decided by using reference tables from literature [192, 198].

| Sample specification | Amide A ($cm^{-1}$) | Absorbance ratio | | | |
|---|---|---|---|---|---|
| | | $A_{1659/1643}$ | $A_{A/CH3}$ | $A_{I/CH3}$ | $A_{II/CH3}$ |
| **Collagen scaffolds 1% , 3 days DHT** | 3326 | 1.08 ± 0.01 | 1.3 ± 0.05 * | 1.68 ± 0.11 * | 1.37 ± 0.05 * |
| **Collagen 1% , non-crosslinked** | 3327 | 1.16 ± 0.08 | 1.75 ± 0.19 | 2.52 ± 0.48 | 1.99 ± 0.22 |

**Table 3.3**: IR characteristics of processing on collagen with freeze drying and DHT comparing to non-crosslinked samples. $A_{1659/1643}$ is the internal amide I absorbance ratio; $A_A$, $A_I$, $A_{II}$ and $A_{CH3}$ are the absorbance intensity of the amide A, amide I, amide II and $CH_3$ bands respectively. * Statistically significant compared to control sample, $p < 0.05$. DHT: dehydrothermal treatment.

## 3.4. CONCLUSION

Collagen scaffolds made of 1% collagen suspension, frozen at -20°C during freeze drying process exhibited a mean pore size and pore size distribution suitable for migration and growth of vascular cells used in this study as well *in vivo* angiogenesis. While EDC increased the scaffold's thermal and mechanical properties, reducing swelling ratio and pore size, DHT increased the mechanical properties and pore size but decreased the denaturation temperature and swelling ratio. DHT samples had a more suitable pore size for endothelial cells and smooth muscle cells ingrowth. The optimal DHT treatment was 3 days DHT as 5 days DHT significantly reduced denaturation temperature. From FTIR analysis, although 3 days DHT treatment reduced denaturation temperature, the overall structure of collagen still in tact. Thus, collagen scaffolds made of 1% collagen, frozen at -20C and cross linked with 3 days DHT will be used to assess cellular ingrowth and vascularisation. Using pins to introduce channels was successful as they preserved their structure and shape after processing. The effect of channels on cellular ingrowths and vascularisation will be investigated in the following chapters.

# CHAPTER 4: ANGIOGENIC CELLS GROWTH ON COLLAGEN SCAFFOLDS *IN VITRO*

## 4.1. INTRODUCTION

Seeding endothelial cells onto polyglycolide polymer scaffolds increased the density of blood vessels at two weeks [203], however, there remains a critical size of scaffold beyond which cells have difficulty in surviving due to poor nutrient diffusion. Artificial vascular systems with inbuilt channels have been developed to overcome this problem [27] and these have improved cellular penetration deep within a scaffold [28]. The microchannels favour an increase in the mass transport of nutrients and oxygen, as well as removal of waste products, throughout the scaffold [27]. Channelled collagen scaffolds have been successfully used in chondrogenesis using bone marrow derived stem cells resulting in good matrix synthesis within the channels and not in the periphery [28, 150].

Is this study, it has been hypothesised that adding channels into porous collagen scaffolds would increase the vascular cells penetration and survival deeper into scaffolds. In vessel formation, both endothelial cells and pericytes are essential for the formation of stable vessels, [10] [11, 12] [14] and co-seeding scaffolds with endothelial cells and smooth muscle cells can enhance assembly of EC into micro vessel like structure [159]. Hence, these cells were assessed in isolation and in combination *in vitro* before assessment of angiogenic cell penetration was carried out *in vivo.*

## 4.2. MATERIALS AND METHODS

### 4.2.1. Cell Culture and Seeding on Scaffolds

Human aorta, vascular smooth muscle cells (HA-VSMC) and human umbilical cord vascular endothelial cells (HUV-EC-C) (LGC Promochem, Middlesex, UK) were kept in liquid nitrogen before thawing in 37°C water bath. They were added to warm full medium, centrifuged to remove frozen media. HA-VSMC cell line was seeded in warm HAM's F12 medium (Lonza Wokingham Ltd, Berkshire, UK) containing 10% fetal bovine serum (FBS) ( Biosera, East Sussex, UK), supplement with insulin, transferring and selenium (ITS) (Lonza Wokingham Ltd, Berkshire, UK), 0.03 mg/ml endothelial cell growth supplement (ECGS) (BD Biosciences, MA, USA), 0.05 mg ascorbic acid, 10 mM Hepes. HUV-EC-C cell line was seeded in HAM's F12 medium containing 10% FBS supplement with 0.03 mg/ml ECGS, 0.1 mg/ml heparin (Sigma-Aldrich). All culture media also contained penicillin (100U/ml) and streptomycin (100 μg/ml) (Lonza, Belgium). Cells were cultured at 37°C in a humidified incubator gassed with 5% $CO_2$ in air.

Initially the scaffolds were prepared for culture; each scaffold type was cut into 0.5-0.6cm slices, washed in 70% ethanol and sonicated for 30mintues. Then, they were washed 3 times in 0.1M Phosphate buffered Saline (PBS) (BioWhittaker, Lonza) for 30 minutes. Finally they were placed in serum free medium at 4°C at least overnight before seeding with cells and kept there till seeding.

After cells were amplified to a sufficient numbers, cells were seeded on scaffolds at $1\times10^5$ cells/well ($5\times10^4$ cells/cm$^2$) for HUV-EC-C and $1\times10^5$ cells/well for HA-

VSMC in 0.5 ml to each well of 24 well tissue culture plates (Greiner Bio-One Ltd, Gloustershire, UK). For co-culture of two types of cells, $0.5\times10^5$ cells/well HUV-EC-C and $0.5\times10^5$ cells/well HA-VSMC were seeded. After cells were settle on the surface of scaffolds in 2 hours, 3 ml of full medium were top up. The Media were replaced every two to three days.

Initially, the scaffolds used for angiogenic cell seeding were made of 1% and 0.5% collagen, frozen at -20°C, and cross linked with 3 days DHT either plain or 3 channelled were investigated and experiment conducted only once an had triplicate of samples. Then, scaffolds made of 1% collagen, frozen at -20°C, and cros slinked with 3 days DHT, plain, 3 channelled and 9 channelled scaffolds were investigated and experiment repeated 3 times, each experiment had triplicate of samples. Those scaffolds were made as explained in chapter 3.

### 4.2.2. Assessment of Cellular Viability

To determine the cells viability and localisation in respect to the channels, live/dead staining and DAPI staining were performed.

For live/dead staining, Live/Dead Viability/Cytotoxicity Kit (Invitrogen, USA) was used. This fluorescent kit contains two fluorescent dyes: calcein AM to stain living cells green and ethidium homodimer-1 (EthD-1) to stain damaged dead cells red. Scaffolds seeded with cells were firstly washed with PBS twice to remove medium, and stained using 0.1% (v/v) calcien and 0.1% (v/v) Ethd-1 (final concentration) in PBS for 30 minutes at 37°C in an incubator. Then, cells were observed without

fixation on surface and cross section of scaffolds under fluorescence microscopy (Axio, Zeiss, Germany).

For DAPI staining, scaffolds cultured with endothelial cells were cut into sections and stained with 4',6-diamidino-2-phenylindole (DAPI) which stains the nucleus blue and viewed under UV light (Axio, Zeiss, Germany). Briefly, sections were first fixed in 4% paraformalaldehyde in PBS for 5 minutes then soaked in 1% Triton X-100 solution for 5 minutes. After that, sections were washed in PBS twice, each time for 2 minutes, stained with DAPI (1:500 in PBS) for 5 minutes in a dark room and washed twice in PBS before viewing under microscope.

### 4.2.3. Assessment of Cellular Attachment and Proliferation

The Alamar Blue$^{TM}$ assay (Biosourse Europe, Nivelles, Belgium) was used to quantify the number of cells at day 1 and 7 according to manufacturer's protocol. Briefly, scaffolds were transferred to new well plate and incubated in 0.5ml of 5% Alamar blue medium solution for 2 hours at 37°C and 5% $CO_2$ at 100% humidity. Then, 400 µl of Alamar blue supernatant was moved to a new plate for analysis and fresh medium was added to scaffolds and put back in incubator. The relative fluorescent units of cell-degraded Alamar blue was measured on a SPECTRAmax GEMINI microplate spectrofluorimeter (Molecular Devices, Berks, UK) at an excitation wavelength of 530 nm and an emission wavelength 590 nm, with a cut-off at 570 nm and converted to cell number based on the standard curve. A standard curve

was produced by sequential dilution of 2:1 of the same cells. The standard curve correlates Relative Fluorescent Unit (RFU) to cell number.

To assess cellular attachment efficacy at day 1, the scaffolds were transferred to empty wells and both the scaffolds and culture wells were assessed by Alamar Blue™ separately. The attachment ratio was calculated as shown in equation (3).

$$\text{Attachment ratio} = \frac{\text{Number of cells on scaffold}}{\text{Number of cells on scaffold + Number of cells on Plates}} \times 100\% \qquad (3)$$

### 4.2.4. Statistics

Results are expressed as mean ± standard of error. One-way analysis of variance (ANOVA) followed by LSD's post hoc test was used where stated with significance set at $p<0.05$. All statistical analyses were performed on SPSS 13.0.

## 4.3. RESULTS

The pore size in collagen can dramatically affect cell behaviour encouraging cell migration and penetration into the scaffold [49]. Initially scaffolds made of different collagen content and thus different pore size were investigated to define optimal pore size for culturing angiogenic cells. Collagen scaffolds made of 0.5% and 1% collagen had an average pore size of 130 and 230 μm (Chapter 3, Figure 3.3). Figure 4.1 shows that 0.5% scaffolds had a significant higher RFU value than 1% scaffolds on day 1 for all types of culture (HUV-EC-C, no channel, 5588 ± 477 vs., 2907 ± 408 and 3x channels, 6146 ± 281 vs. 4155 ± 457, HAV-SMC no channel, 13437 ± 327 vs., 7627

± 851 and 3x channels, 11651 ± 890 vs. 9522 ± 485, and co-culture no channel, 7914 ± 1354 vs. 5162 ± 495 and 3x channels, 8902 ± 933 vs. 6419 ± 442). However, on day 7, there was no difference between 1% and 0.5% scaffolds on all types of culture. Unfortunately, the data from day 3 and day 7 could not be compared as the scaffolds were not transferred to new wells before doing Alamar Blue® on day 3. Thus numbers on day 3 are reflective of cells attached to scaffolds and cells attached to plate wells.

The live/dead staining of scaffolds made of 1% or 0.5% with and without channels showed majority of cells were viable on all scaffolds (Figure 4.2). In conclusion, all scaffolds supported the growth of three types of culture to similar extent and 0.5% collagen scaffolds with higher pore size did not offer any better cellular proliferation; however, the 0.5% collagen scaffold were mechanically weak and difficult to handle. This agrees with literature when pore size increases, mechanical properties lower. Lower collagen content result in less dense scaffolds with reduced stiffness [150, 193]. Thus, we concluded that 1% collagen scaffolds with average pore size of 130μm were more suitable for our study which correlates well with other published literature [204].

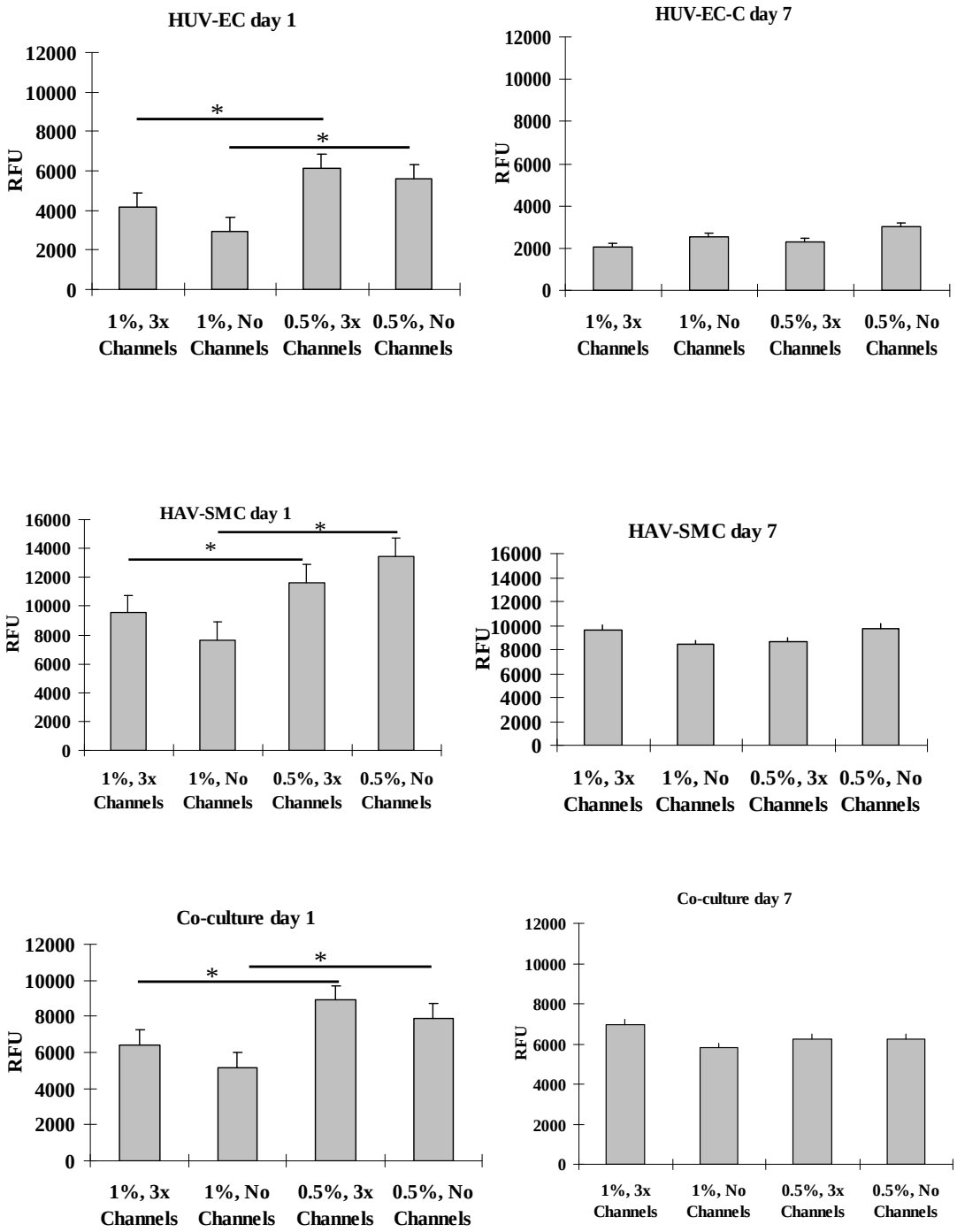



**Figure 4.1**: Assessment of Cell proliferation on scaffolds made of different collagen concentrations over time using Alamar Blue assays. RFU: Relative Fluorescence Unit. * Statistically significant, $p < 0.05$. All scaffolds supported the growth of three types of culture to similar extent. HUV-EC: endothelial cells. HAV.SMC: smooth muscle cells.

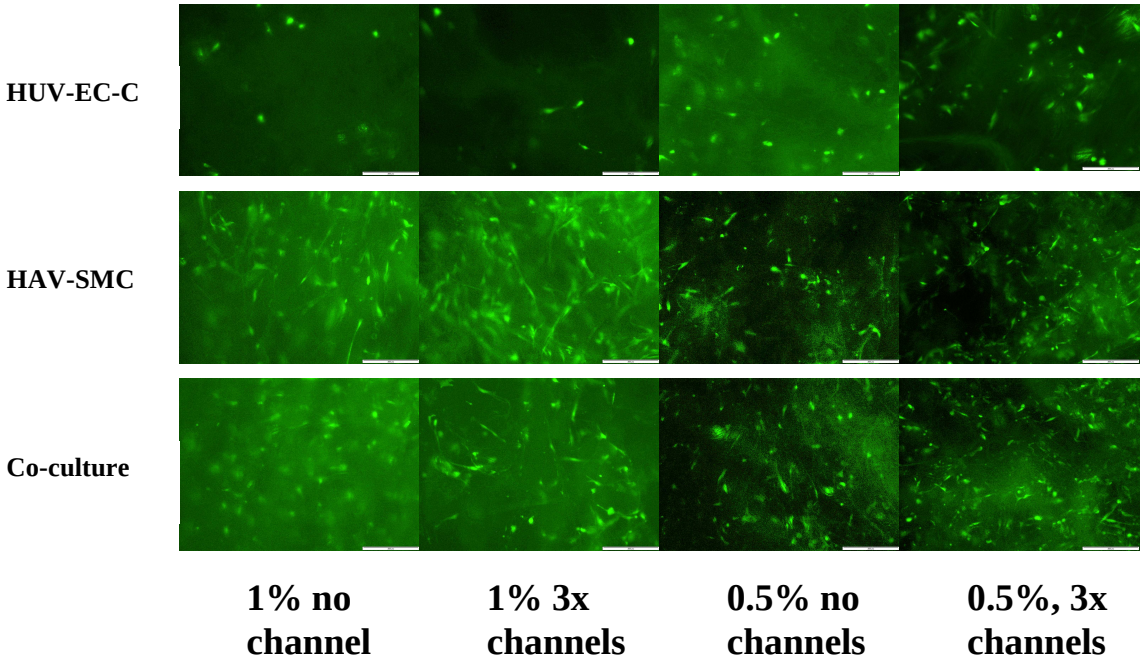



**Figure 4.2:** Live/Dead Staining of scaffolds made of 1% and 0.5% collagen, with and without channels. Scale bar = 200μm HUV-EC: endothelial cells. HAV.SMC: smooth muscle cells.

As a result, more channels were introduced in scaffolds made of 1% collagen and investigated whether the channels would offer a better angiogenic cells attachment and proliferation. HUV-EC-C, HAV-SMC and co-culture cells all attached to and proliferated on all scaffold over 7 days (Figure 4.3). There was more HUV-EC-C (attachment ratio 45%, 49% and 56% for no channels, 3 channels and 9 channels respectively) and co-culture (attachment ratio 34%, 56% and 59% for no channels, 3 channels and 9 channels respectively) cellular attachment to scaffolds compared to HAV-SMC-C (attachment ratio 26%, 24% and 35% for no channels, 3 channels and 9 channels respectively) (Figure 4.3-A). Addition of channels improved cellular attachment as compared to scaffolds without channels, however, only significantly in co-culture seeded scaffolds [0 channel (34%) < 3 channels (56%) < 9 channels (59%), $p<0.05$]. For all samples, HUV-EC-C had a significantly higher attachment ratio of

45% (0 channel), 49% (3 channels), and 56% (9 channels) ($p$<0.05) than HA-VSMC [26% (0 channel), 24% (3 channels) and 35% (9 channels) ($p$<0.05)]. There was no significant difference between HUV-EC-C and co-culture cells attachment ratios, however, there was a significant higher attachment of co-culture cells to 3 and 9 channels scaffolds (56 and 59 % ($p$<0.05) respectively) compared to HA-VSMC (24% and 39% ($p$<0.05) respectively). Co-culture 9 channels seeded scaffolds had the highest attachment ratio of 59%.

At day 1, there was no significant difference in cell number between different scaffolds or different cell cultures (Figure 4.3-B). From day 1 to day 7, HUV-EC-C (47982 ± 5253 vs. 101830 ± 3326 , 40931 ± 5202 vs. 95401 ± 7330, 47873 ± 4058 vs.107218 ± 6443 cells/scaffold for no channels, 3 channels and 9 channels respectively), HA-VSMC (42609 ± 7400 vs. 133392 ± 8678, 27971 ± 3207 vs. 109693 ± 12765 , 38922 ± 6482 vs.145310 ± 15559 cells/scaffold for no channels, 3 channels and 9 channels respectively) and co-culture cells (23133 ± 6392 vs. 68417 ± 10544, 33632 ± 8328 vs. 92899 ± 18455, 31629 ± 5475 vs.74410 ± 12653 cells/scaffold for no channels, 3 channels and 9 channels respectively) proliferated on all samples significantly ($p$<0.05). At day 7, for HUV-EC-C, there was no significant difference in cell number between scaffolds with and without channels (101830± 3326 vs. 95401 ± 7330 vs. 107218 ± 6443 for no channels, 3 channels and 9 channels respectively). However for HA-VSMC and co-culture cells, there was significant difference between scaffolds with and without channels. For HA-VSMC, scaffolds with 9 channels (145310 ± 15559 cells/scaffold, $p$<0.05) had a significantly higher cell number than 3 channels scaffolds (109693 ± 12765 cells, $p$<0.05). For co-culture cells, scaffolds with 3 channels (92899 ± 18455 cells/scaffold, $p$<0.05) had a

significantly higher cell number than scaffolds without channels (68417 ± 10544 cells/scaffold, $p<0.05$). For 9 channels scaffolds, HA-VSMC had a significantly higher cell number (145310 ± 15559 cells/scaffold, $p<0.05$) than HUV-EC-C (107218 ± 6443 cells/scaffold, $p<0.05$) which in turn higher than co-culture cell number (74410 ± 12653 cells/scaffolds, $p<0.05$). Similar trend was seen for scaffolds without channels (133392 ± 8678 HA-VSMC, 101830 ± 3326 HUV-EC-C and 68417 ± 10544 co-culture cells/scaffold, $p<0.05$), however, there was no significant difference for 3 channels samples.

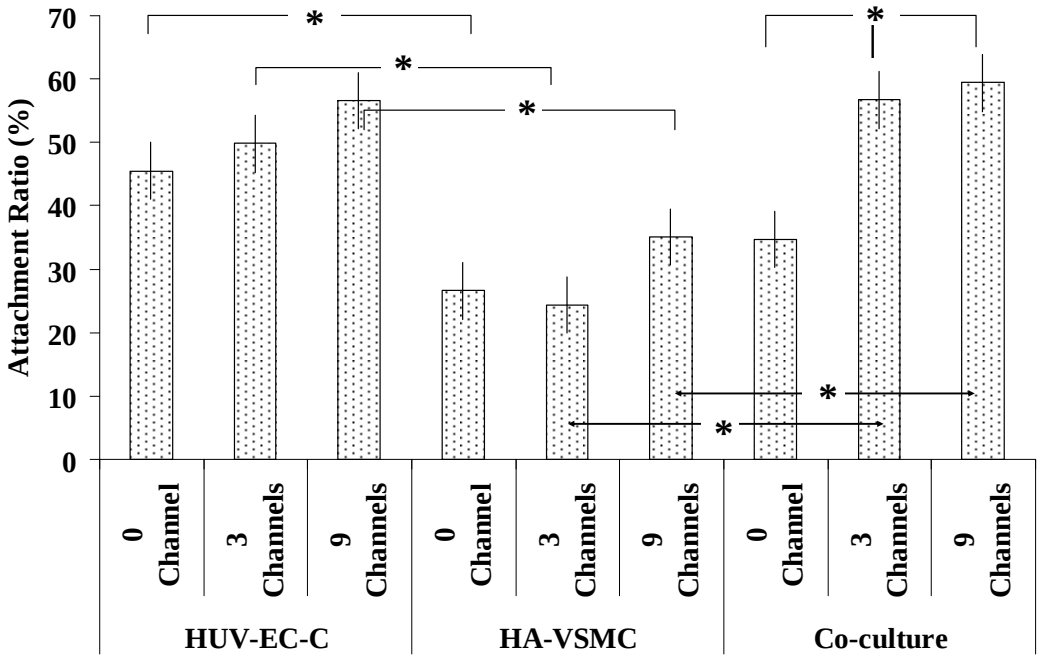



**Figure 4.3-A:** Attachment ratio of HUV-EC-C (endothelial cells), HA-VSMC (smooth muscle cells) and co-culture cells on collagen scaffolds at day 1 after 24 hours incubation examined by Alamar Blue™ Assay. HUV-EC-C and co-culture had higher attachment ratio to scaffolds. Addition of channels improved cellular attachment as compared to scaffolds without channels. Co-culture 9 channels seeded scaffolds had the highest attachment ratio. * Significant difference, $p<0.05$.

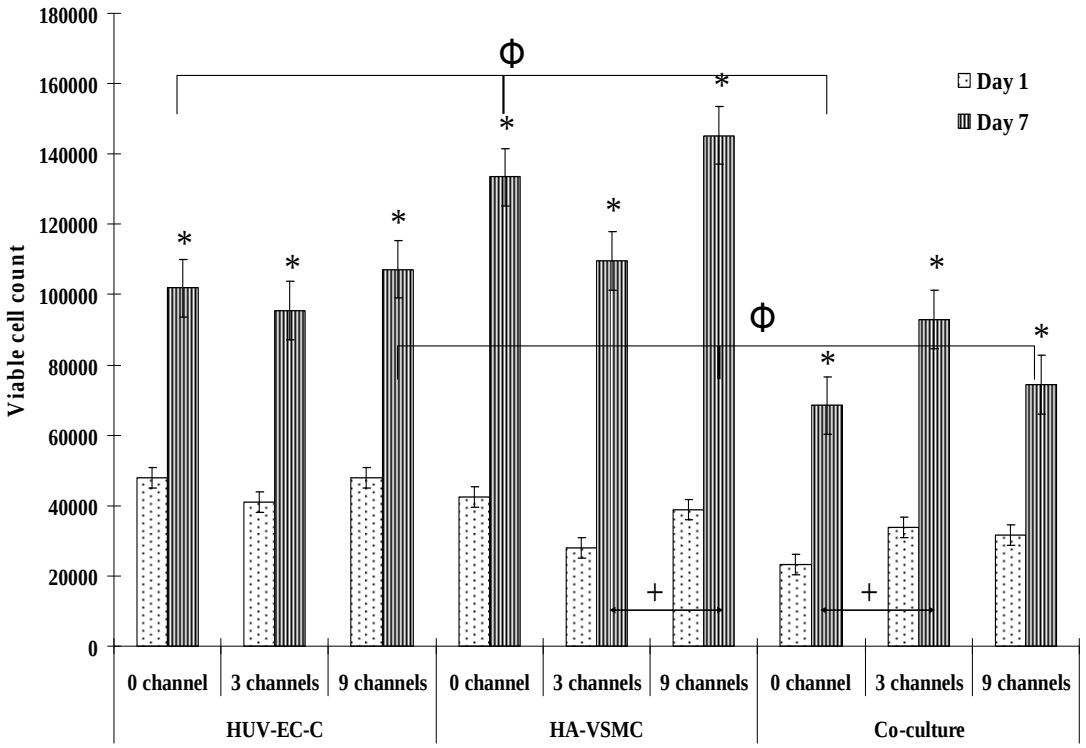
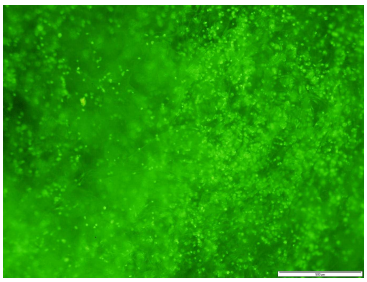


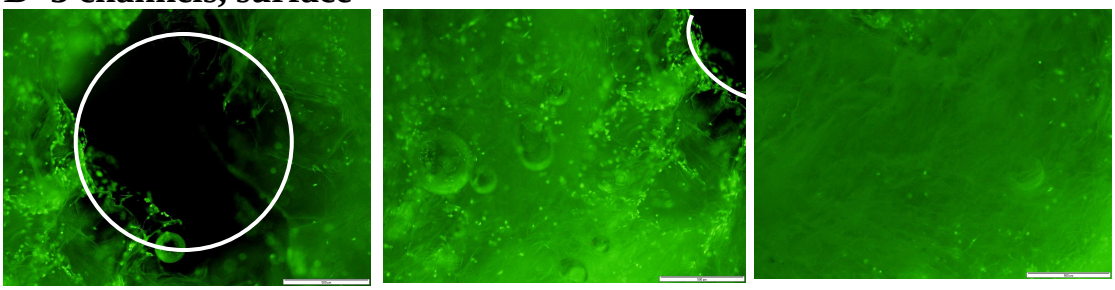

**Figure 4.3-B** Proliferation of HUV-EC-C (endothelial cells), HA-VSMC (smooth muscle cells) and co-culture cells on collagen scaffolds from day 1 to day 7. At day 1, no significant difference in cell number between different scaffolds or different cell cultures. From day 1 to day 7, different cell cultures proliferated significantly on all scaffolds. At day 7, there was significant difference in cell number between scaffolds with and without channels for HA-VSMC and co-culture cells but not for HUV-EC-C. 9 and 0 channels, but not 3 channels scaffolds, had higher cell number of HA-VSMC than HUV-EC-C which is turn higher than co-culture cells. * compared with same type of scaffolds and cell culture at day 1. Φ comparison of same scaffold type seeded with different cells. + comparison between different scaffolds seeded with same type of cells. $p<0.05$

Live/Dead staining images (Figure 4.4 & 4.5). For all three types of culture, the cells reside mainly around the channels (Figure 4.4-B & D and Figure 4.5-B, C & D) and migrate along the channels (Figure 4.4-C). In the sample with 3 channels, the area between two channels seemed to be less invaded with cells (Figure 4.4- B3 & C3 and Figure 4.5-B3 & C3) compared with samples with 9 channels (Figure 4.4-D3 and Figure 4.5-D1) where more cells were seen in the area between channels. This could be explained by the fact that smaller and more channels makes channels in close proximity and thus cells will be distributed all over the scaffold as they seek to get to close to the channel. Similarly, DAPI images (Figure 4.6) demonstrate that in absence of channels (Figure 4.6-A), the HUV-EC cells are distributed sparingly as single cells. However, in presence of channel (Figure 4.6-B&C), the cells form a bright cell galaxy along the channel with fewer cells in the area far from channel.

**A- No channel**

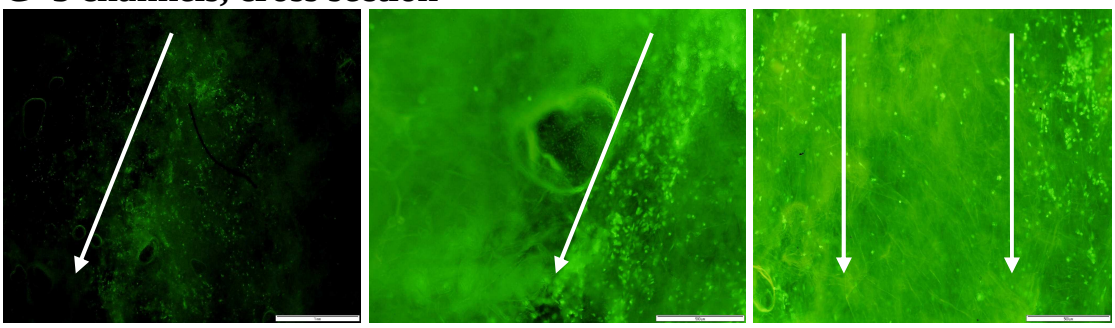


**B- 3 channels, surface**



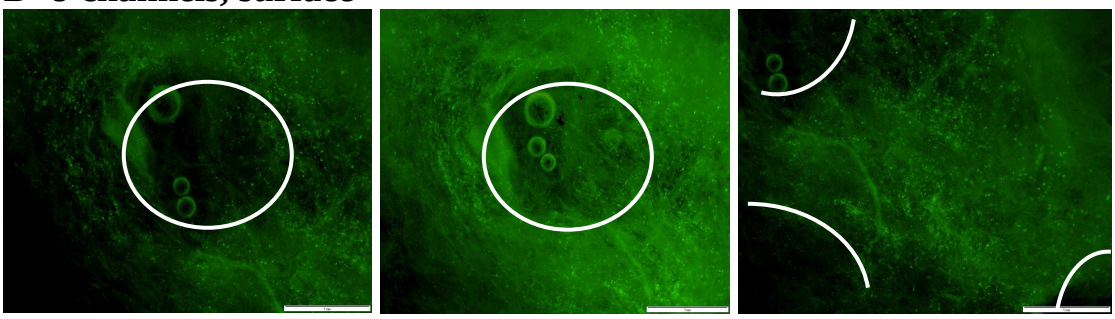
**B-1 View of channel** **B-2 Area close to channel** **B-3 Area far from channel**

**C- 3 channels, cross section**



**C-1 Along channel** **C-2 Along channel** **C-3 Between 2 channels**

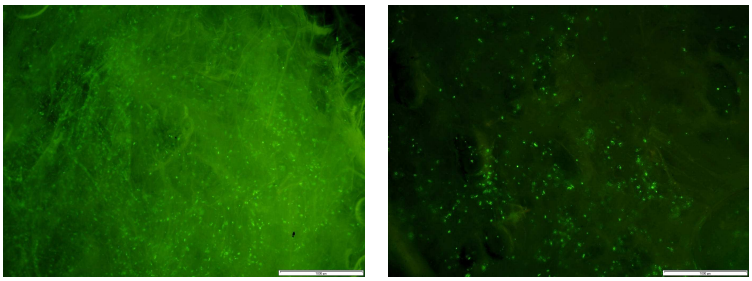
**D- 9 channels, surface**



**D-1 View of channel** **D-2 View of channel 2** **D-3 Area between 3 channels**

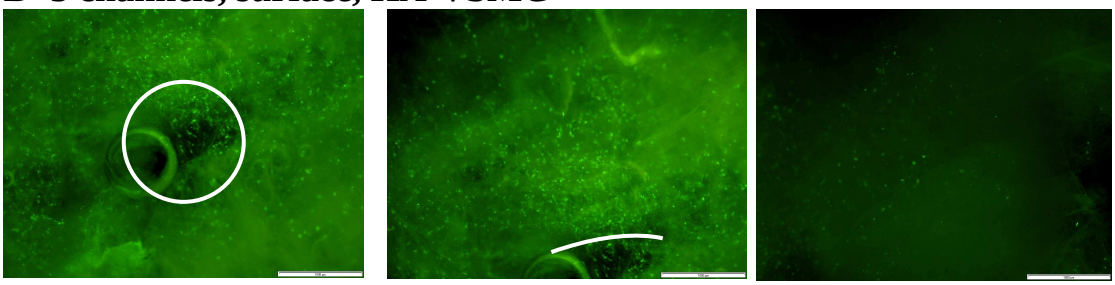
**Figure 4.4:** Live/Dead staining of HUV-EC-C (endothelial cells) seeded scaffolds (green colour for live cells). The cells reside mainly around the channels and migrate along the channels. For 9 channels scaffolds, there are more cells between channels compared to 3 channels ones due to smaller distance between channels (B3 vs. D3). Scale bar= 500µm for A, B, C-2 and C-3 and =1mm for C-1, D.

**A- No channel**



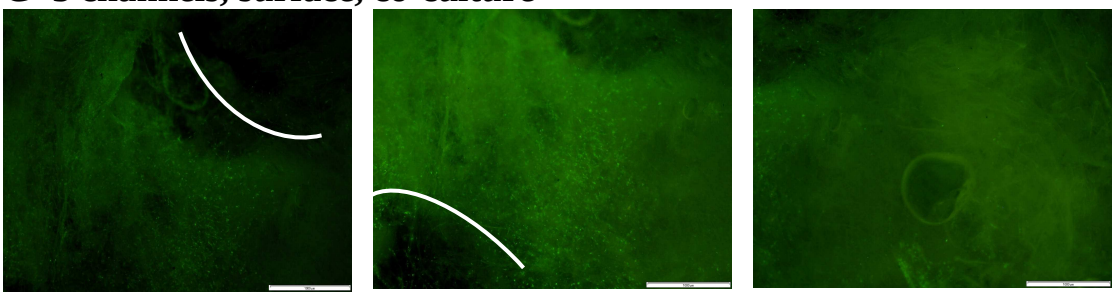
**A-1 surface- HA-VSMC** **A-2 surface- Co-culture**

**B- 3 channels, surface, HA-VSMC**



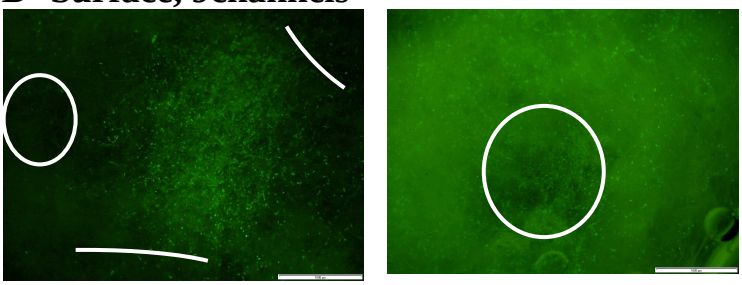
**B-1 View of channel** **B-2 Area close to channel** **B-3 Area far from channel**

**C- 3 channels, surface, co-culture**



**C-1 View of channel** **C-2 Area close/between Channel** **C-3 Area far from channel**

**D- Surface, 9channels**



**D-1 HA-SMC, area between Channels** **D-2 co-culture, view of channel**

**Figure 4.5:** Live/Dead staining of HA-VSMC (smooth muscle cells) and co-culture seeded scaffolds (green colour for live cells). The cells reside mainly around the channels. For 9 channels scaffolds, there are more cells between channels compared to 3 channels ones due to smaller distance between channels (B3 vs. D1 for HA-VSMC). Scale bar =1mm

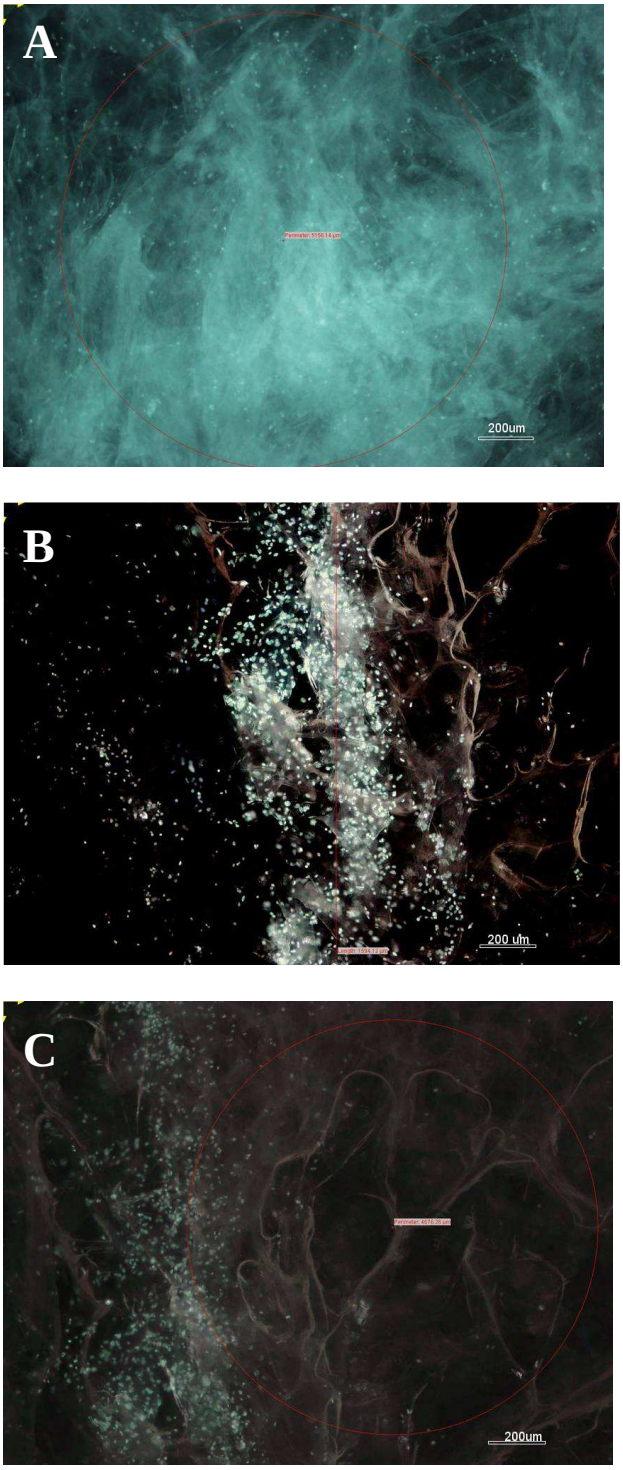



**Figure 4.6:** DAPI staining of HUV-EC-C (endothelial cells) seeded collagen scaffolds *in vitro*. **A-** Scaffold with no channels. **B-** Sample with 3 channels, view of cross section through 1 channel. **C-** Sample with 3 channels, view area far from channel. The cells appear as bright galaxy along the channel with fewer cells far away from channel.

## 4.4. DISCUSSION AND CONCLUSION

Channels were developed in a porous 3-D collagen scaffolds and used to promote rapid ingress of angiogenic cells. Initial studies conducted *in vitro* demonstrated that the scaffolds supported the angiogenic cells in growth in culture and the channels improved the depth of penetration of cells into the scaffold. The cells reside mainly around the channels and migrate along the channels as shown by galaxy images and cell number suggesting an advantage for channels.

These initial experiments were conducted to ascertain the optimum scaffold composition. The pore size of the scaffold relates to angiogenesis; a diameter of 250 to 300µm was most effective for new vessel ingrowth using poly (ether ester) block-copolymer scaffolds [205]. Using collagen scaffolds, a pore size ranging from 50 to 200µm is suitable for endothelial and smooth muscle cells infiltration *in vitro* and *in vivo* and angiogenesis [17, 162, 179-181] [204], which is consistent with our samples. We investigated the effect of pore size on angiogenic cells proliferation *in vitro*. 1% and 0.5% collagen scaffolds with average pore size of 130 and 230µm were tested. 0.5% collagen scaffolds with higher pore size did not offer any better cellular proliferation. Although the initial experiments appear to show that there was overall better attachment on day 1 in the 0.5% group, this advantage was not transferred to day 7 where there was no difference between the groups (figure 4.1). Though no mechanical testing was done on 0.5% collagen scaffold, it is well documented in literature that increased pore size affect scaffold structural integrity lowering its mechanical properties. Lower collagen content result in less dense scaffolds with

reduced stiffness [150, 193]. These could possibly explain why 0.5% collagen scaffolds did not have better cellular growth on it after 7 days though they had bigger pore size. There was no increase in proliferation of the scaffolds with channels in these initial experiments on 0.5% collagen scaffolds, possibly due to increased dead cells on the 0.5% scaffolds. The pore size needs to be optimal for cell growth as bigger pore size provides less room for cells to make contact and proliferate. In addition, weak mechanical strength created by bigger pore size could potentially be worsened by the void created with channels. In 1% collagen scaffolds, though not significant, there was a slight increase in proliferation in presence of channels. Thus, we concluded that 1% collagen scaffolds with average pore size of 130μm were more suitable for our study which correlates well with other published literature [204].

Improved cell penetration has previously been noted in agarose hydrogel scaffolds seeded with NIH-3T3 with microfluidic channels. The cell viability decreased with increasing distance from the channels and NIH-3T3 cells viability was maximised closer to the microfluidic channels with the depletion of nutrients across the hydrogel diminishing with increased distance from the channels [206]. Furthermore, the incorporation of channels in collagen scaffolds using solid free form fabrication improved penetration of higher number of human bone marrow derived mesenchymal stem cells (HBMSCs) towards the centre of scaffolds resulting in better chondrogenesis [28]. In our study, the channels did confer an advantage for angiogenic cells attachment with increased channel number (figure 4.3). There was less attachment of smooth muscle cells compared to endothelial cell. This could be explained by the different mechanism of attachment to collagen surface. However, the proliferation is important. On of the most important finding is that cells proliferated in

all groups on the scaffolds. Cell count in this experiment reflects the actual cell number attached to scaffold compared to RFU values in the initial experiment where it relies only on the metabolic activity of cells. It should be taken into consideration that metabolic activity of cells could be different at different passages and cultures. Thus, using a standard curve to count cells is more reliable that RFU values. This could be the reason no difference in proliferation in presence of channels was seen in the initial experiment

It has not been previously reported that angiogenic cells attach and proliferate greatly on 5cm thick collagen scaffolds. Although, from figure 4.2, the channels might have not greatly contributed to proliferation of cells, however, from figure 4.3 and 4.4, they encouraged cells to migrate down in the scaffolds. This greatly improves cell survival as with time, if cells proliferate greatly only on surface, they will suffer diffusion constraint and cells will die.

If tissue engineering is to develop beyond the incorporation of cellular scaffolds to the incorporation of scaffolds containing task specific cells to perform specific functions, rapid vascularisation is essential. As cells migrate deep into foam scaffolds and proliferate, diffusion of nutrients and oxygen is limited to only a few hundred micrometres from the scaffold's periphery [144]. *In vivo,* cells require a constant supply of nutrients and oxygen from the capillaries nearby. Thus, in order to keep cells alive in a tissue engineered construct, the scaffold needs to be invaded by vascular network. Therefore, creating internal channels to permit the flow of nutrient-rich medium throughout the scaffold is one strategy proposed for maintaining cell survival deep within the scaffold [206-208]. The channelled scaffolds support the

growth and migration of angiogenic channels as shown in our study, which could in turn help to speed up the rate of vascular tubule formation. This could be used in one of two ways either allowing for establishing pre existing vascular networks within scaffolds or for the incorporation of task specific cells within the construct. Thus, this study delineates the potential of using channelled scaffolds to promote capillary network formation *in vitro* in a 3-D collagen scaffold. Furthermore, the channels offer the possibility of rapid blood vessels infiltration into material from host anastomosing with a preformed network which is investigated in the next chapter. A cellularized tissue engineered scaffold could have a host of clinical applications including rapidly vascularised constructs for use for cutaneous resurfacing as well as incorporation of task specific cells for bone engineering.

Another strategy to promote angiogenesis in engineered tissues is the delivery of pro angiogenic factors with cell-polymer construct. However, this strategy has been of limited use as these molecules are inactivated *in vivo* leading to reduced effective concentration over time as well as potential risk of unwanted tissue and toxic side effects [209, 210]. The effect of growth factor incorporation in addition to channels is not known but would be an attractive venue of future research, concentrating on attempting to incorporate growth factors into the polymer which would be potentially possible due to the low temperature production method used.

# CHAPTER 5: MACROPAHGE-MEDIATED BIODEGRADATION OF DIFFERENT CROSSLINKED COLLAGEN SCAFFOLDS

## 5.1. INTRODUCTION

The degradation of porous scaffolds affects cell viability, growth as well as host response. Once a scaffold is implanted *in vivo* it needs to maintain its mechanical properties until the cells lay down enough extracellular matrix (ECM), then it should be completely degraded and adsorbed [115]. Both the rate of cellular infiltration and the rate of degradation depend on the properties of the biomaterial, including chemical composition, porosity, pore size, cross linking degree and enzyme levels at the site of implantation [118]. Collagen turnover is required for connective tissue remodelling during growth and development [119]. *In vivo* degradation of collagen scaffolds is complex; implants are infiltrated by various cells including fibroblasts which contract the implant, macrophages and neutrophils which release collagen degrading enzymes. These enzymes are metalloproteinases (MMPs) [211] and may be divided according to their primary structure and substrate specificity into five subclasses: collagenases, gelatinases, stromelysins, membrane-type MMPs and non-classified MMPs. There are 4 collagenases: MMP-1 (collagenase-1), MMP-8 (neutrophil collagenase), MMP-13 (collagenase-3) and MMP-18 (collagenase-4)[120]. Collagenases cleave tropocollagen (TC) at one single site, producing two fragments: $TC_1$ at about ¾ and $TC_2$ at about ¼ of the original molecule as a result of the hydrolysis of a single Gly-

Ile/Leu bond in each α chain of the collagen molecule allowing for further digestion by other MMPs, including gelatinases [50, 51] . Apart from collagenases, gelatinases play an important role in degrading rapidly denatured collagen and collagen fragments [50].

A critical factor in biocompatibility of polymer such as collagen is the balance between the mechanical properties and degradation resistance. Degradation profile, degradation product form and toxicity are variables that influence the host response. Amongst other major characteristics of the generic host response to biomaterials is macrophage activation, foreign body giant cell production and granulation tissue formation [212]. Macrophages participate in the biodegradation of extracellular matrices such as collagen by releasing enzymes, in organization of angiogenesis, and in regulation of tissue regeneration [116, 213]. Foreign body giant cells as well respond to a foreign material. They are a distinct population of cells derived from macrophages fusion [214].

In order to degrade a scaffold macrophages need first to attach and adhere to the material. Macrophages express extracellular membrane integrin receptors that recognise the Arginine-Glycine-Aspartic acid sequence (RGD sequence) found in a variety of ECM proteins including collagens [215]. This integrin meditated adhesion leads to signalling events that regulate cellular function and movement as well as cell proliferation and survival [216]. Macrophages actively respond to polymeric materials both *in vitro* [52] and *in vivo* [117] by adhesion, proliferation and formation of giant cells, engulfment and degradation of material [116, 213]. Since macrophages are involved in the immune response, inflammation and toxicity, their presence after

biomaterials' implantation has been regarded as negative. However macrophages play a critical role in tissue regeneration as well as degradation of degradable biomaterials [217, 218].

Collagen degradation requires water and enzyme penetration as well as digestion of linkages. Though collagen swells to a certain extent upon exposure to water, it can only be digested completely when collagenases take part. Whilst tissue collagenases cleave one time cross all three chains as described above, collagenases from clostridium histolyticum (CHC) make multiple scissions per chain [122]. Those enzymes cleave undenatured helical regions at physiological pH and temperature [123]. Other non-specific proteinases, like pepsin, can only attack telopeptides or denatured helical regions. This makes them responsible for further degradation down to amino acids[124].

*In vitro,* the rate of degradation of collagen scaffolds is determined using bacterial collagenases such as clostridium histolyticum collagenase (CHC). This enzyme preferentially hydrolyzes the X-Gly bond in a sequence R-Pro- X-Gly-Pro. This sequence is found almost exclusively in collagen and susceptibility to the enzyme is often used as a criterion for collagen [127, 128, 219]. CHC is widely available in purified forms and has a broad spectrum of action cleaving all types of collagen [125]. *In vivo/in vitro* correlation is possible as its specificity is similar to human neutrophil and fibroblast collagenase [126].

Collagenase is too big to penetrate into fibrils of collagen and thus digestion occurs at the fibril surface [129]. The formation of cross links between the triple helical regions

of adjacent molecules restricts access and reduces the number of specific cleavage sites [118]. Cross linking is used to achieve tissue formation- implant degradation match. It improves the physical properties of a collagen scaffold as well as the resorption/degradation rate [134, 187]. Synthetic cross links can be achieved either by using chemical crosslinking agents or physical crosslinking methods. A variety of chemical methods have been described including glutaraldehyde, formaldehyde, polyepoxy compounds, acyl azide, carbodiimides and hexamethylene-diisocyanate[54]. There are concerns over the cytotoxicity of their residues or their degraded products [220], either *in vitro* or *in vivo.* Carbodiimides (CDA or EDC) show promise as they contain no potentially cytotoxic residuals and do not remain active. The nontoxic urea derivative released when the crosslink is generated is easily rinsed from the collagen, leaving no residual chemicals [141]. Physical crosslinking can be achieved by heat, dehydrothermal treatment (DHT), ultraviolet (UV) and γ-irradiation. In DHT, crosslinking is induced by simply heating dry collagen under vacuum to approximately 100°C [118], but this can partially denature the collagen molecule as discussed in the previous chapter [142].

Previous studies have investigated collagenase driven degradation of collagen scaffolds at body temperature and under mechanical stimuli of 1Hz to partially mimic the *in vivo* conditions of biodegradation in the absence of cells encountered *in vivo* [150, 221]. In this study, it had been hypothesised that *in vitro* collagenase degradation would correlate with *in vitro* degradation by macrophages. There is currently there is no previously published data confirming the correlation between enzymatic collagen degradation and an *in vitro* model of macrophage degradation. This is useful as it allows for the characteristics of scaffolds to be defined in a more

biological fashion and will help to design scaffolds with task specific profile for use in tissue engineering.

This chapter assesses the macrophage-mediated biodegradation of different cross linked collagen scaffolds *in vitro* and correlates the chemical degradation of scaffolds with an *in vitro* model of scaffold degradation. The extent and effect of crosslinking has been examined, in chapter 3, using mechanical testing (Young's modulus) and measurements of the denaturation temperature and swelling ratio. These data have been used to correlate with the degradation studies.

## 5.2. MATERIALS AND METHODS

### 5.2.1. Cell Culture and Seeding on Scaffolds

BALB/c murine macrophage cell line RAW264.7 (Lonza, UK) were expanded in α-minimal essential medium (α-MEM) ( Gibco, Invitrogen, U.K.) supplemented with 10% Foetal Bovine Serum (FBS) ( Biosera, Sussex, U.K.), 1% antibiotics (Lonza, Belgium) and maintained at 37°C and 5% $CO_2$. Initially the scaffolds were prepared for culture; each scaffold type was cut into 0.5-0.6cm slices, washed in 70% ethanol and sonicated for 30mintues. Then, they were washed 3 times in 0.1M Phosphate buffered Saline (PBS) (BioWhittaker, Lonza) for 30 minutes. Finally they were placed in serum free medium at 4°C at least overnight before seeding with cells and kept there till seeding.

The concentrated macrophage solutions ($3x10^6$/ml) were seeded to the collagen scaffolds in 1ml of medium per well and cultured at 37°C and 5% $CO_2$ at 100% humidity. The composite were incubated for 7 days. Medium was changed every 3 days. In order to assess the effect on collagen scaffolds degradation of two different cross linking methods, one physical and the other chemical, the collagen scaffolds seeded with macrophages were made of 1% collagen, frozen at -20°C and cross linked using DHT (1 day, 3 days and 5 days) and EDC crosslinked (10mM, 33mM and 50mM) using methods explained in chapter 3.

### 5.2.2. Assessment of Macrophage Attachment, Proliferation and Morphology on collagen scaffolds

The Alamar Blue™ assay (Biosourse Europe, Nivelles, Belgium) was used to quantify the number of cells at day 1 and 7 according to manufacturer's protocol. Briefly, scaffolds were transferred to new well plate and incubated in 0.5ml of 5% Alamar blue medium solution for 2 hours at 37°C and 5% $CO_2$ at 100% humidity. Then, 400 µl of Alamar blue supernatant was moved to a new plate for analysis and fresh medium was added to scaffolds and put back in incubator. The relative fluorescent units of cell-degraded Alamar blue was measured on a SPECTRAmax GEMINI microplate spectrofluorimeter (Molecular Devices, Berks, UK) at an excitation wavelength of 530 nm and an emission wavelength 590 nm, with a cut-off at 570 and converted to cell number based on the standard curve. A standard curve was produced by sequential dilution of 2:1 of the same cells. The standard curve correlates Relative Fluorescent Unit (RFU) to cell number.

To assess cellular attachment efficacy at day 1, the scaffolds were transferred to empty wells and both the scaffolds and culture wells were assessed by Alamar Blue™ separately. The attachment ratio was calculated as shown in equation (3) used in chapter 4.

To assess the morphology and behaviour of cells attached to collagen scaffolds, samples were examined using SEM. At day 7, murine macrophage-laden scaffolds were rinsed in 0.1M PBS and fixed in 4% Glutaraldehyde (BDH Limited, UK), 0.1M PBS, and pH7.3 overnight at 4°C. Samples were then serially dehydrated in 40%, 70%, 80%, 90%, 95% and 100% ethanol solutions for 15 minutes each, infiltrated in 50% (v/v) hexamethyldisilazane (Sigma-Aldrich, USA) in ethanol and 100% hexamethyldisilazane once each for 30 minutes. Finally the samples were washed with fresh 100% hexamethyldisilazane again and left overnight in a fume cabinet to air dry.

The dried specimens were placed on aluminium stubs, sputter coated with Platinum using a Polaron SC502 Sputter Coater (Fison Instruments, UK), and examined using JEOL JSM-840F scanning electron microscope (Peabody, MA) at 3kV.

### 5.2.3. Assessment of Collagen Scaffolds Degradation

#### 5.2.3.1. Assessment of Scaffolds Degradation by Collagenases

Collagen scaffolds of about 5 mg (mean 5.11 ±0.17 mg) were measured dry and incubated at 37°C with 1 ml of 0.1 M Tris-HCl (pH 7.4) containing 50 mM CaCl2 for

30 minutes. One ml of 0.1 M Tris-HCl containing 50 Units of Clostridial Bacterial Type I Collagenase (Sigma Aldrich, UK) was added to the solution and scaffolds were subjected to 1 Hz in a shaker bath for 1 hour. Samples were removed and placed on ice with 0.2 ml of 0.25M EDTA. The samples were rinsed three times in water and then in ethanol over a period of three hours. The samples were then dried under a flow cabinet for 24 hours, remeasured dry and the percentage degradation calculated as the difference between the original and final dry mass. A control scaffold was also measured without the addition of collagenase [150].

#### 5.2.3.2. Assessment of Scaffolds Degradation by Macrophages

Culture medium was changed every 3 days and collected every time medium was changed and frozen in sealed vials at −20 °C before replenishment. Sircol™ soluble collagen assay was used according to the manufacturer's instructions and measured using Dynex Technologies MRX spectrophotometer. Briefly, equal volumes of samples, collagen standards and fresh unused tissue culture medium were placed in centrifuge tubes with 1ml Sircol dye reagent for 30 minutes. After centrifugation, the unbound dye was discarded and the bound dye was resuspended in 1ml of Alkali reagent and the absorbance read at 520nm. Collagen standards were used to plot a standard curve used to calculate collagen content of test samples. To allow for any collagen that has been released rather than degraded by cells, scaffolds without cells were incubated for the duration of the experiment in the absence of cells. The medium

was assessed for collagen as described and this value subtracted from value obtained from true samples.

### 5.2.4. Statistics Correlation Analysis

Results are expressed as mean ± standard deviation. One-way analysis of variance (ANOVA) followed by LSD's post hoc test was used where stated with significance set at $p<0.05$. Multiple linear regression analysis was used to examine correlations between enzymatic degradation and macrophage mediated degradation as well mechanical properties and thermal properties examined in chapter 3. The independence of the different parameters tested was evaluated using Pearson's product-moment correlations ($r$) between parameters with significance set at $p<0.01$. All statistical analyses were performed on SPSS 13.0.

## 5.3. RESULTS

### 5.3.1. Macrophage Attachment, Proliferation and Morphology on Collagen Scaffolds

Correlation between enzymatic degradation of collagen *in vitro* and *in vivo* in the presence of crosslinking is well established [222]. Yet, there is no previously published data confirming the correlation between enzymatic collagen degradation and an *in vitro* model of macrophage degradation. To investigate the potential roles of macrophages in collagen degradation, RAW264.7, a murine monocyte/macrophage cell line were seeded on different cross linked collagen scaffolds.

Macrophages attached to and proliferated on all scaffold (Figure 5.1). There was better macrophage attachment to cross linked samples of both types (Figure 5.1-A). Physical treatment with DHT improved macrophage attachment as compared to EDC chemical cross linking. Crosslinking with DHT produced a significant improvement in the ratio of attachment when compared with non cross linked samples. Cross linking with DHT for 1 day and 5 days caused a 38% ($p<0.05$) and 62% ($p<0.05$) attachment respectively. The optimum physical treatment condition for macrophage attachment on these collagen scaffolds is 3 days DHT with an attachment ratio of 79% ($p<0.05$). For chemical treatment, only 33mM EDC significantly improved macrophages attachment compared to non cross linked samples with a ratio of 37% *($p<0.05$)* (compared to only 17% and 12% for 10mM and 50mM EDC respectively).

More macrophages were observed on cross linked samples at day 1 (Figure 5.1-B). From day 1 to day 7, macrophages proliferated on all samples but only significantly on non cross linked (4-fold increase), 3 days DHT (1.5-fold increase), 5 days DHT (5-fold increase) and 50mM EDC (1.5-fold increase). At day 7, cell number was the highest on 3 days DHT treated samples (254764 cells) and the lowest on 50mM EDC treated samples (70488 cells).

The SEM images (Figure 5.2) show the macrophages behaving as expected on the collagen scaffolds, producing podosomes and fusing into multinucleated giant cells.

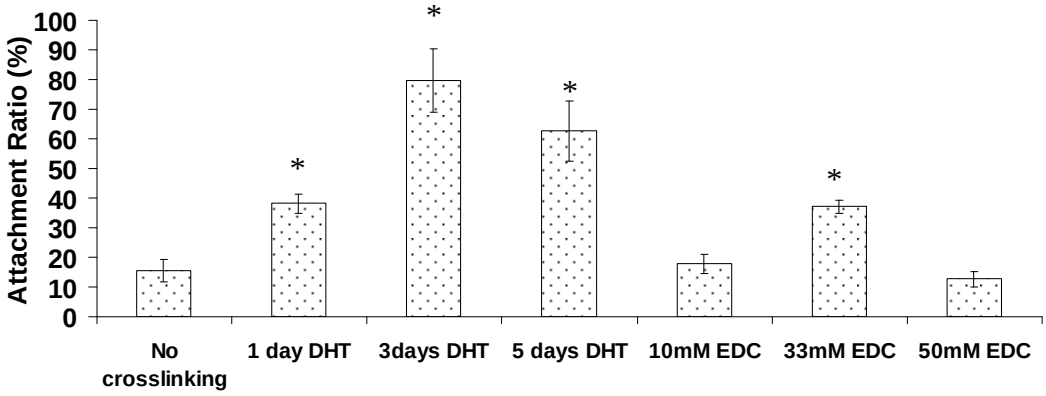



**Figure 5.1-A:** Attachment ratio of RAW264.7 macrophages on collagen scaffolds at day 1 after 24 hours incubation examined by Alamar Blue$^{TM}$ Assay. Cross linking improves macrophages attachment compared to non cross linked samples. Physical treatment of collagen scaffolds (DHT: dehydrothermal treatment) significantly improved attachment compared to chemical treatment (EDC: carbodiimide). The optimum condition for macrophage attachment on these collagen scaffolds is 3 days DHT with an attachment ratio of 79%. * compared with non cross linked samples $p<0.05$

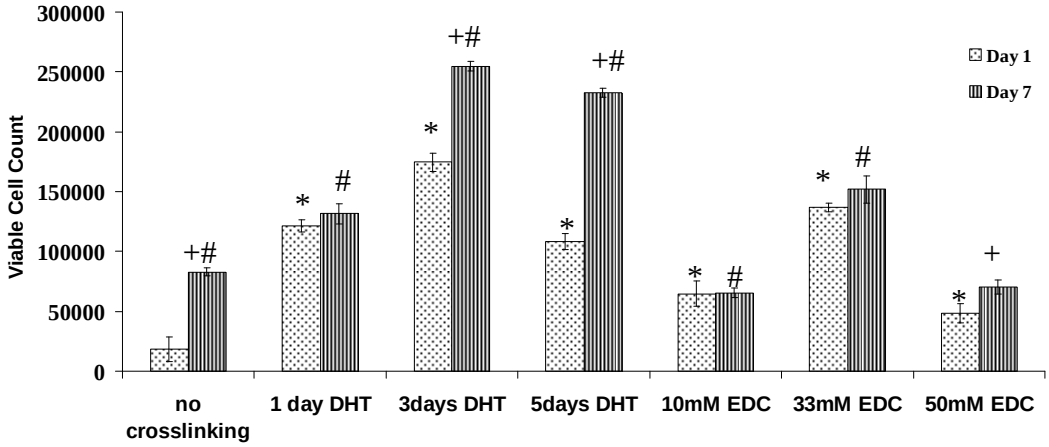



**Figure 5.1-B:** Proliferation of RAW264.7 macrophages on collagen scaffolds from day 1 to day 7. At day 1, more macrophages were observed on cross linked samples. From day 1 to day 7, macrophages proliferated on all samples. At day 7, cell number was significantly more on cross linked samples compared to non cross linked samples except 50mM EDC (carbodiimide). * compared with non crosslinked at day 1. # compared with non crosslinked at day 7. + compared to day 1 within groups, $p<0.05$. DHT: dehydrothermal treatment.

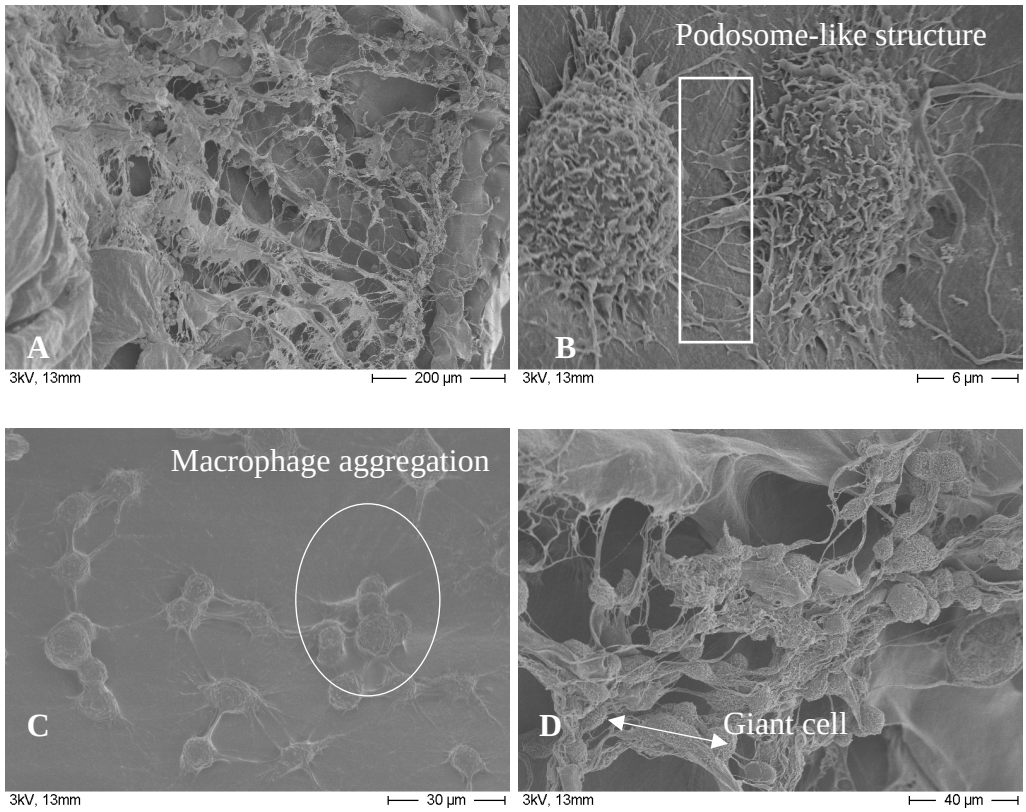



**Figure 5.2.** Scanning Electron micrographs illustrating RAW264.7 macrophages attaching to collagen scaffolds *in vitro*. **A-** Murine 264.7 macrophages attached and proliferated on collagen scaffolds, scale bar = 200µm. **B-** Cells firmly attached to the collagen surface via Podosome-like structure, scale bar = 6µm. **C-** Macrophages aggregation and fusion to form Giant cells, scale bar = 30µm. **D-** Note the formations of giant cells, scale bar = 40µm.

### 5.3.2. Collagenase and Macrophages- mediated Biodegradation of Collagen Scaffolds

Cross linking with DHT reduced amount of collagen degraded by macrophages (Figure 5.3-A) but only significantly for 3 and 5 days treatments where the amount of collagen degraded reduced from 0.092µg/µl for non cross linked samples to

0.025µg/µl ($p$<0.05) and 0.017µg/µl ($p$<0.05) for 3 and 5 days respectively. Similar trend was seen in collagenase mediated degradation (Figure 5.3-B) where rate of degradation reduced significantly for 3 and 5 days DHT treatment (non cross linked 83% vs. 60% ($p$<0.05) and 35% ($p$<0.05) for 3 and 5 days respectively). For chemical treatment, the amount of collagen degraded by macrophages (Figure 5.3-A) reduced significantly to 0.023µg/µl ($p$<0.05) and 0.010µg/µl ($p$<0.05) for 33mM and 50mM EDC. However, in collagenase mediated degradation (Figure 5.3-B), the rate of degradation reduced significantly at all EDC concentrations (38% ($p$<0.05) for 10mM EDC, 16% ($p$<0.05) for 33mM EDC and 3% ($p$<0.05) for 50mM EDC). Cross linking the scaffolds with either DHT or EDC increased the resistance of the scaffold to degradation by both collagenase (Figure 5.3-A) and macrophage (Figure 5.3-B). EDC crosslinking is far more effective than DHT crosslinking in preventing collagenase degradation and macrophage degradation.

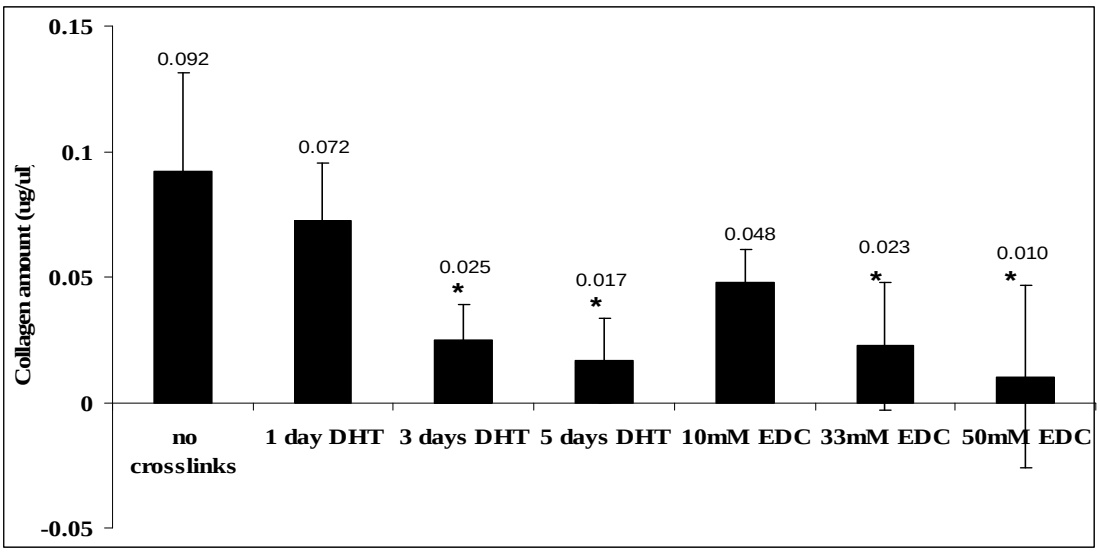



**Figure 5.3-A:** Collagen degradation by macrophages measured by Sircol$^{TM}$ soluble collagen assay. The amount of collagen released decreases with increasing cross linking. * compared with non cross linked samples $p$<0.05. EDC: carbodiimide, DHT: dehydrothermal treatment.

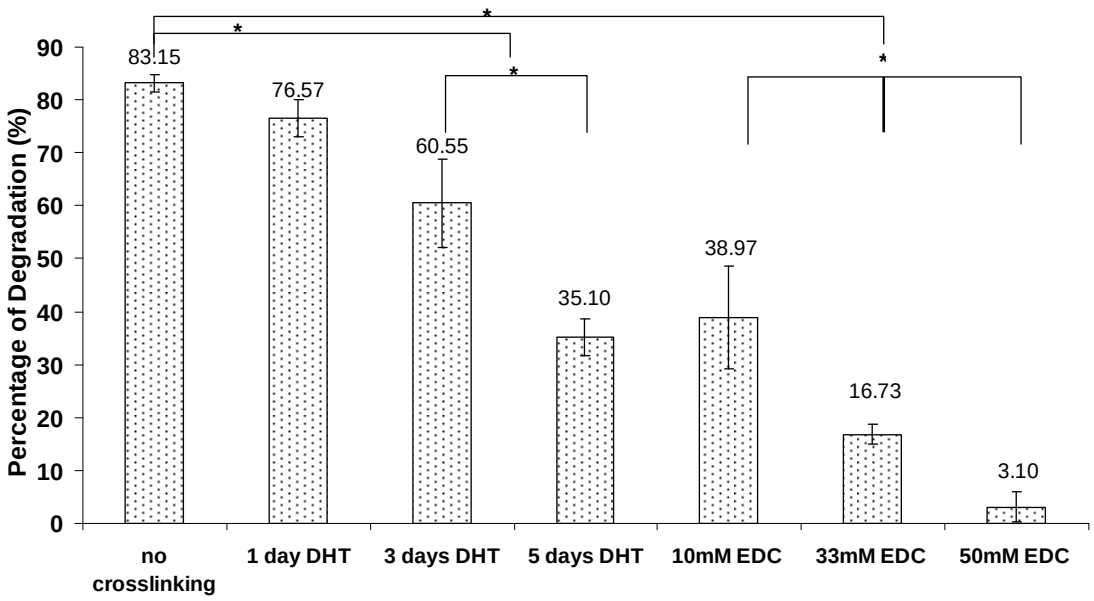



**Figure 5.3-B.** Enzymatic degradation of 1% collagen scaffolds after different cross linking using 50Units bacterial clostridial type I collagenase at 37°C for 1 hour. Increasing crosslinking increases resistance to enzymatic degradation. * compared with non cross linked samples $p<0.05$. EDC: carbodiimide, DHT: dehydrothermal treatment.

### 5.3.3. Linear Regression and Correlations

Multiple linear regression analysis was carried out to investigate the correlations between enzymatic degradation and cross linking degree ($T_d$, $E$ and Q) investigated in the chapter 3 as well as enzymatic degradation and macrophage degradation. The enzymatic degradation was found to be highly negatively correlated with the denaturation temperature ($T_d$) (Figure 5.4-A, $p<0.01$, $R^2 = 0.78$, $r = -0.883$) as well as with Young's modulus ($E$) (Figure 5.4-B, $p<0.01$, $R^2 = 0.593$, $r = -0.770$). The enzymatic degradation was correlated with swelling ratio (Q) (Figure 5.4-C, $p<0.01$, $R^2 = 0.868$, $r = 0.931$) and with macrophage degradation (Figure 5.4-D, $p<0.01$, $R^2 = 0.433$, $r = 0.658$).

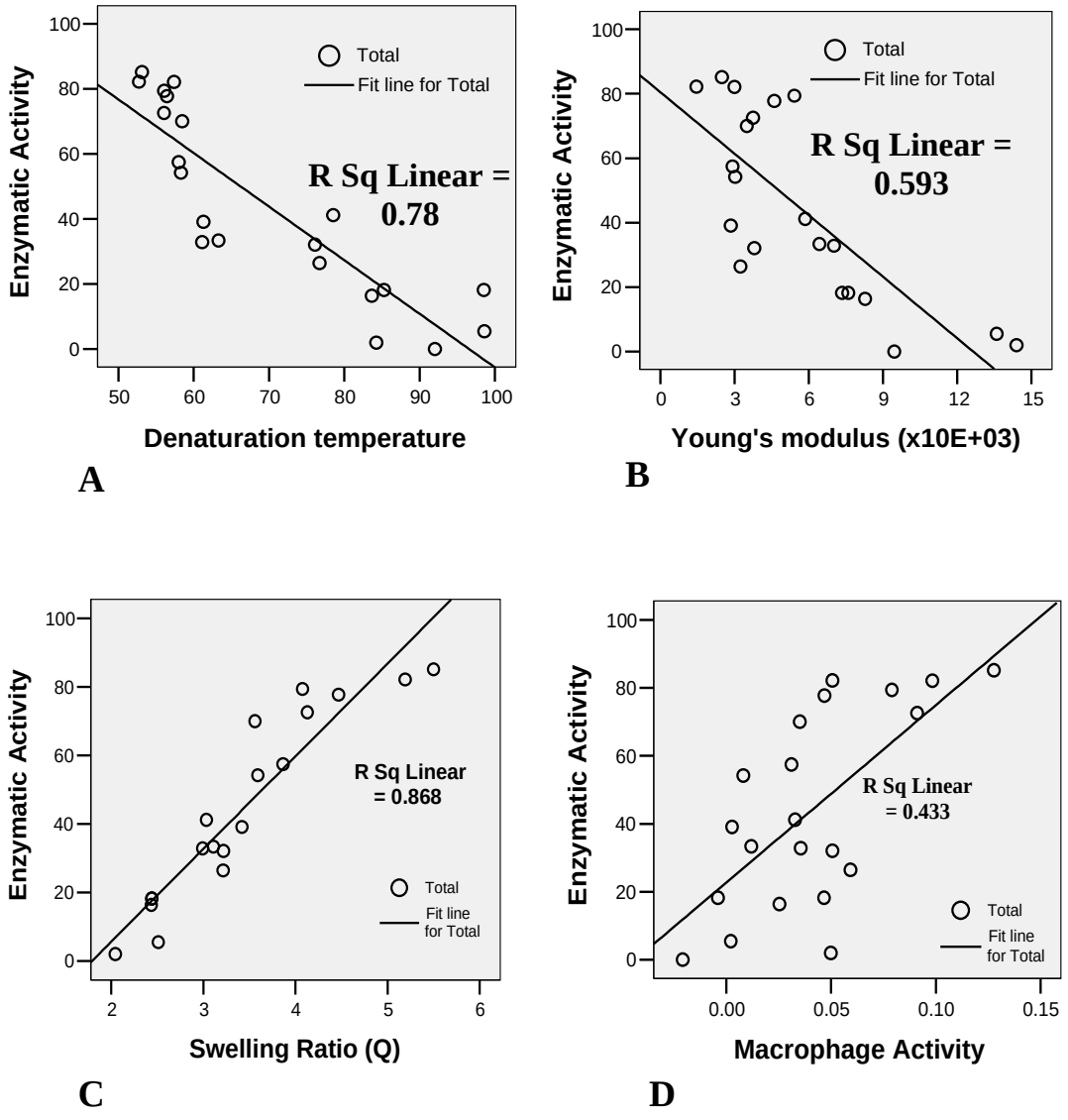



**Figure 5.4:** Linear regressions of enzymatic degradation against macrophage degradation, Young's modulus ($E$) and denaturation temperature ($T_d$). Enzymatic degradation correlated with **A**- denaturation temperature, **B**- Young's modulus, **C**- swelling ratio and **D**- macrophage activity. Enzymatic activity is the amount of collagen degraded by Clostridial Bacterial Type I Collagenase. Macrophage activity is the amount of collagen degraded by macrophages and released in the culture medium.

## 5.4. DISCUSSION AND CONCLUSION

RAW 264.7 attached to collagen scaffolds, proliferated, and exhibited macrophage aggregation to form giant cells. Cross linking the scaffolds with either DHT or EDC increased the resistance of the scaffold to degradation by macrophages. Cross linking collagen increases its resistance to degradation and this has been shown using a variety of methods of cross linking including ultra violet radiation, diphenylphosphorylazide, hydrazine and glutaraldehyde [134, 223, 224]. The differences presented here, showing that EDC cross linked samples are more resistant to degradation than DHT cross linked samples, corroborates previously published data [225].

EDC cross linking caused a far more pronounced resistance to collagenase even at the lowest concentration compared to DHT. This could be due to increased cross linking degree by EDC compared to DHT as confirmed by increased denaturation temperature and Young's modulus (Table 3.1, Chapter 3) which both correlate well with enzymatic degradation ($r$ = -0.883 against $T_d$ and $r$ = -0.770 against $E$). Increasing the cross linking density reduces the freedom of collagen chain movement. This increases the resistance to network expansion resulting in a decreased swelling ratio[197]. Both treatments decreased swelling ratio (Table 3.1, Chapter 3) due to increased cross linking density which correlates well with enzymatic degradation (r = 0.931), however, the effect was more pronounced with EDC treated samples. The

swelling ratio also suggests that the degree of cross linking was higher in EDC crosslinked samples compared to DHT.

Other potential reasons for the EDC resistance to collagenase are different cross linking locations on the collagen, where EDC cross linking sites restricts the collagenase cleaving sites [225], or due to the partial denaturation of the collagen in DHT treatment, as shown by the decreased denaturation temperature [118, 150, 221].

The traditional view of the macrophage as simply an immune activating cell is being questioned as subpopulations of macrophages have been identified [226]. These appear to have either a pro-inflammatory or pro angiogenic function, based on their cytokine expression [227]. They have a role in collagen degradation, allowing for collagen turnover and hence potentially for incorporation of a tissue engineered scaffold [117]. Altering cross linking of the scaffolds positively influences the rate of macrophage attachment as well as inhibiting the scaffold degradation; however the method of cross linking is important. Lower attachment was seen in EDC cross linked scaffolds. This is in keeping with other data assessing fibroblast, keratinocyte [228] and HUVEC [138] behaviour. EDC may be reducing cellular adherenence by masking receptor binding sites on the collagen. The surface property of a scaffold is important in determining cellular attachment and proliferation [229]. It is possible that changes in surface property caused by EDC led to reduced degradation by bacterial collagenase, reduced macrophage attachment and could possibly affect sensitivity to macrophages' MMPs.

It is well known that the surface microstructure, such as pore size, distribution and shape, plays an important effect on cell attachment, proliferation and function [55, 194]. For cell adhesion, it is important to have surface features that are equal or larger than the cell itself. The results suggest that the changes in morphology are due to the rehydration and refreezing process in the EDC cross linking treatment before freeze drying. Pore formation occurs as result of ice crystals formation during the freezing of the collagen suspension that are removed by freeze drying leaving a void that forms the pores. As discussed in chapter 3, this additional refreezing can lead to the fusion of some smaller pores, possible secondary larger ice crystals formation or the collapse of the scaffold which can oppose small pores fusion [55, 194]. Hence, in our samples, collapse effect is more prominent than the fusion resulting in overall smaller pores especially at higher EDC concentration.

Scaffolds cross linked by DHT have a higher cellular attachment rate, but conversely are degraded far quicker. The mechanism for this effect remains unclear. It could be due to the lower mechanical properties of the DHT treated samples (Table 3.1, Chapter 3). The more organized pore structure and slightly bigger pores could have encouraged more cellular adhesion (Figure 3.5 & 3.6, Chapter 3). During DHT, the further dehydration removes more water molecules which causes overall shrinkage in sample size but increases the pore size. However, human macrophages are on average about 21 μm in diameter [230], this is much smaller than even the smallest pore in our sample (Figure 3.6, Chapter 3). The size of the pore size per se does not explain the decreased cell adhesion or resistance to degradation.

It is also possible that the interaction between the scaffold and the macrophage affects the rate at which the cell releases collagenases or MMP's. Macrophages secrete diverse MMPs, such as MMP-9 that contribute to the degradation of extracellular matrix components [231, 232] with regulation of MMPs expression in macrophages being influenced by contact with matrix components. [231-233]. Macrophages, activated by interaction with type I collagen, secrete MMPs including MMP-9 which has a matrix degrading effect [234]. Further work will be needed to elucidate this difference, culturing macrophages on different scaffolds. Unfortunately the study of MMP expression by macrophages *in vitro* is difficult [231].

The overall degradation of collagen scaffolds by macrophages must therefore be influenced not only by the extent of attachment, but also by the method and degree of cross linking and denaturation extent of the collagen. This difference in behaviour could well be important in producing scaffolds with task specific roles *in vivo*.

In conclusion, macrophages play a key role in collagen degradation allowing for collagen turnover and incorporation of a tissue engineered scaffold into the host. This study shows that altering the scaffold properties by cross linking affects the rate of degradation by macrophages which is correlated with chemical degradation, denaturation temperature, mechanical properties and swelling ratio of the scaffold. This is useful as it allows for the characteristics of scaffolds to be defined in a more biological fashion and will help to design scaffolds with task specific profile for use in tissue engineering.

# Chapter 6: *IN VIVO* ASSESSMENT OF VASCULARISATION IN CHANNELLED COLLAGEN SCAFFOLDS

## 6.1. INTRODUCTION

Channels were developed in a porous 3-D collagen scaffolds and used to promote rapid ingress of angiogenic cells. Initial studies conducted *in vitro*, summarised in chapter 4, demonstrated that the scaffolds supported the angiogenic cells in growth in culture and the channels improved the depth of penetration of cells into the scaffold. The cells reside mainly around the channels and migrate along the channels.

However, it is equally important that the scaffolds promote a rapid vascular infiltration from the host into scaffolds offering the possibility of anastomosing with a preformed network. Thus, in this chapter, channelled and non-channelled collagen scaffolds were tested *in vivo*. Also, collagen scaffolds pre-seeded with endothelial and mesenchymal stem cells we assessed.

Blood vessels are usually encouraged to infiltrate into an implant by angiogenic growth factors diffusing from the implant. However, the release of such growth factors needs to be tightly controlled in order to avoid the development of disorganized, leaky and haemorrhagic vessels [235]. Here, we hypothesis that the presence of channel on collagen scaffolds alone will encourage the infiltration of blood vessels into collagen implants.

There has been some preliminary *in vivo* success with implanted cell-seeded constructs [14]. Hereby, endothelial cells and human bone marrow mesenchymal stem cells pre seeded collagen scaffolds were assessed *in vivo*. The effect of channels on those samples in promoting infiltration of angiogenic cells was explored.

## 6.2. MATERIALS AND METHODS

### 6.2.1. Sample Preparation Prior to *In Vivo* Implantation

#### 6.2.1.1. Plain (non-cell seeded) Collagen Scaffolds

In order to asses the vascular infiltration of plain collagen scaffolds *in vivo*, 7 samples without channel and 7 samples with one channel were implanted *in vivo* (Figure 6.1-A) . Prior implantation, 2 rounds of scaffolds (13mm in diameter and 0.5cm thick) were cut in eighths (8) each. Scaffolds were soaked in ethanol for 30minutes then washed in PBS twice before being soaked in PBS overnight.

#### 6.2.1.2. Cell-seeded Collagen Scaffolds

In order to asses the vascular infiltration of cell-seeded collagen scaffolds *in vivo*, 7 samples without channel, 7 samples with one channel and 7 samples with two smaller channel were implanted *in vivo* (Figure 6.1-A&B)

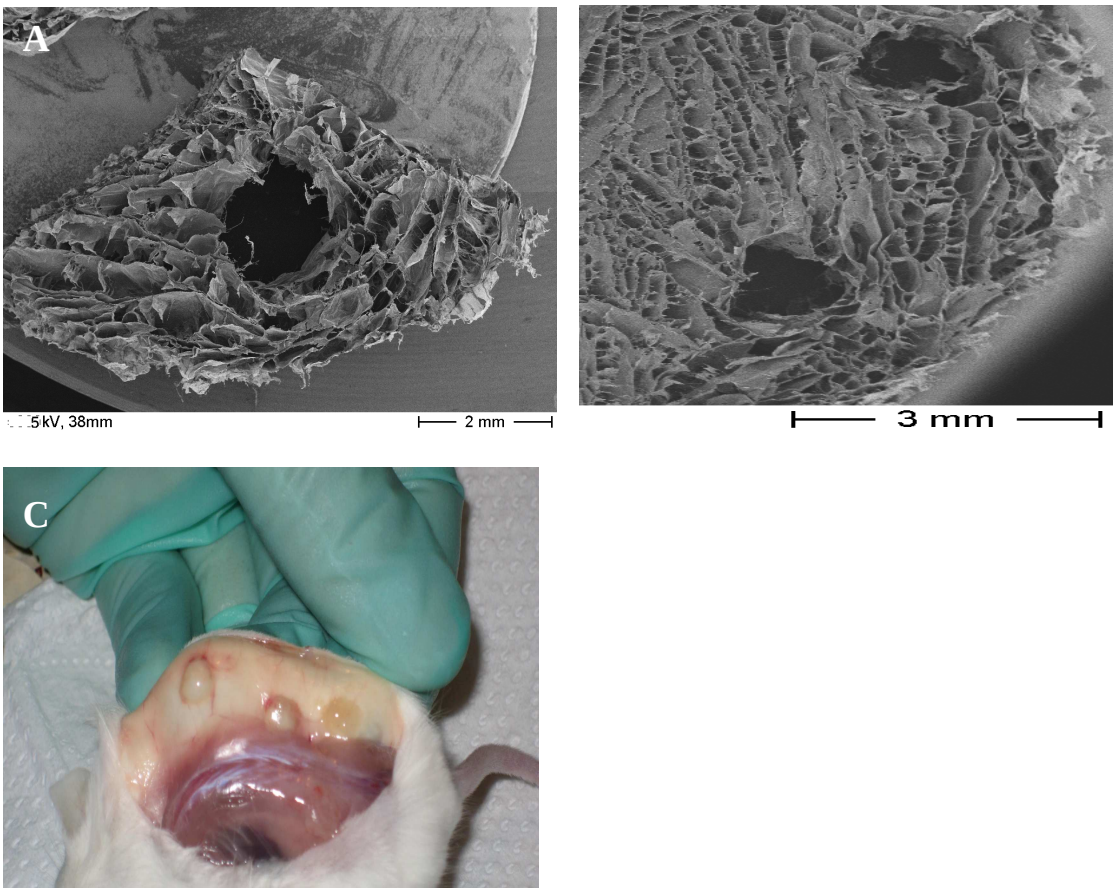



**Figure 6.1:** Scanning Electron micrographs illustrating cross-sectional view of channelled collagen scaffold implanted in mice, **A-** sample with one channel, average channel diameter measured at 2.02 ± 0.15mm, **B-** sample with two channels, average channel diameter measured at 1.17 ± 0.14mm. **C-** Photograph of the implanted collagen scaffolds just before retrieval. 3 samples were implanted each side subcutaneously.

Human bone marrow stromal cells (hBMSCs) and human umbilical vein endothelial cells (HUVECs) were used in this experiment. The HUVECs were purchased from BD Biosciences (cat. #354151), cultured (100mL Medium 200 [Cascade Bioscience,

Winchester, MA (#M-200-500)] mixed with 2mL LSGS [#S-003-10] and 1mL PenStrep). The hBMSCs were H-120 from National Institutes of Health (NIH) laboratory collection of hBMSCs derived from bone samples obtained as the by products of surgical procedures carried out by collaborators, and received according to National Institute of Dental and Craniofacial Animal Study (NIDCR) approved protocol for use of surgical waste. The bone sample from which the H-120 strain was derived was generated from a 19-year-old male donor undergoing surgery for flat foot correction. The hBMSCs were cultured in a 20% FBS media supplemented with 100 U/ml penicillin, 100 μg/ml streptomycin, and 1x Glutamax$^{TM}$ (Gibco, Grand Island, NY).

Prior to transplantation the scaffolds were rinsed in Ethanol to sterilize them, and then washed two times with aMEM and left to soak in aMEM for 10 minutes in order to eliminate the Ethanol and equilibrate the scaffold. The desired cells were spun down and resuspended in 40uL of aMEM. After soaking the scaffolds were blotted to remove moisture then placed in the cell solution to ensure that the cells were soaked into the scaffold and not just on the surface. HUVECs seeded at passage 6 with $1.5x10^6$ per scaffold, and hBMSCs at passage 5 with $2.0x10^6$ per scaffold.

### 6.2.2. *In Vivo* Implantation

#### 6.2.2.1. Plain (non-cell seeded) Collagen Scaffolds

All experiments were carried out under license at the University of Oxford with the ethical approval of the University of Oxford Research and Ethics Committee. A total of eight Female BALB/c mice aged between 3 and 6 weeks were used (Biomedical

services, University of Oxford, UK). Six scaffolds were implanted subcutaneously on the dorsal aspect of each mouse through incision under general anaesthesia using Isoflurane (Figure 1.6-C). After surgery and recovery, mice were fed basic laboratory diet and given water ad libitum. Four animals were euthanized by cervical dislocation under general anaesthesia either at week 1 or week 2 and the scaffolds were harvested for further analysis.

#### 6.2.2.2. Cell-seeded Collagen Scaffolds

Scaffolds seeded with cells were placed subcutaneously in the backs of NIH III Nude mice according to (NIDCR, Proposal #07-448). The mice were fed a standard diet and kept in a social environment in accordance with the ethical and animal welfare requirements of the NIH. After either 4 or 8 weeks, the scaffolds were harvested, fixed (in 10% formalin for 3 days), and processed for paraffin embedding. Scaffolds embedded in paraffin and cut into 6μm sections.

### 6.2.3. Light Microscopy Examination of Plain Collagen Scaffolds

Specimens as they were harvested were placed in 1.5mL cold PBS each and placed onto ice and viewed under light microscope. Images were then taken and Image analysis software (ImageJ, Wayne Rasband) was used to quantify the area occupied by blood vessels/granulation tissue.

### 6.2.4. Haematoxylin/Eosin (H&E) Staining of Plain Collagen Scaffolds

Immediately after light microscopy examination, implanted plain collagen scaffolds were cryosectioned, mounted on glass slides and frozen at -20°C till further analysis. Sections were routinely haematoxylin–eosin stained.

### 6.2.5. Immunohistochemistry

#### 6.2.5.1. F40/80 Staining

Immunofluorescence microscopy was used to study the invasion of macrophages onto implanted plain collagen scaffolds. Slides were defrosted at 37°C, wet in PBS, fixed in 10% formaldehyde and washed with PBS and 0.1% Triton X100. Sections were then incubated with rat anti mouse F40/80 antigen (1:50) (ABD SEROTEC, MCA 497G) for 1 hour at room temperature, washed with PBS and 0.1 Triton X100 , followed by 30 minutes incubation with anti-rat IgG NL557 Conjugated Goat IgG secondary antibody (1:200) (R&D systems). Both antibodies were diluted in PBS. For control slide, only PBS was added. DAPI was used a counter staining. Section were washed and mounted in and viewed under microscope. Image analysis software (ImageJ, Wayne Rasband) was used to quantify macrophage population using antibody stained sections.

### 6.2.5.2. vWF Staining

The total number of cells and vascular endothelial cells invaded implanted plain collagen scaffolds was calculated by DAPI staining and vWF immunostaining respectively. Sections (5 μm) were cut by using a cryomicrotome (Leica Microsystems, Wetzlar, Germany) at -25 $^{o}$C placed on positively charged slides (Superfrost Plus ™, Thermo Scientific, Braunschweig, Germany) and stored at -20 $^{o}$C before analysis. The slides were defrosted at room temperature for 10 minutes before being fixed with 4% paraformaldahyde for 10 minutes. The numbers of vascular endothelial cells in the scaffold was calculated by using vWF immunostaining (rabbit anti vWF Dako, Denmark). Goat anti-rabbit Alexa Fluor 546 (Invitrogen, USA) was used as secondary antibody and DAPI were used for nuclear staining. Several thin optical slices (thickness < 0.7 μm) of high-resolution were obtained by sequential confocal scanning by using a confocal microscope (Nikon eC1 plus, TE2000E, Japan) of scaffold sections were acquired to identify cells. Following acquisition of images, the numbers of cell nuclei stained with DAPI were calculated, as were the number of angiogenic cells stained with vWF. The total area of cells in the section was calculated and cell numbers were standardized to cells per 0.1 mm$^2$ as well as vWF particle count**.** Images were analysed using ImageJ analysis software (ImageJ, NIH, Bethseda, USA).

### 6.2.5.3. Alpha Smooth Muscle Actin (α-SMA) Staining

Since α-SMA detects the actin in smooth muscle cells only expressed in blood vessel lining, it was used quantity of staining as a measure of blood vessels present in the

implanted cell-seeded collagen scaffolds. The slides were placed at 60°C for 10 minutes to melt paraffin before being fixed with xylene and ethanol for 10 minutes. Alpha smooth muscle actin (α-SMA – Zymed, San Francisco, CA) immunohistochemistry was then used with a 3, 3'-diaminobenzidine (Superpicture HRP Conjugate Broad Spectrum [DAB], Zymed, Carlsbad, CA) secondary antibody system. Samples were then dehydrated and mounted for imaging. Images were analysed using ImageJ analysis software (ImageJ, NIH, Bethseda, USA).

### 6.2.6. Statistics

Results are expressed as mean ± standard deviation. One-way analysis of variance (ANOVA) followed by LSD's post hoc test was used where stated with significance set at $p<0.05$ unless otherwise stated. All statistical analyses were performed on SPSS 13.0.

## 6.3. RESULTS AND DISCUSSION

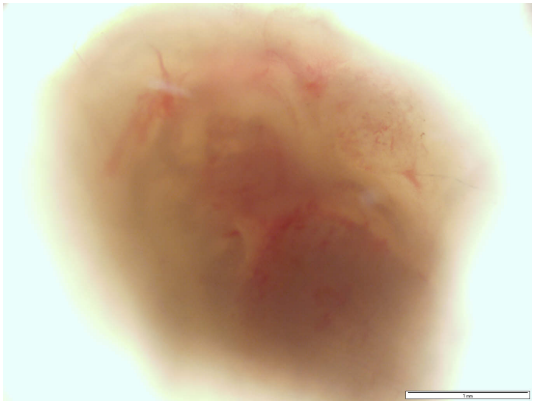
### 6.3.1. Vascularisation of Implanted Plain Collagen Scaffolds

#### 6.3.1.1. Vascular and angiogenic cells Penetration

Evidence of increased vascular penetration was seen a week 1 in channelled samples compared with those without channels (Figure 6.2- A & B). After 2 weeks explantation, scaffolds showed a clear branched vascular network of micro vessels in

the channelled samples. This structure was not apparent in the non-channelled samples (Figure 6.2-C& D). At week 1 the total area of granulation tissue was significantly higher in channelled samples compared to non-channelled samples (299078 $\mu m^2$ vs. 60297 $\mu m^2$, $p < 0.001$) (Figure 6.3). At week 2, the total granulated area increased significantly in both samples but channelled samples still had higher granulated area than non channeled samples (669637 $\mu m^2$ vs. 222657 $\mu m^2$, $p < 0.001$). The presence of channels increased the total area of granulation tissue (Figure 6.2-A). A more organized and mature vasculature was produced in the presence of channels than in their absence (Figure 6.2). Samples with channels preserved the porous structure and pores were much more populated with cells compared to non channelled samples, as shown in H&E staining (Figure 6.4) and DAPI staining (Figure 6.6-A).

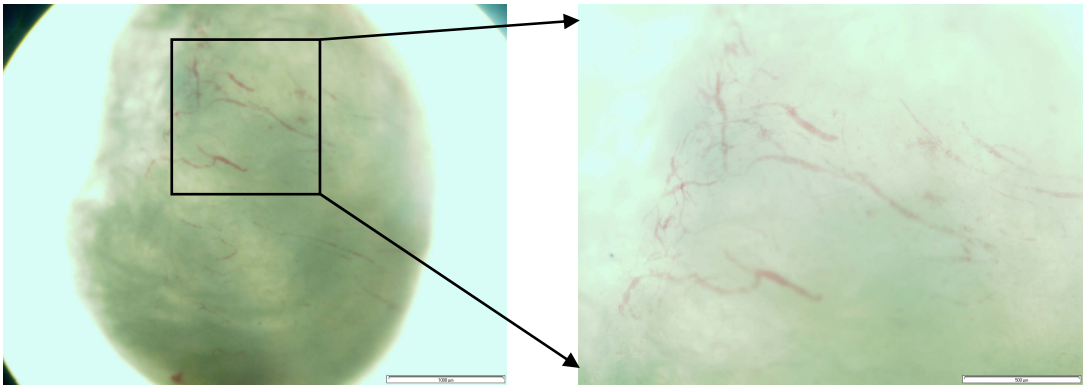
**A- Week 1 no channel**



**B- Week 1 with channel**



**C- Week 2 no channel**



**D- Week 2 with channel**

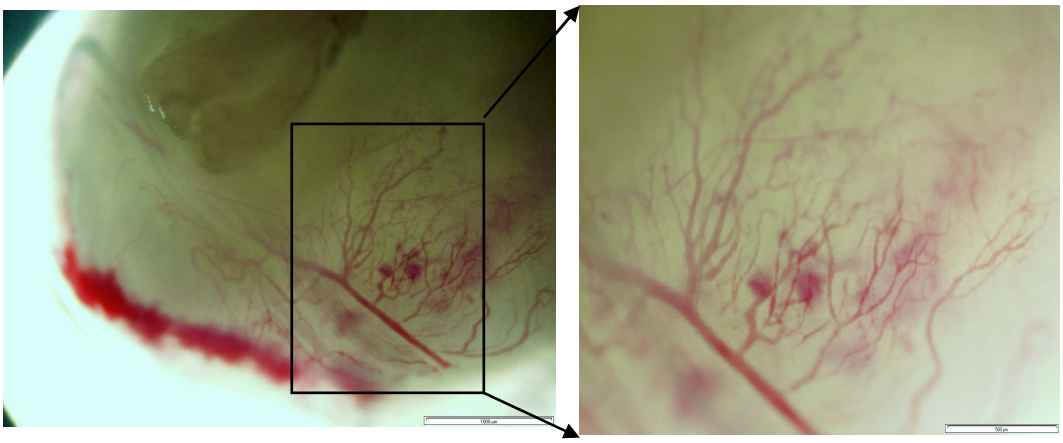


**Figure 6.2:** Photographs of scaffolds taken at time of explantation. The presence of channels in the scaffolds allows for the development of a more rapid and more mature vasculature**,** scale bar A, B, C (left) and D (left) = 1mm and C & D (right), 500µm.

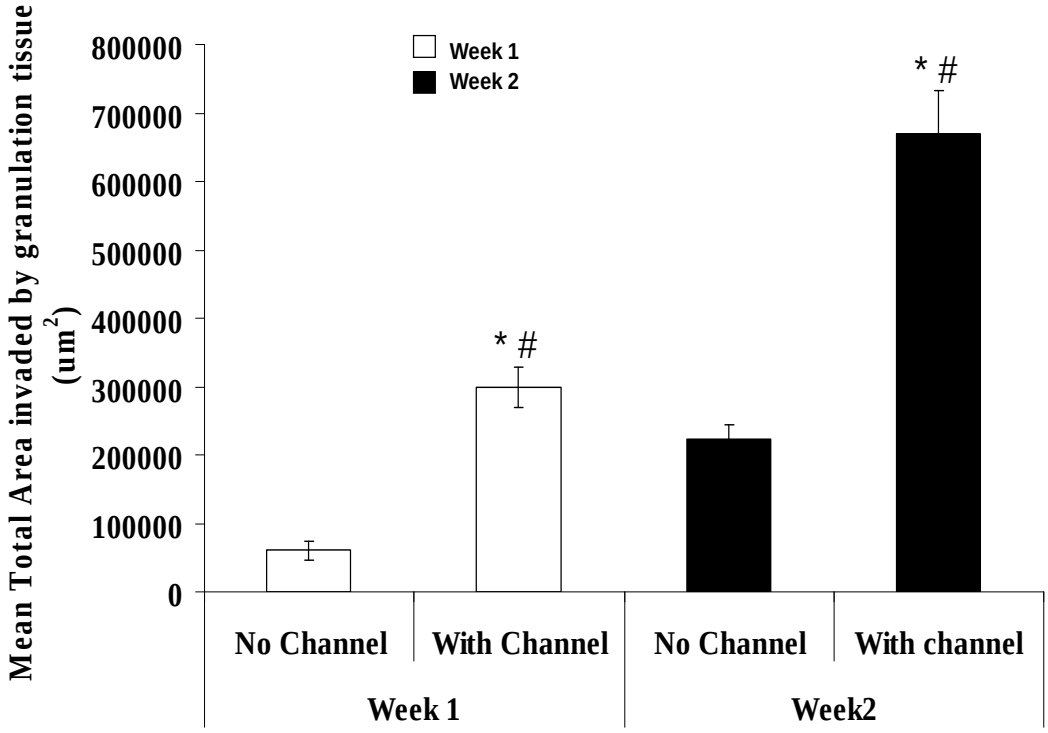



**Figure 6.3: Vascular penetration in plain collagen scaffolds.** Mean total area of collagen invaded by granulation tissue/blood vessels after 2 weeks implantation. Channels increase the rate of blood vessel development. * compared to sample without channel at the same time point. # compared to same type of sample at week 1 ($P < 0.001$).

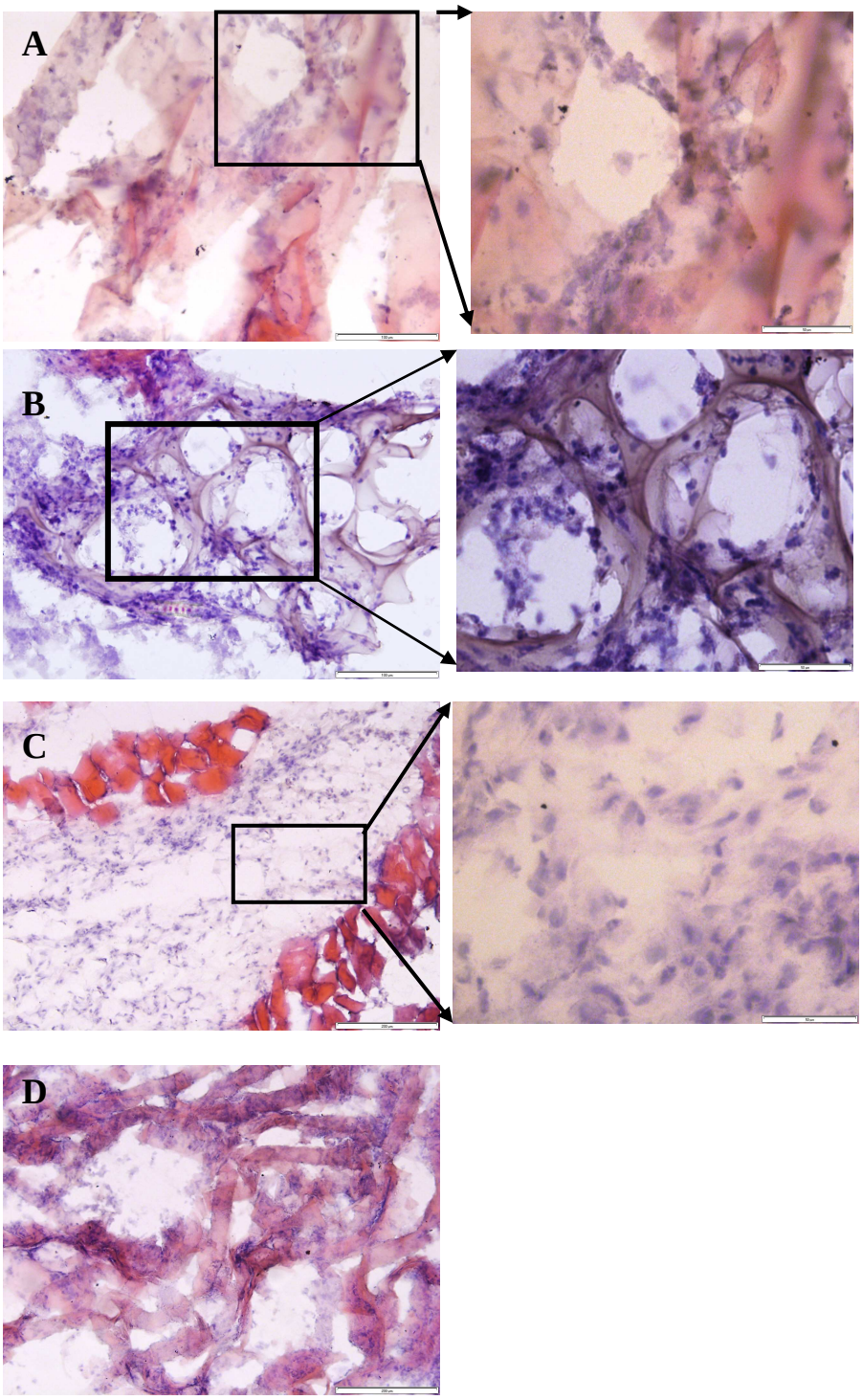
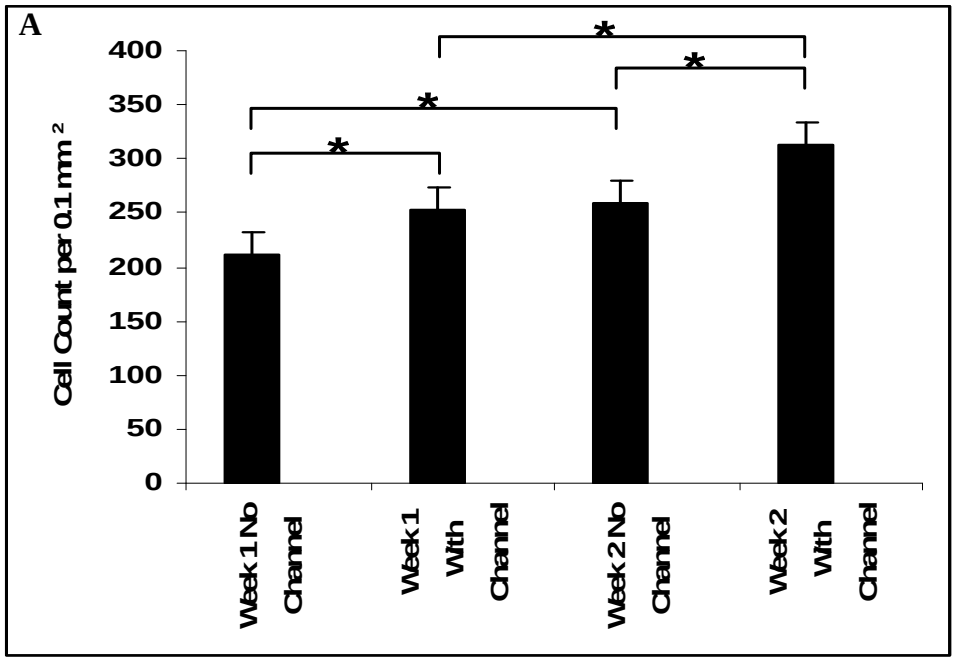



**Figure 6.4:** H&E staining of plain collagen scaffolds explants. **A-** Week 1 without channel, scale bar = 100 and 50µm. **B-** Week 1 with channels, scale bar = 100 and 50µm. **C-** Week 2 without channels, scale bar = 200 and 50µm. **D-** Week 2 with channels, scale bar = 200µm.

Overall, the presence of channels increased the cell migration into scaffolds as shown by increased total cell numbers (Figure 6.5-A). At week 1, the total cell number was significantly higher in the channelled samples compared to non-channelled ones (211 vs. 252 cell/0.1mm$^2$, $p < 0.05$). At week 2, total cell increased in both samples reaching 312 cell/0.1mm$^2$ in channelled samples and 259 cell/0.1mm$^2$ cells in non-channelled samples ($p < 0.05$). The total cell number was significantly higher in channelled samples compared to non-channelled samples at week 2 (312 vs. 259 cell/0.1mm$^2$, $p < 0.05$)

Figure 6.6-B shows vWF staining as indicator of angiogenic cells penetration into scaffolds. From figure 6.5-B, the particle count of vWF increased significantly in samples with channels. The vWF particle count increased significantly in both type of samples from week 1 to week 2 (49 and 76 at week 1 for non channelled and channelled samples respectively compared to 87 and 127 at week 2 for non channelled and channelled samples respectively, $p < 0.05$) (Figure 6.5-B). At either week 1 or 2, the presence of channels increased significantly vWF count (week 1 non-channelled, 49 vs. week 1 channeled, 76 and week 2 non channelled, 87 vs. week 2 channelled 127, $p < 0.05$) (Figure 6.5-B).



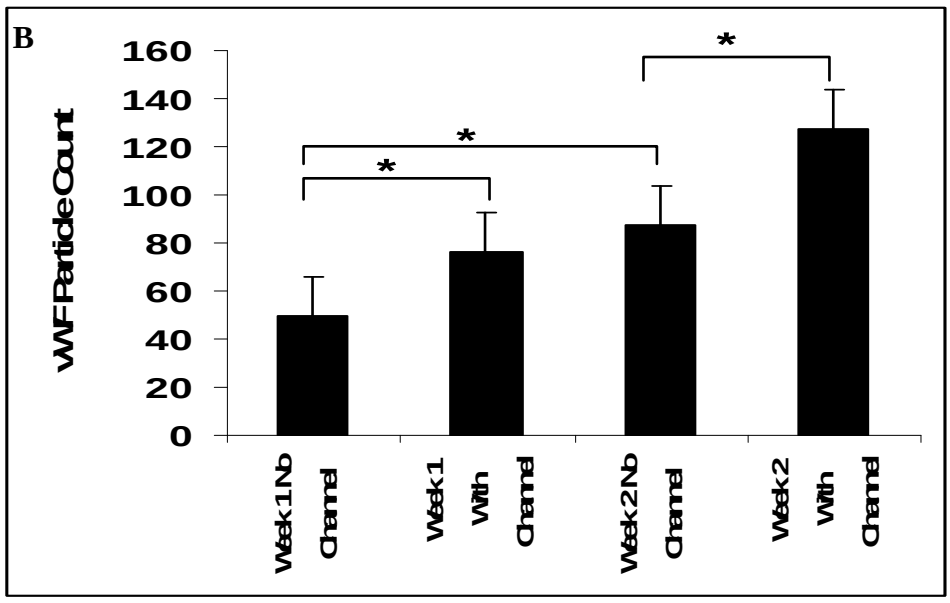




**Figure 6.5:** Angiogenic Cell penetration in plain collagen scaffolds. **A-** Total cell number invasion into collagen scaffolds with or without channels. The total cell number was significantly higher in channelled samples compared to non-channelled samples at week 1 & 2, * statistically significant, $p<0.05$. **B-** The vWF particle count as measure of angiogenic cells invasion into collagen scaffolds. At either week 1 or 2, the presence of channels increased significantly vWF count, * statistically significant, $p<0.05$.

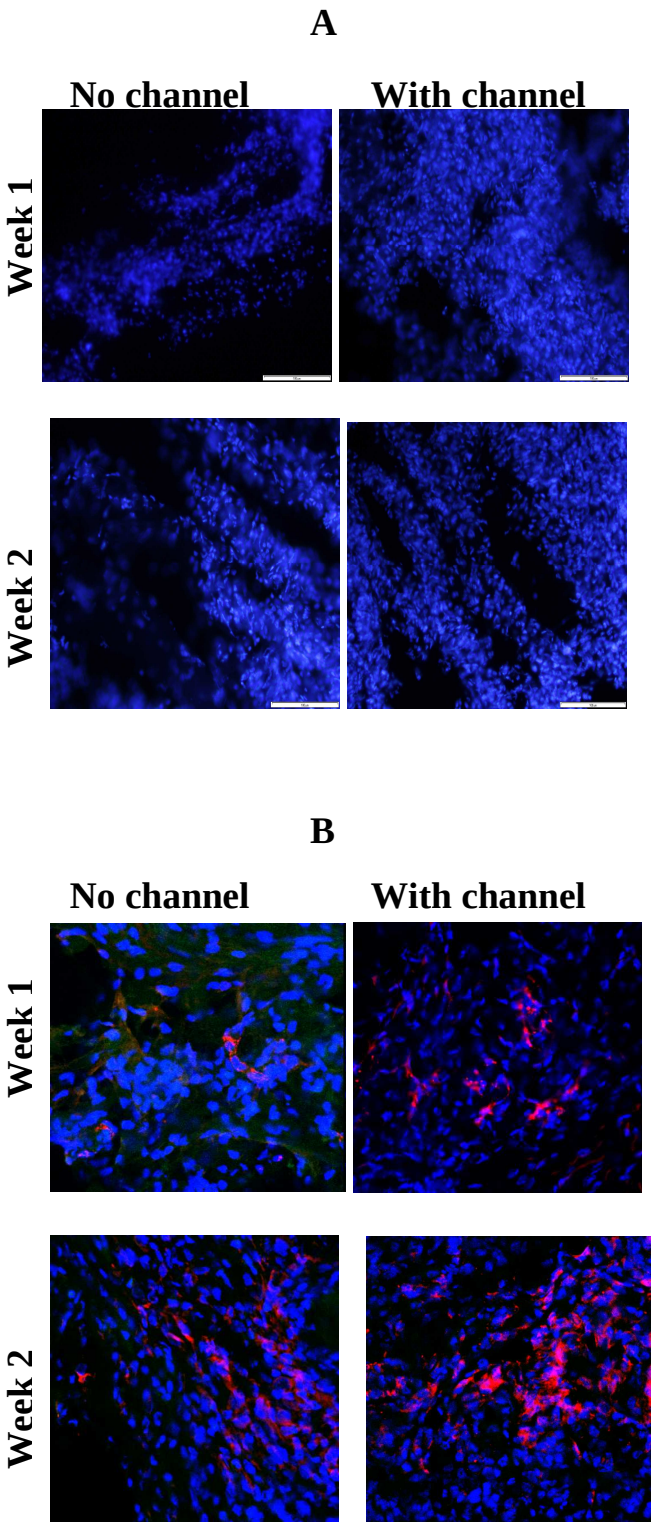



**Figure 6.6: A-** DAPI staining of collagen scaffolds after explantation, scale bar = 100µm. **B-** vWF staining of collagen scaffolds after explantation, 60x magnification.

#### 6.3.1.2. Macrophage Cells Penetration

Cellular and angiogenic cells invasion correlates well with macrophage invasion into scaffolds (Figure 6.7) since angiogenesis *in vivo* is usually accompanied by infiltration of macrophages [236]. The macrophages invasion into scaffolds was quicker in channelled samples where the area ratio of macrophages to other cells was 0.53 at week 1 which is significantly higher than 0.019 in the case of non channelled samples ($p < 0.05$). However, at week 2, the macrophages invasion increased considerably in non channelled samples to 0.29 whilst it leveled off to 0.43 in channelled samples ($p < 0.05$).

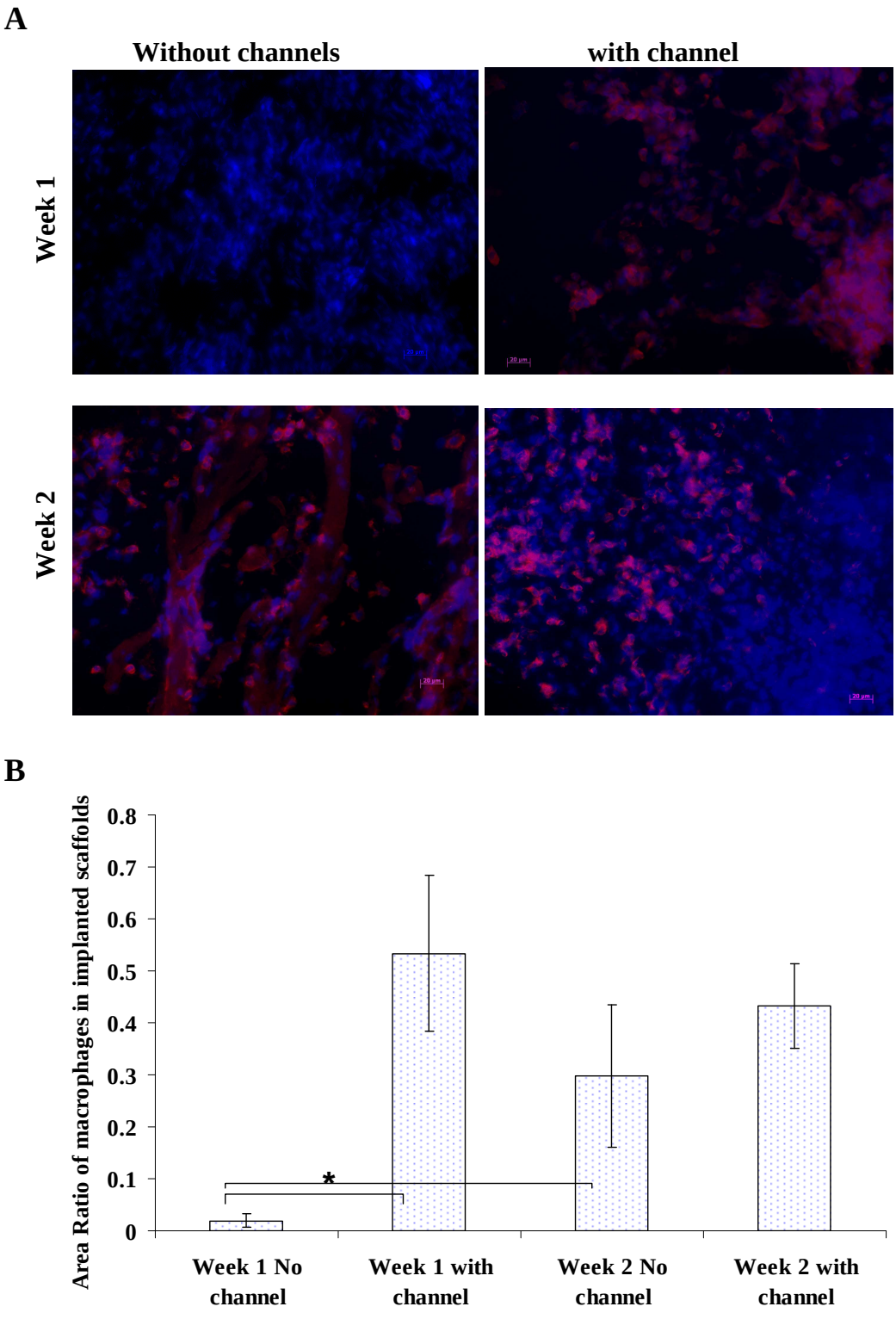



**Figure 6.7: A-** F4/80 staining scale bar = 20μm. **B-** Macrophage invasion into collagen scaffolds with or without channels. * compared to week 1 without channels $p<0.05$. The presence of channels increased macrophage invasion into scaffolds.

### 6.3.2. *Angiogenic Cells penetration into Cell-seeded Collagen Scaffolds*

Figure 6.8 shows α-SMA staining as indicator of angiogenic cells penetration into scaffolds. From figure 6.7, 4 weeks after implantation, the area fraction of α-SMA increased in EC- seeded samples in channeled samples compared to samples with no channels but only significantly in samples with 2 small channels (0.02 vs. 0.06 vs. 0.13 for samples with no channel, 1 large channel and 2 small channels respectively, $p < 0.05$). However, at the same time, hBMSC- seeded samples had a significant increase of α-SMA area fraction in sample with 1 large channel though it increased in sample with two small channels compared to non-channeled sample but not significantly (0.012 vs. 0.17 vs. 0.10 for samples with no channel, 1 large channel and 2 small channels respectively, $p < 0.05$). α-SMA area fraction of samples with one large channel was significantly higher for hBMSC compared to EC-seeded samples (0.06 vs. 0.17 for sample with large channel EC-seeded and hBMSC seeded respectively, $p < 0.05$).

At week 8, hBMSC-seeded samples had more or less the same area fraction cross all samples compared to EC-seeded samples where the staining area fraction increased significantly in sample with 2 small channels compared to the other samples (0.05 vs. 0.07 vs. 0.27 for samples with no channel, 1 large channel and 2 small channels respectively, $p < 0.05$).

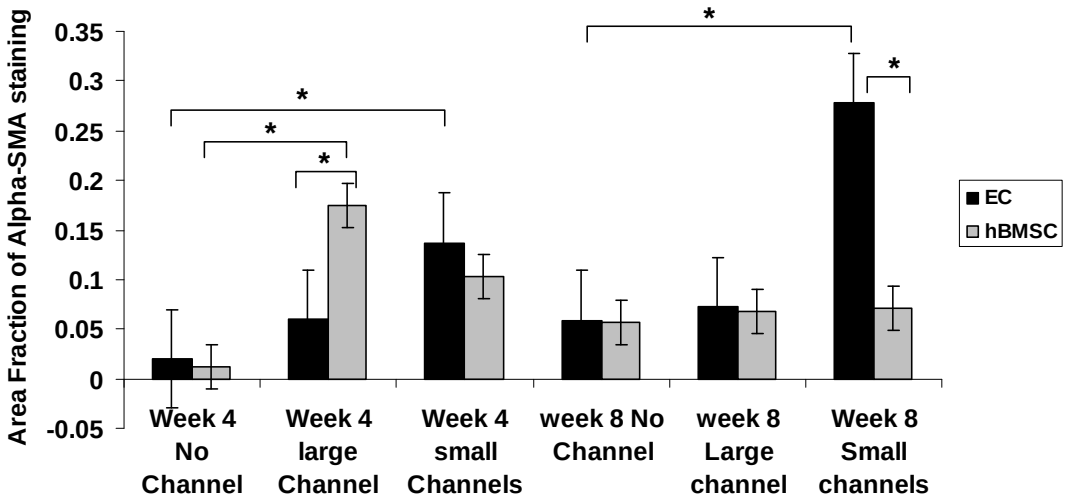
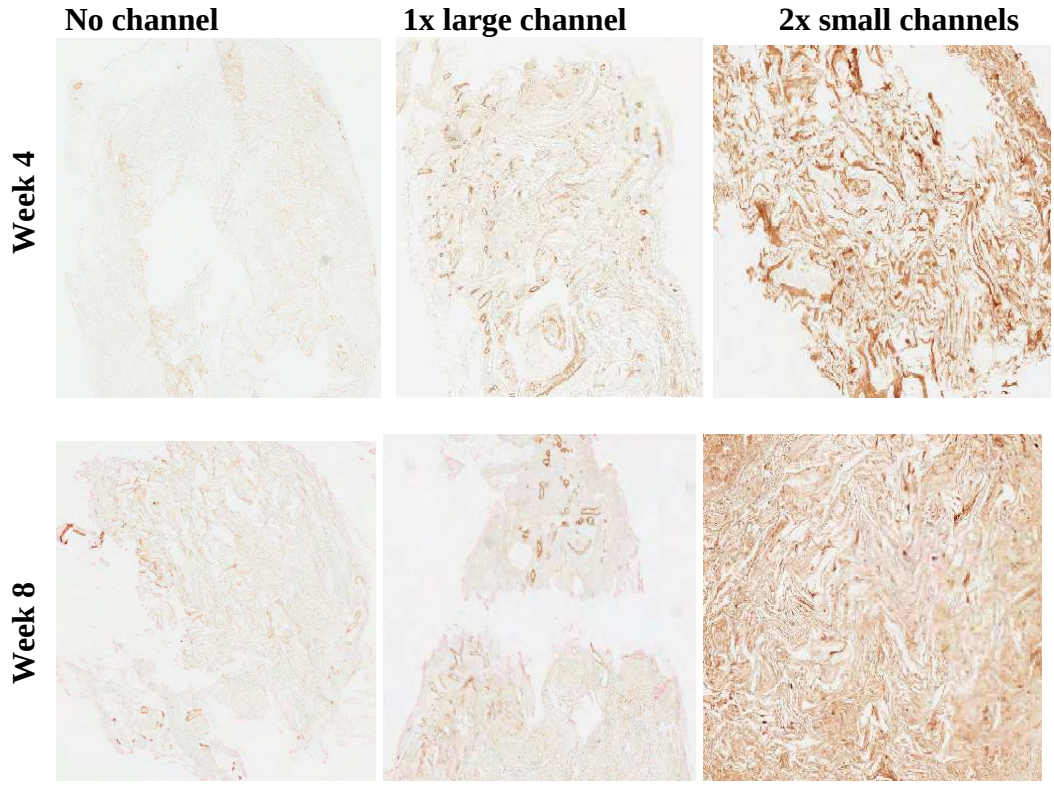



**Figure 6.8:** The area fraction of α-SMA staining in cell-seeded collagen scaffolds after implantation in mice. * Statistically significant $p < 0.05$. 4 weeks after implantation, the area fraction of α-SMA increased in EC (endothelial cells)- seeded samples in channeled same but significantly in samples with 2 small channels whilst hBMSC (mesenchymal stem cells)- seeded samples had a significant increase of α-SMA area fraction in sample with 1 large channel. At week 8, hBMSC-seeded samples had more or less the same area fraction cross all samples compared to EC-seeded samples where the staining area fraction increased significantly in sample with 2 small channels compared to the other samples.

**HUV-EC seeded scaffolds**




**hBMSC seeded scaffolds**

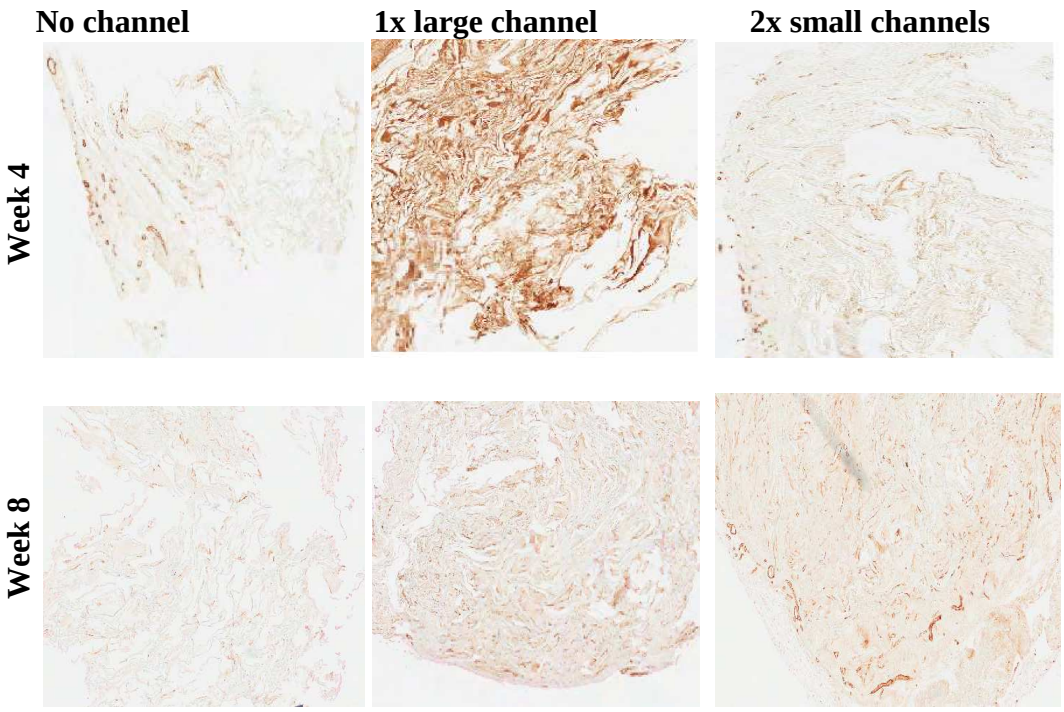



**Figure 6.9:** α-SMA staining of cell HUV-EC and hBMSC (mesenchymal stem cells) pre-seeded collagen scaffolds after explantation.

## 6.4. DISCUSSION

Overall, channels increased cell migration into scaffold and in particular angiogenic cells as determined by endothelial cells markers and macrophages markersx. Samples showed a clear branched vascular network of microvessels after 2 weeks in the plain channelled samples. This structure was not apparent in the plain non channelled samples. Thus, in growth of blood vessel cells are increased in these collagen scaffolds in the presence of channels. Due to limited sample size in the animal licence used, the channelled samples with all three and nine channels used in the *in vitro* testing were too big to be used in the *in vivo* study. Blood vessel infiltration was more rapid and extensive in plain samples with channels compared to plain non-channeled samples. In chapter 4, it was shown that the channelled scaffolds support the growth and migration of angiogenic channels. This might speed up the tubular like network formation. More importantly, once the vascular like network is present, the material should be easily invaded by host vasculature to anastomose with the already available network. In this chapter, the presence of channels allowed more rapid infiltration of host blood vessels and allowed the development of a mature vasculature. Thus, the channels offer the possibility of rapid blood vessels infiltration into material from host anastomosing with a preformed network.

3-D printing can be used to create micro channels [144]. Solid freeform fabrication (SFF) can produce scaffolds with predefined and reproducible internal morphology to act as an artificial vascular system [145]. The traditional SFF technique drawbacks as they are processed at high temperatures limiting the choice of materials and preventing the incorporation of biological molecules. A novel SFF technique has been

developed producing collagen scaffolds with complex internal morphology using a sacrificial mould and critical point drying technique. The moulds can contain predefined and reproducible features as small as 200μm [27]. These channelled collagen scaffolds have been successfully used in chondrogenesis using bone marrow derived stem cells resulting in good matrix synthesis within the channels and not in the periphery [28, 150]. However, this method is very time consuming with low producibility. Thus the method presented in this paper provides an easy way to test the efficacy and benefit of channelled scaffolds to achieve rapid angiogenesis. However, since those prove to be successful, the next step will be to produce scaffolds with more defined features using the indirect SFF.

It was expected that implanted scaffolds will elicit a light foreign body response from the host; this is characterised by the recruitment of inflammatory cells (e.g. macrophages, monocytes, neutrophils) to the area which together with local cells (e.g. fibroblasts) promote angiogenesis [237]. The traditional view of the macrophage as simply an immune activating cell [226, 237] is being questioned as subpopulations of macrophages have been identified. These appear to have either a pro-inflammatory or pro angiogenic function, based on their cytokine expression [227]. Macrophages play a central role in angiogenesis and integration of implanted biomaterial into tissue by producing several potent angiogenic factors such as: VEGF [238], b-FGF [239], TGF-β [240] and IL-8 [241]. Equally, they play a key role in the initiation of implants degradation [117] as demonstrated in the study summarised in chapter 5. Macrophages have been found in tissue section ongoing angiogenesis and are perquisite for neovascularisation [242]. Macrophages may elaborate in formation or

invasion of blood vessels by drilling tunnels using metalloproteinases which can facilitate the access of other blood components and setting up a tubular network [243]. Macrophages release different metalloproteases (e.g. collagenases) and serine proteinases (e.g. plasminogen activator, which degrade ECM components, modulate ECM mechanical properties and release angiogenic fragment from ECM molecules as well as releasing ECM-bound growth factors such as b-FGF through urokinase-type tissue plasminogen expression [244-246]. Therefore, the fact that macrophages presence was higher in sample with channels at weeks 1 then levelled off after 2 weeks compared to non channelled samples where the process was slower and still ongoing (Figure 6.7) could emphasis that neovascularisation is quicker in samples with channel. Thus, there need to be a balanced well controlled macrophage response to biomaterials as this critically determines the fate of tissue engineered implants.

Pre seeding channelled scaffolds with cells did improve the area fraction of SMA both for large and small channels at week 4 for both HUV-EC and hBMSC. However, for hBMSC, the area fraction was diminished at week 8 (Figure 6.8). This could be explained by the fact that channels gave the cells adequate time to invade after 4 weeks. This fits with the argument of more rapid cell infiltration in the presence of channels. However, time and financial constraints of only doing this experiment once makes it hard to draw conclusive observations. Ideally the experiment should be repeated.

Bone marrow mesenchymal stem cells are characterized by their ability to differentiate into smooth muscle cells, endothelial cells and hematopoietic supporting stroma [247, 248]. Due to these attributes bMSCs have the potential to support the

development of a microvascular network. Vitalization of collagen scaffolds with osteoblast-like cells, bone marrow mesenchymal stem cells or both cells in combination significantly enhanced vascularisation of scaffolds after implantation into the dorsal skinfold chamber of balb/c mice. However, the speed of vascularisation was independent of seeded cell type [249]. This led to the conclusion that accelerated vascularisation is rather cells released VEGF- related rather than ability of mesenchymal cells to differentiate into different vascular cells type [249]. In our study, hBMSCs promoted infiltration of angiogenic cells into collagen scaffolds but to far less extend then HUV-EC cells. A possible explanation could be the VEGF released by HUV-EC was greater than hBMSCs. Thus, expression of VEGF in close vicinity of cell-seeded implants could shed more light on the possible reasons. More interestingly, further investigations of *in vivo* differentiation processes of pluripotent stem cells would appear promising for tissue engineering approaches.

Silk fibroin scaffolds pre seeded with microvascular endothelial cells showed no infiltration of host vasculature after 14 days implantation *in vivo* [250]. However, inoculated microvascular ECs derived from the human dermis when inoculated onto de-epidermized acellular dermis and implanted the engineered tissue blocks into nude mice, the contribution of ECs to vascularization was then observed [251]. In this study, HUV-EC cells promoted angiogenic cells infiltration into collagen scaffolds to a greater extent than hBMSC. The presence of channels improved the infiltration with samples of smaller channels offering a significant increase in angiogenic cells infiltration. Thus, it could be concluded that pre-seeding channelled collagen scaffolds with endothelial cells has potential of speeding up vascularisation of implanted scaffolds.

## 6.5. CONCLUSION

The addition of channels improves the speed of cellularisation of collagen scaffolds. The channels offer the possibility of rapid blood vessel infiltration into the material from the host, anastomosing with a preformed network. This strategy can be adopted when rapid cellularisation is essential or to allow for rapid closure of defects in reconstructive surgery.

# CHAPTER 7: CONCLUSIONS AND FUTURE WORK

## 7.1. CONCLUSIONS

Collagen scaffolds made of 1% collagen suspension, frozen at -20°C during freeze drying process exhibited a mean pore size and pore size distribution suitable for migration and growth of vascular cells used in this study. While EDC increased the scaffold's thermal and mechanical properties, reducing swelling ratio and pore size, DHT increased the mechanical properties and pore size but decreased the denaturation temperature and swelling ratio. DHT samples had a more suitable pore size for endothelial cells and smooth muscle cells ingrowth. Thus, collagen scaffolds made of 1% collagen, frozen at -20C and cross linked with 3 days DHT were used to assess cellular ingrowth and vascularisation. Using pins to introduce channels was successful as they preserved their structure and shape after processing.

The scaffolds supported the angiogenic cells in growth in culture in *vitro* and the channels improved the depth of penetration of cells into the scaffold. The cells reside mainly around the channels and migrate along the channels suggesting an advantage for channels. The presence of channels increased the cell migration into scaffolds *in vivo,* in particular angiogenic cells. Blood vessel infiltration was more rapid and extensive *in vivo* in samples with channels compared to non channelled samples. Channels could aid production of tissue engineered constructs. These channels offer the possibility of rapid blood vessel penetration from the host into the scaffold biomaterial to form anastomoses with a preformed network. Pre-seeding

collagen scaffolds before *in vivo* implantation with endothelial cells could speed-up the vascularisation of implants compared to pre-seeding with hBMSCs, .

Channelled collagen scaffolds had rapid dual invasion of angiogenic cells and macrophages *in vivo*. The later subsided after 2 weeks implantation compared to non-channelled samples where the process was slower. This emphasises the fact that macrophages have both pro-inflammatory and pro-angiogenic role which is important in determining the fate of the implanted scaffold. Furthermore, they play a role on the degradation of the implanted scaffolds which is important to be tightly controlled as there need to be a balance between tissue formation and material degradation. Macrophages play a key role in collagen degradation allowing for collagen turnover and incorporation of a tissue engineered scaffold into the host. This study showed that altering the scaffold properties by cross linking affects the rate of degradation by macrophages which is correlated with chemical degradation, denaturation temperature, mechanical properties and swelling ratio of the scaffold. This is useful as it allows for the characteristics of scaffolds to be defined in a more biological fashion and will help to design scaffolds with task specific profile for use in tissue engineering.

## 7.2. FUTURE WORK

The scaffolds supported the angiogenic cells growth and penetration in the scaffolds *in vitro* as well as rapid vascular penetration *in vivo*. Thus, in future work, it would be interesting to culture angiogenic cells on those scaffolds and promote them to form tubules *in vitro* first before implantation and evaluate whether those will anastomoses with host vasculature and more importantly, how rapid this will be. This has potential use in constructing scaffolds for tissue engineering of bulk tissues.

In the co-culture model, a pre tagging of cells would be valuable as this will allow examining how the cells lie in parallel to each other on the scaffolds. As a result, it will determine whether it is better the culture both cells together at same time or culture one before the other.

The delivery of pro angiogenic factors with cell-polymer construct could be a method to promote angiogenesis in engineered tissues. The effect of growth factor incorporation in addition to channels is not known but would be an attractive venue of future research, concentrating on attempting to incorporate growth factors into the polymer which would be potentially possible due to the low temperature production methods used.

The method presented in this paper to make channelled scaffolds provides an easy way to test the efficacy and benefit of channelled scaffolds to achieve rapid

angiogenesis. The results tends to support the addition of more and small channels rather than few and large channels. However, since those prove to be successful, the next step could be to produce scaffolds with more defined features using the indirect SFF. In this method, collagen scaffolds are produced with complex internal morphology using a sacrificial mould and critical point drying technique. The moulds can contain predefined and reproducible features as small as 200μm [28, 150].

Pre seeding collagen scaffolds with HUV-EC and hBMSC experiment could be repeated and more tests needs to be conducted. Primarily, it will be interesting to quantify VEFG expression by cells in the close vicinity of the implants. Furthermore, investigation of hBMSCs differentiation on collagen scaffolds before implantation could help to shed light on possible reasons of vascularisation. Similarly, the fate of their differentiation could be investigated after implantation.

## REFERENCES


1. Rose FR, Hou Q, Oreffo RO. Delivery systems for bone growth factors - the new players in skeletal regeneration. The Journal of pharmacy and pharmacology 2004 Apr;56(4):415-427.

2. Lee KY, Mooney DJ. Hydrogels for tissue engineering. Chem Rev 2001 Jul;101(7):1869-1879.

3. Frerich B, Lindemann N, Kurtz-Hoffmann J, Oertel K. In vitro model of a vascular stroma for the engineering of vascularized tissues. Int J Oral Maxillofac Surg 2001 Oct;30(5):414-420.

4. Nomi M, Atala A, Coppi PD, Soker S. Principles of neovascularization for tissue engineering. Mol Aspects Med 2002 Dec;23(6):463-483.

5. Mikos AGTJS. Formation of highly porous biodegradable scaffolds for tissue engineering. Electronic Journal of Biotechnology 2000;3(2):114-119.

6. Vunjak-Novakovic G, Freed LE. Culture of organized cell communities. Adv Drug Deliv Rev 1998 Aug 3;33(1-2):15-30.

7. Arosarena O. Tissue engineering. Current opinion in otolaryngology & head and neck surgery 2005 Aug;13(4):233-241.

8. Griffith CK, Miller C, Sainson RC, Calvert JW, Jeon NL, Hughes CC, et al. Diffusion limits of an in vitro thick prevascularized tissue. Tissue Eng 2005 Jan-Feb;11(1-2):257-266.

9. Kannan RY, Salacinski HJ, Sales K, Butler P, Seifalian AM. The roles of tissue engineering and vascularisation in the development of micro-vascular networks: a review. Biomaterials 2005 May;26(14):1857-1875.

10. Risau W. Mechanisms of angiogenesis. Nature 1997 Apr 17;386(6626):671-674.

11. Laschke MW, Harder Y, Amon M, Martin I, Farhadi J, Ring A, et al. Angiogenesis in tissue engineering: breathing life into constructed tissue substitutes. Tissue Eng 2006 Aug;12(8):2093-2104.

12. Soker S, Machado M, Atala A. Systems for therapeutic angiogenesis in tissue engineering. World J Urol 2000 Feb;18(1):10-18.

13. Walgenbach KJ, Voigt M, Riabikhin AW, Andree C, Schaefer DJ, Galla TJ, et al. Tissue engineering in plastic reconstructive surgery. Anat Rec 2001 Aug 1;263(4):372-378.

14. Ko HC, Milthorpe BK, McFarland CD. Engineering thick tissues-the vascularisation problem. European cells & materials 2007;14:1-18; discussion 18-19.

15. Nillesen ST, Geutjes PJ, Wismans R, Schalkwijk J, Daamen WF, van Kuppevelt TH. Increased angiogenesis and blood vessel maturation in acellular collagen-heparin scaffolds containing both FGF2 and VEGF. Biomaterials 2007 Feb;28(6):1123-1131.

16. Pieper JS, Hafmans T, van Wachem PB, van Luyn MJ, Brouwer LA, Veerkamp JH, et al. Loading of collagen-heparan sulfate matrices with bFGF promotes angiogenesis and tissue generation in rats. Journal of biomedical materials research 2002 Nov;62(2):185-194.

17. O'Brien FJ, Harley BA, Yannas IV, Gibson LJ. The effect of pore size on cell adhesion in collagen-GAG scaffolds. Biomaterials 2005 Feb;26(4):433-441.

18. Cassell OC, Hofer SO, Morrison WA, Knight KR. Vascularisation of tissue-engineered grafts: the regulation of angiogenesis in reconstructive surgery and in disease states. Br J Plast Surg 2002 Dec;55(8):603-610.

19. Montesano R, Orci L, Vassalli P. In vitro rapid organization of endothelial cells into capillary-like networks is promoted by collagen matrices. The Journal of cell biology 1983 Nov;97(5 Pt 1):1648-1652.

20. Yang J, Richards J, Guzman R, Imagawa W, Nandi S. Sustained growth in primary culture of normal mammary epithelial cells embedded in collagen gels. Proceedings of the National Academy of Sciences of the United States of America 1980 Apr;77(4):2088-2092.

21. Zhang Y. Bladder reconstruction by tissue engineering--with or without cells? The Journal of urology 2008 Jul;180(1):10-11.

22. Kim BS, Atala A, Yoo JJ. A collagen matrix derived from bladder can be used to engineer smooth muscle tissue. World journal of urology 2008 Aug;26(4):307-314.

23. Tonello C, Vindigni V, Zavan B, Abatangelo S, Abatangelo G, Brun P, et al. In vitro reconstruction of an endothelialized skin substitute provided with a microcapillary network using biopolymer scaffolds. Faseb J 2005 Sep;19(11):1546-1548.

24. Kirsner RS, Falanga V, Eaglstein WH. The development of bioengineered skin. Trends in biotechnology 1998 Jun;16(6):246-249.

25. Landman KA, Cai AQ. Cell proliferation and oxygen diffusion in a vascularising scaffold. Bulletin of mathematical biology 2007 Oct;69(7):2405-2428.

26. Malda J, Klein TJ, Upton Z. The roles of hypoxia in the in vitro engineering of tissues. Tissue engineering 2007 Sep;13(9):2153-2162.

27. Sachlos E, Reis N, Ainsley C, Derby B, Czernuszka JT. Novel collagen scaffolds with predefined internal morphology made by solid freeform fabrication. Biomaterials 2003 Apr;24(8):1487-1497.

28. Dawson JI, Wahl DA, Lanham SA, Kanczler JM, Czernuszka JT, Oreffo RO. Development of specific collagen scaffolds to support the osteogenic and chondrogenic differentiation of human bone marrow stromal cells. Biomaterials 2008 Jul;29(21):3105-3116.

29. Gelse K, Poschl E, Aigner T. Collagens--structure, function, and biosynthesis. Advanced drug delivery reviews 2003 Nov 28;55(12):1531-1546.

30. Kucharz EJ. The collagens: biochemistry and pathophysiology. Berlin; London: Springer-Verlag 1992;xviii, 430p. : ill; 25cm.

31. Friess W. Collagen--biomaterial for drug delivery. Eur J Pharm Biopharm 1998 Mar;45(2):113-136.

32. Lee CH, Singla A, Lee Y. Biomedical applications of collagen. International journal of pharmaceutics 2001 Jun 19;221(1-2):1-22.

33. Martini FH. Fundamentals of anatomy and physiology. 4th ed. London: Prentice Hall Internation, 1998.

34. Davis GE, Senger DR. Endothelial extracellular matrix: biosynthesis, remodeling, and functions during vascular morphogenesis and neovessel stabilization. Circulation research 2005 Nov 25;97(11):1093-1107.

35. Xin Liu HW, Michael Byrne, Stephen Krane, and Rudolf Jaenisch. Type III collagen is crucial for collagen I fibrillogenesis and for normal cardiovascular development. PNAS March 4, 1997;94(5):1852-1856.

36. Lohler J, Timpl R, Jaenisch R. Embryonic lethal mutation in mouse collagen I gene causes rupture of blood vessels and is associated with erythropoietic and mesenchymal cell death. Cell 1984 Sep;38(2):597-607.

37. George EL, Baldwin HS, Hynes RO. Fibronectins are essential for heart and blood vessel morphogenesis but are dispensable for initial specification of precursor cells. Blood 1997 Oct 15;90(8):3073-3081.

38. Hutmacher DW, Cool S. Concepts of scaffold-based tissue engineering--the rationale to use solid free-form fabrication techniques. Journal of cellular and molecular medicine 2007 Jul-Aug;11(4):654-669.

39. Chvapil M, Holusa R. Experimental experiences with the collagen sponge as hemostaticum and tampon. Journal of biomedical materials research 1968 Jun;2(2):245-264.

40. Leighton J, Mark R, Justh G. Patterns of three-dimensional growth in vitro in collagen-coated cellulose sponge: carcinomas and embryonic tissues. Cancer Res 1968 Feb;28(2):286-296.

41. Oluwasanmi J, Chvapil M. A comparative study of four materials in local burn care in rabbit model. J Trauma 1976 May;16(5):348-353.

42. C. Liu, Z. Xia and J. T. Czernuszka. Design and development of three dimensional scaffolds for tissue engineering. Trans IChemE, Part A, Chemical Engineering Research and Design 2007;85(A7):1051-1064.

43. K.F. Leonga CKC, N. Sudarmadjia, W.Y. Yeonga. Engineering functionally graded tissue engineering scaffolds. Journal of the Mechanical Behavior of Biomedical Materials 2008 April 2008;1(2):140-152.

44. Hoi-Yan Cheung K-TL, Tung-Po Lu, David Hui A critical review on polymer-based bio-engineered materials for scaffold development Composites: part B 2007;28:291-300.

45. Causa F, Netti PA, Ambrosio L. A multi-functional scaffold for tissue regeneration: The need to engineer a tissue analogue. Biomaterials 2007 Dec;28(34):5093-5099.

46. Rucker M, Laschke MW, Junker D, Carvalho C, Tavassol F, Mulhaupt R, et al. Vascularization and biocompatibility of scaffolds consisting of different calcium phosphate compounds. J Biomed Mater Res A 2008 Sep 15;86(4):1002-1011.

47. Miyata T, Taira T, Noishiki Y. Collagen engineering for biomaterial use. Clinical materials 1992;9(3-4):139-148.

48. Tabesh H, Amoabediny G, Nik NS, Heydari M, Yosefifard M, Siadat SO, et al. The role of biodegradable engineered scaffolds seeded with Schwann cells for spinal cord regeneration. Neurochemistry international 2009 Feb;54(2):73-83.

49. Hubbell JA. Biomaterials in tissue engineering. Bio/technology (Nature Publishing Company) 1995 Jun;13(6):565-576.

50. Aimes RT, Quigley JP. Matrix metalloproteinase-2 is an interstitial collagenase. Inhibitor-free enzyme catalyzes the cleavage of collagen fibrils and soluble native type I collagen generating the specific 3/4- and 1/4-length fragments. The Journal of biological chemistry 1995 Mar 17;270(11):5872-5876.

51. Gross J, Harper E, Harris ED, McCroskery PA, Highberger JH, Corbett C, et al. Animal collagenases: specificity of action, and structures of the substrate cleavage site. Biochemical and biophysical research communications 1974 Nov 27;61(2):605-612.

52. Abraham LC, Dice JF, Lee K, Kaplan DL. Phagocytosis and remodeling of collagen matrices. Experimental cell research 2007 Mar 10;313(5):1045-1055.

53. Jayakrishnan A, Jameela SR. Glutaraldehyde as a fixative in bioprostheses and drug delivery matrices. Biomaterials 1996 Mar;17(5):471-484.

54. Khor E. Methods for the treatment of collagenous tissues for bioprostheses. Biomaterials 1997 Jan;18(2):95-105.

55. Park SN, Park JC, Kim HO, Song MJ, Suh H. Characterization of porous collagen/hyaluronic acid scaffold modified by 1-ethyl-3-(3-dimethylaminopropyl)carbodiimide cross-linking. Biomaterials 2002 Feb;23(4):1205-1212.

56. Sionkowska A, Wess T. Mechanical properties of UV irradiated rat tail tendon (RTT) collagen. International journal of biological macromolecules 2004 Apr;34(1-2):9-12.

57. Weadock KS, Miller EJ, Bellincampi LD, Zawadsky JP, Dunn MG. Physical crosslinking of collagen fibers: comparison of ultraviolet irradiation and dehydrothermal treatment. Journal of biomedical materials research 1995 Nov;29(11):1373-1379.

58. Zhao W, Chen B, Li X, Lin H, Sun W, Zhao Y, et al. Vascularization and cellularization of collagen scaffolds incorporated with two different collagen-targeting human basic fibroblast growth factors. J Biomed Mater Res A 2007 Sep 1;82(3):630-636.

59. Pang Y, Wang X, Ucuzian AA, Brey EM, Burgess WH, Jones KJ, et al. Local delivery of a collagen-binding FGF-1 chimera to smooth muscle cells in collagen scaffolds for vascular tissue engineering. Biomaterials Feb;31(5):878-885.

60. C. Liu Z. Xia. J. T. Czernuszka. Design and Development of Three-Dimensional Scaffolds for Tissue Engineering. Chemical Engineering Research and Design 2007;85(7):1051-1064.

61. Chvapil M. Collagen sponge: theory and practice of medical applications. Journal of biomedical materials research 1977 Sep;11(5):721-741.

62. Kleinman HK, Klebe RJ, Martin GR. Role of collagenous matrices in the adhesion and growth of cells. The Journal of cell biology 1981 Mar;88(3):473-485.

63. Rosso F, Giordano A, Barbarisi M, Barbarisi A. From cell-ECM interactions to tissue engineering. Journal of cellular physiology 2004 May;199(2):174-180.

64. Gunatillake PA, Adhikari R. Biodegradable synthetic polymers for tissue engineering. European cells & materials 2003 May 20;5:1-16; discussion 16.

65. Lakshmi S. Naira CTL. Biodegradable polymers as biomaterials. Prog Polym Sci 2007;32:762-798.

66. Chen G, Sato T, Ushida T, Ochiai N, Tateishi T. Tissue engineering of cartilage using a hybrid scaffold of synthetic polymer and collagen. Tissue engineering 2004 Mar-Apr;10(3-4):323-330.

67. S. Nehrer PV, R. Dorotka, Austria. Biomaterials in cartilage repair. Osteoarthritis and Cartilage Vol 15, Supplement B, Abstracts of ICRS 2007, Warsaw, Poland 2007.

68. Place ES, George JH, Williams CK, Stevens MM. Synthetic polymer scaffolds for tissue engineering. Chemical Society reviews 2009 Apr;38(4):1139-1151.

69. Duda DG, Fukumura D, Jain RK. Role of eNOS in neovascularization: NO for endothelial progenitor cells. Trends in molecular medicine 2004 Apr;10(4):143-145.

70. Ziche M, Morbidelli L, Choudhuri R, Zhang HT, Donnini S, Granger HJ, et al. Nitric oxide synthase lies downstream from vascular endothelial growth factor-induced but not basic fibroblast growth factor-induced angiogenesis. The Journal of clinical investigation 1997 Jun 1;99(11):2625-2634.

71. Eming SA, Brachvogel B, Odorisio T, Koch M. Regulation of angiogenesis: wound healing as a model. Progress in histochemistry and cytochemistry 2007;42(3):115-170.

72. Carmeliet P. Mechanisms of angiogenesis and arteriogenesis. Nat Med 2000 Apr;6(4):389-395.

73. Mettouchi A, Meneguzzi G. Distinct roles of beta1 integrins during angiogenesis. European journal of cell biology 2006 Apr;85(3-4):243-247.

74. Birkedal-Hansen H, Moore WG, Bodden MK, Windsor LJ, Birkedal-Hansen B, DeCarlo A, et al. Matrix metalloproteinases: a review. Crit Rev Oral Biol Med 1993;4(2):197-250.

75. Auerbach W, Auerbach R. Angiogenesis inhibition: a review. Pharmacol Ther 1994 Sep;63(3):265-311.

76. Benjamin LE, Hemo I, Keshet E. A plasticity window for blood vessel remodelling is defined by pericyte coverage of the preformed endothelial network and is regulated by PDGF-B and VEGF. Development (Cambridge, England) 1998 May;125(9):1591-1598.

77. Beck L, Jr., D'Amore PA. Vascular development: cellular and molecular regulation. Faseb J 1997 Apr;11(5):365-373.

78. Hirschi KK, Rohovsky SA, D'Amore PA. PDGF, TGF-beta, and heterotypic cell-cell interactions mediate endothelial cell-induced recruitment of 10T1/2 cells and their differentiation to a smooth muscle fate. The Journal of cell biology 1998 May 4;141(3):805-814.

79. Cen L, Liu W, Cui L, Zhang W, Cao Y. Collagen tissue engineering: development of novel biomaterials and applications. Pediatric research 2008 May;63(5):492-496.

80. Aszodi A, Legate KR, Nakchbandi I, Fassler R. What mouse mutants teach us about extracellular matrix function. Annual review of cell and developmental biology 2006;22:591-621.

81. Yang J, Richards J, Bowman P, Guzman R, Enami J, McCormick K, et al. Sustained growth and three-dimensional organization of primary mammary tumor epithelial cells embedded in collagen gels. Proceedings of the National Academy of Sciences of the United States of America 1979 Jul;76(7):3401-3405.

82. Montesano R, Mouron P, Amherdt M, Orci L. Collagen matrix promotes reorganization of pancreatic endocrine cell monolayers into islet-like organoids. The Journal of cell biology 1983 Sep;97(3):935-939.

83. S.J. Wilkinson DWLH. Determination of collagen fibril structure and orientation in connective tissues by X-ray diffraction. Radiation Physics and Chemistry 1999;56:197-204

84. Vernon RB, Sage EH. Contraction of fibrillar type I collagen by endothelial cells: a study in vitro. Journal of cellular biochemistry 1996 Feb;60(2):185-197.

85. Patino MG, Neiders ME, Andreana S, Noble B, Cohen RE. Cellular inflammatory response to porcine collagen membranes. Journal of periodontal research 2003 Oct;38(5):458-464.

86. Liu L, Kuffova L, Griffith M, Dang Z, Muckersie E, Liu Y, et al. Immunological responses in mice to full-thickness corneal grafts engineered from porcine collagen. Biomaterials 2007 Sep;28(26):3807-3814.

87. Charriere G, Bejot M, Schnitzler L, Ville G, Hartmann DJ. Reactions to a bovine collagen implant. Clinical and immunologic study in 705 patients. Journal of the American Academy of Dermatology 1989 Dec;21(6):1203-1208.

88. Belbachir K, Noreen R, Gouspillou G, Petibois C. Collagen types analysis and differentiation by FTIR spectroscopy. Analytical and bioanalytical chemistry 2009 Oct;395(3):829-837.

89. Raul Fleischmajer BRO, Klaus Kúhn. Biology, chemistry, and pathology of collagen. Annals of the New York Academy of Sciences, 0077-892 1985;460:537p. : ill. : 523 cm.

90. van der Rest M, Garrone R. Collagen family of proteins. Faseb J 1991 Oct;5(13):2814-2823.

91. Banga I. Structure and function of elastin and collagen. Budapest: Akadémiai Kiadó 1966;xii, 224p.: ill; 25cm.

92. J. Brinckmann HN, P.K.Muller. Collagen: Primer in structure , processing and Assemble. Springer-Verlag Berlin Heidelberg 2005.

93. Nimni ME. Collagen: Its structure and function in normal and pathological connective tissues. Seminars in arthritis and rheumatism 1974 Winter;4(2):95-150.

94. Kleinman HK, Martin GR, Fishman PH. Ganglioside inhibition of fibronectin-mediated cell adhesion to collagen. Proceedings of the National Academy of Sciences of the United States of America 1979 Jul;76(7):3367-3371.

95. Klebe RJ. Isolation of a collagen-dependent cell attachment factor. Nature 1974 Jul 19;250(463):248-251.

96. Klebe RJ. Cell attachment to collagen: the requirement for energy. Journal of cellular physiology 1975 Oct;86(2 Pt 1):231-236.

97. Messent AJ, Tuckwell DS, Knauper V, Humphries MJ, Murphy G, Gavrilovic J. Effects of collagenase-cleavage of type I collagen on alpha2beta1 integrin-mediated cell adhesion. Journal of cell science 1998 Apr;111 ( Pt 8):1127-1135.

98. Leitinger B, Hohenester E. Mammalian collagen receptors. Matrix Biol 2007 Apr;26(3):146-155.

99. Balian G, Click EM, Crouch E, Davidson JM, Bornstein P. Isolation of a collagen-binding fragment from fibronectin and cold-insoluble globulin. J Biol Chem 1979 Mar 10;254(5):1429-1432.

100. Senger DR, Perruzzi CA, Streit M, Koteliansky VE, de Fougerolles AR, Detmar M. The alpha(1)beta(1) and alpha(2)beta(1) integrins provide critical support for vascular endothelial growth factor signaling, endothelial cell migration, and tumor angiogenesis. Am J Pathol 2002 Jan;160(1):195-204.

101. Dejana E, Languino LR, Polentarutti N, Balconi G, Ryckewaert JJ, Larrieu MJ, et al. Interaction between fibrinogen and cultured endothelial cells. Induction of migration and specific binding. The Journal of clinical investigation 1985 Jan;75(1):11-18.

102. Francis ME, Uriel S, Brey EM. Endothelial Cell-Matrix Interactions in Neovascularization. Tissue engineering 2008 Jan 21.

103. Zhang X, Groopman JE, Wang JF. Extracellular matrix regulates endothelial functions through interaction of VEGFR-3 and integrin alpha5beta1. Journal of cellular physiology 2005 Jan;202(1):205-214.

104. Mallery SR, Lantry LE, Toms MC, Titterington LC, Hout BL, Brierley GP, et al. Human microvascular endothelial cell-extracellular matrix interaction in cellular growth state determination. Cell Tissue Res 1995 Jan;279(1):37-45.

105. Short SM, Talbott GA, Juliano RL. Integrin-mediated signaling events in human endothelial cells. Molecular biology of the cell 1998 Aug;9(8):1969-1980.

106. Delvos U, Gajdusek C, Sage H, Harker LA, Schwartz SM. Interactions of vascular wall cells with collagen gels. Laboratory investigation; a journal of technical methods and pathology 1982 Jan;46(1):61-72.

107. Feder J, Marasa JC, Olander JV. The formation of capillary-like tubes by calf aortic endothelial cells grown in vitro. Journal of cellular physiology 1983 Jul;116(1):1-6.

108. Schor AM, Schor SL, Allen TD. Effects of culture conditions on the proliferation, morphology and migration of bovine aortic endothelial cells. Journal of cell science 1983 Jul;62:267-285.

109. Madri JA, Williams SK. Capillary endothelial cell cultures: phenotypic modulation by matrix components. The Journal of cell biology 1983 Jul;97(1):153-165.

110. Jackson CJ, Jenkins KL. Type I collagen fibrils promote rapid vascular tube formation upon contact with the apical side of cultured endothelium. Experimental cell research 1991 Jan;192(1):319-323.

111. Powell RJ, Hydowski J, Frank O, Bhargava J, Sumpio BE. Endothelial cell effect on smooth muscle cell collagen synthesis. The Journal of surgical research 1997 Apr;69(1):113-118.

112. K. Habursky KTa, M. Burrows, R.V. Iozzo, S. Choi, W.F. DeGrado, J.D. San Antonio Endothelial cell-collagen interactions in angiogenesis. Matrix Biology 2006;25:S58.

113. Carey DJ. Control of growth and differentiation of vascular cells by extracellular matrix proteins. Annual review of physiology 1991;53:161-177.

114. Pickering JG. Regulation of vascular cell behavior by collagen : form is function. Circulation research 2001 Mar 16;88(5):458-459.

115. Wu L, Ding J. In vitro degradation of three-dimensional porous poly(D,L-lactide-co-glycolide) scaffolds for tissue engineering. Biomaterials 2004 Dec;25(27):5821-5830.

116. Xia Z, Huang Y, Adamopoulos IE, Walpole A, Triffitt JT, Cui Z. Macrophage-mediated biodegradation of poly(DL-lactide-co-glycolide) in vitro. Journal of biomedical materials research 2006 Dec 1;79(3):582-590.

117. Valentin JE, Stewart-Akers AM, Gilbert TW, Badylak SF. Macrophage participation in the degradation and remodeling of extracellular matrix scaffolds. Tissue Eng Part A 2009 Jul;15(7):1687-1694.

118. Gorham SD, Light ND, Diamond AM, Willins MJ, Bailey AJ, Wess TJ, et al. Effect of chemical modifications on the susceptibility of collagen to proteolysis. II. Dehydrothermal crosslinking. International journal of biological macromolecules 1992 Jun;14(3):129-138.

119. Ottl J, Gabriel D, Murphy G, Knauper V, Tominaga Y, Nagase H, et al. Recognition and catabolism of synthetic heterotrimeric collagen peptides by matrix metalloproteinases. Chemistry & biology 2000 Feb;7(2):119-132.

120. Verma RP, Hansch C. Matrix metalloproteinases (MMPs): chemical-biological functions and (Q)SARs. Bioorganic & medicinal chemistry 2007 Mar 15;15(6):2223-2268.

121. Ala-aho R, Kahari VM. Collagenases in cancer. Biochimie 2005 Mar-Apr;87(3-4):273-286.

122. Riley KN, Herman IM. Collagenase promotes the cellular responses to injury and wound healing in vivo. Journal of burns and wounds 2005;4:e8.

123. Harrington DJ. Bacterial collagenases and collagen-degrading enzymes and their potential role in human disease. Infection and immunity 1996 Jun;64(6):1885-1891.

124. Weiss JB. Enzymic degradation of collagen. International review of connective tissue research 1976;7:101-157.

125. Welgus HG, Kobayashi DK, Jeffrey JJ. The collagen substrate specificity of rat uterus collagenase. The Journal of biological chemistry 1983 Dec 10;258(23):14162-14165.

126. Mookhtiar KA, Van Wart HE. Clostridium histolyticum collagenases: a new look at some old enzymes. Matrix (Stuttgart, Germany) 1992;1:116-126.

127. Fujimoto D. Action of bacterial collagenase on Ascaris cuticle collagen. Journal of biochemistry 1975 Nov;78(5):905-909.

128. Nagai Y, Sakakibara S, Noda H, Akabori S. Hydrolysis of synthetic peptides by collagenase. Biochimica et biophysica acta 1960 Jan 29;37:567-569.

129. Steven FS. Polymeric collagen fibrils. An example of substrate-mediated steric obstruction of enzymic digestion. Biochimica et biophysica acta 1976 Nov 8;452(1):151-160.

130. Duan X, Sheardown H. Dendrimer crosslinked collagen as a corneal tissue engineering scaffold: mechanical properties and corneal epithelial cell interactions. Biomaterials 2006 Sep;27(26):4608-4617.

131. Angele P, Abke J, Kujat R, Faltermeier H, Schumann D, Nerlich M, et al. Influence of different collagen species on physico-chemical properties of crosslinked collagen matrices. Biomaterials 2004 Jun;25(14):2831-2841.

132. Koide T, Daito M. Effects of various collagen crosslinking techniques on mechanical properties of collagen film. Dental materials journal 1997 Jun;16(1):1-9.

133. Charulatha V, Rajaram A. Influence of different crosslinking treatments on the physical properties of collagen membranes. Biomaterials 2003 Feb;24(5):759-767.

134. Weadock KS, Miller EJ, Keuffel EL, Dunn MG. Effect of physical crosslinking methods on collagen-fiber durability in proteolytic solutions. Journal of biomedical materials research 1996 Oct;32(2):221-226.

135. Madhavan K, Belchenko D, Motta A, Tan W. Evaluation of composition and crosslinking effects on collagen-based composite constructs. Acta biomaterialia Apr;6(4):1413-1422.

136. Heath Y and Da RJ. Collagen stabilization and modification using a polyepoxide, triglycidyl isocyanurate Polymer Degradation and Stability October 2009;94(10):1684-1692.

137. Petite H, Rault I, Huc A, Menasche P, Herbage D. Use of the acyl azide method for cross-linking collagen-rich tissues such as pericardium. Journal of biomedical materials research 1990 Feb;24(2):179-187.

138. Wissink MJ, van Luyn MJ, Beernink R, Dijk F, Poot AA, Engbers GH, et al. Endothelial cell seeding on crosslinked collagen: effects of crosslinking on endothelial cell proliferation and functional parameters. Thromb Haemost 2000 Aug;84(2):325-331.

139. Jarman-Smith ML, Bodamyali T, Stevens C, Howell JA, Horrocks M, Chaudhuri JB. Porcine collagen crosslinking, degradation and its capability for fibroblast adhesion and proliferation. Journal of materials science 2004 Aug;15(8):925-932.

140. Chan BP, So KF. Photochemical crosslinking improves the physicochemical properties of collagen scaffolds. J Biomed Mater Res A 2005 Dec 1;75(3):689-701.

141. Billiar K, Murray J, Laude D, Abraham G, Bachrach N. Effects of carbodiimide crosslinking conditions on the physical properties of laminated intestinal submucosa. Journal of biomedical materials research 2001 Jul;56(1):101-108.

142. Yunoki S, Suzuki T, Takai M. Stabilization of low denaturation temperature collagen from fish by physical cross-linking methods. Journal of bioscience and bioengineering 2003;96(6):575-577.

143. Sionkowska A. Thermal denaturation of UV-irradiated wet rat tail tendon collagen. International journal of biological macromolecules 2005 Apr;35(3-4):145-149.

144. Sachlos E, Wahl DA, Triffitt JT, Czernuszka JT. The impact of critical point drying with liquid carbon dioxide on collagen-hydroxyapatite composite scaffolds. Acta biomaterialia 2008 Sep;4(5):1322-1331.

145. Sachlos E, Czernuszka JT. Making tissue engineering scaffolds work. Review: the application of solid freeform fabrication technology to the production of tissue engineering scaffolds. European cells & materials 2003 Jun 30;5:29-39; discussion 39-40.

146. Park A, Wu B, Griffith LG. Integration of surface modification and 3D fabrication techniques to prepare patterned poly(L-lactide) substrates allowing regionally selective cell adhesion. Journal of biomaterials science 1998;9(2):89-110.

147. Giordano RA, Wu BM, Borland SW, Cima LG, Sachs EM, Cima MJ. Mechanical properties of dense polylactic acid structures fabricated by three dimensional printing. Journal of biomaterials science 1996;8(1):63-75.

148. Griffith LG, Wu B, Cima MJ, Powers MJ, Chaignaud B, Vacanti JP. In vitro organogenesis of liver tissue. Annals of the New York Academy of Sciences 1997 Dec 31;831:382-397.

149. Michelle L. Griffith JWH. Freeform Fabrication of Ceramics via Stereolithography. Journal of the American Ceramic Society 1996;79(10):2601-2608.

150. Wahl DA, Sachlos E, Liu C, Czernuszka JT. Controlling the processing of collagen-hydroxyapatite scaffolds for bone tissue engineering. Journal of materials science 2007 Feb;18(2):201-209.

151. Peters MC, Polverini PJ, Mooney DJ. Engineering vascular networks in porous polymer matrices. Journal of biomedical materials research 2002 Jun 15;60(4):668-678.

152. Lee H, Cusick RA, Browne F, Ho Kim T, Ma PX, Utsunomiya H, et al. Local delivery of basic fibroblast growth factor increases both angiogenesis and engraftment of hepatocytes in tissue-engineered polymer devices. Transplantation 2002 May 27;73(10):1589-1593.

153. Novosel EC, Kleinhans C, Kluger PJ. Vascularization is the key challenge in tissue engineering. Advanced drug delivery reviews 2011 Apr 30;63(4-5):300-311.

154. Chen X, Aledia AS, Ghajar CM, Griffith CK, Putnam AJ, Hughes CC, et al. Prevascularization of a fibrin-based tissue construct accelerates the formation of functional anastomosis with host vasculature. Tissue engineering 2009 Jun;15(6):1363-1371.

155. Gibot L, Galbraith T, Huot J, Auger FA. A pre existing microvascular network benefits in vivo revascularization of a microvascularized tissue-engineered skin substitute. Tissue Eng Part A 2010 Oct;16(10):3199-3206.

156. Tremblay PL, Hudon V, Berthod F, Germain L, Auger FA. Inosculation of tissue-engineered capillaries with the host's vasculature in a reconstructed skin transplanted on mice. Am J Transplant 2005 May;5(5):1002-1010.

157. Jansen RG, Kuijpers-Jagtman AM, van Kuppevelt TH, Von den Hoff JW. Collagen scaffolds implanted in the palatal mucosa. The Journal of craniofacial surgery 2008 May;19(3):599-608.

158. Callegari A, Bollini S, Iop L, Chiavegato A, Torregrossa G, Pozzobon M, et al. Neovascularization induced by porous collagen scaffold implanted on intact and cryoinjured rat hearts. Biomaterials 2007 Dec;28(36):5449-5461.

159. Wu X, Rabkin-Aikawa E, Guleserian KJ, Perry TE, Masuda Y, Sutherland FW, et al. Tissue-engineered microvessels on three-dimensional biodegradable scaffolds using human endothelial progenitor cells. American journal of physiology 2004 Aug; 287(2):H480-487.

160. Melero-Martin JM, Khan ZA, Picard A, Wu X, Paruchuri S, Bischoff J. In vivo vasculogenic potential of human blood-derived endothelial progenitor cells. Blood 2007 Jun 1; 109(11):4761-4768.

161. Borselli C, Ungaro F, Oliviero O, d'Angelo I, Quaglia F, La Rotonda MI, et al. Bioactivation of collagen matrices through sustained VEGF release from PLGA microspheres. J Biomed Mater Res A 2010 Jan; 92(1):94-102.

162. Shen YH, Shoichet MS, Radisic M. Vascular endothelial growth factor immobilized in collagen scaffold promotes penetration and proliferation of endothelial cells. Acta biomaterialia 2008 May;4(3):477-489.

163. Steffens GC, Yao C, Prevel P, Markowicz M, Schenck P, Noah EM, et al. Modulation of angiogenic potential of collagen matrices by covalent incorporation

of heparin and loading with vascular endothelial growth factor. Tissue engineering 2004 Sep-Oct; 10(9-10):1502-1509.

164. Yao C, Markowicz M, Pallua N, Noah EM, Steffens G. The effect of cross-linking of collagen matrices on their angiogenic capability. Biomaterials 2008 Jan;29(1):66-74.

165. Nakatsu MN, Sainson RC, Aoto JN, Taylor KL, Aitkenhead M, Perez-del-Pulgar S, et al. Angiogenic sprouting and capillary lumen formation modeled by human umbilical vein endothelial cells (HUVEC) in fibrin gels: the role of fibroblasts and Angiopoietin-1. Microvascular research 2003 Sep; 66(2):102-112.

166. Chiu LL, Radisic M. Scaffolds with covalently immobilized VEGF and Angiopoietin-1 for vascularization of engineered tissues. Biomaterials 2010 Jan; 31(2):226-241.

167. Hosper NA, Eggink AJ, Roelofs LA, Wijnen RM, van Luyn MJ, Bank RA, et al. Intra-uterine tissue engineering of full-thickness skin defects in a fetal sheep model. Biomaterials 2010 May; 31(14):3910-3919.

168. Somasundaram R, Schuppan D. Type I, II, III, IV, V, and VI collagens serve as extracellular ligands for the isoforms of platelet-derived growth factor (AA, BB, and AB). The Journal of biological chemistry 1996 Oct 25; 271(43):26884-26891.

169. Paralkar VM, Vukicevic S, Reddi AH. Transforming growth factor beta type 1 binds to collagen IV of basement membrane matrix: implications for development. Developmental biology 1991 Feb; 143(2):303-308.

170. Yang Y, Zhao Y, Chen B, Han Q, Sun W, Xiao Z, et al. Collagen-binding human epidermal growth factor promotes cellularization of collagen scaffolds. Tissue Eng Part A 2009 Nov; 15(11):3589-3596.

171. Linke K, Schanz J, Hansmann J, Walles T, Brunner H, Mertsching H. Engineered liver-like tissue on a capillarized matrix for applied research. Tissue Eng 2007 Nov; 13(11):2699-2707.

172. Brown DL, Meagher PJ, Knight KR, Keramidaris E, Romeo-Meeuw R, Penington AJ, et al. Survival and function of transplanted islet cells on an in vivo, vascularized tissue engineering platform in the rat: A pilot study. Cell transplantation 2006; 15(4):319-324.

173. Weinberg CB, Bell E. A blood vessel model constructed from collagen and cultured vascular cells. Science (New York, NY 1986 Jan 24; 231(4736):397-400.

174. L'Heureux N, Paquet S, Labbe R, Germain L, Auger FA. A completely biological tissue-engineered human blood vessel. Faseb J 1998 Jan;12(1):47-56.

175. Dagalakis N, Flink J, Stasikelis P, Burke JF, Yannas IV. Design of an artificial skin. Part III. Control of pore structure. Journal of biomedical materials research 1980 Jul; 14(4):511-528.

176. Schoeters G, Leppens H, Van Gorp U, Van Den Heuvel R. Haemopoietic long-term bone marrow cultures from adult mice show osteogenic capacity in vitro on 3-dimensional collagen sponges. Cell proliferation 1992 Nov; 25(6):587-603.

177. Yannas IV, editor. Tissue and organ regeneration in adults. New York: Springer, 2001.

178. Yannas IV, Tzeranis DS, Harley BA, So PT. Biologically active collagen-based scaffolds: advances in processing and characterization. Philosophical transactions 2010 Apr 28; 368(1917):2123-2139.

179. Yahyouche A, Zhidao X, Czernuszka JT, Clover AJ. Macrophage-mediated degradation of crosslinked collagen scaffolds. Acta biomaterialia 2011 Jan;7(1):278-286.

180. Kanematsu A, Yamamoto S, Ozeki M, Noguchi T, Kanatani I, Ogawa O, et al. Collagenous matrices as release carriers of exogenous growth factors. Biomaterials 2004 Aug; 25(18):4513-4520.

181. Danielsson C, Ruault S, Basset-Dardare A, Frey P. Modified collagen fleece, a scaffold for transplantation of human bladder smooth muscle cells. Biomaterials 2006 Mar; 27(7):1054-1060.

182. Schoof H, Apel J, Heschel I, Rau G. Control of pore structure and size in freeze-dried collagen sponges. Journal of biomedical materials research 2001; 58(4):352-357.

183. O'Brien FJ, Harley BA, Yannas IV, Gibson L. Influence of freezing rate on pore structure in freeze-dried collagen-GAG scaffolds. Biomaterials 2004 Mar; 25(6):1077-1086.

184. Doillon CJ, Whyne CF, Brandwein S, Silver FH. Collagen-based wound dressings: control of the pore structure and morphology. Journal of biomedical materials research 1986 Oct; 20(8):1219-1228.

185. Jun Ping Zheng CZW, Xiu Xing Wanga, Hong Yan Wanga, Hong Zhuanga and Kang De Yao. Preparation of biomimetic three-dimensional gelatin/montmorillonite–chitosan scaffold for tissue engineering Reactive and Functional Polymers 2007;67(9):780-788.

186. Haugh MG, Jaasma MJ, O'Brien FJ. The effect of dehydrothermal treatment on the mechanical and structural properties of collagen-GAG scaffolds. J Biomed Mater Res A 2009 May; 89(2):363-369.

187. Thompson JI, Czernuszka JT. The effect of two types of cross-linking on some mechanical properties of collagen. Bio-medical materials and engineering 1995; 5(1):37-48.

188. Yannas IV, Tobolsky AV. Cross-linking of gelatine by dehydration. Nature 1967 Jul 29; 215(5100):509-510.

189. Buttafoco L, Engbers-Buijtenhuijs P, Poot AA, Dijkstra PJ, Daamen WF, van Kuppevelt TH, et al. First steps towards tissue engineering of small-diameter blood vessels: preparation of flat scaffolds of collagen and elastin by means of freeze drying. J Biomed Mater Res B Appl Biomater 2006 May; 77(2):357-368.

190. Flandin F, Buffevant C, Herbage D. A differential scanning calorimetry analysis of the age-related changes in the thermal stability of rat skin collagen. Biochim Biophys Acta 1984 Dec 7; 791(2):205-211.

191. Weadock K, Olson RM, Silver FH. Evaluation of collagen crosslinking techniques. Biomater Med Devices Artif Organs 1983;11(4):293-318.

192. Jackson M, Choo LP, Watson PH, Halliday WC, Mantsch HH. Beware of connective tissue proteins: assignment and implications of collagen absorptions in infrared spectra of human tissues. Biochim Biophys Acta 1995 Jan 25; 1270(1):1-6.

193. Karageorgiou V, Kaplan D. Porosity of 3D biomaterial scaffolds and osteogenesis. Biomaterials 2005 Sep; 26(27):5474-5491.

194. Ma L, Gao C, Mao Z, Zhou J, Shen J, Hu X, et al. Collagen/chitosan porous scaffolds with improved biostability for skin tissue engineering. Biomaterials 2003 Nov; 24(26):4833-4841.

195. Pietrucha K. Changes in denaturation and rheological properties of collagen-hyaluronic acid scaffolds as a result of temperature dependencies. International journal of biological macromolecules 2005 Sep 28; 36(5):299-304.

196. Koide M, Osaki K, Konishi J, Oyamada K, Katakura T, Takahashi A, et al. A new type of biomaterial for artificial skin: dehydrothermally cross-linked

composites of fibrillar and denatured collagens. Journal of biomedical materials research 1993 Jan; 27(1):79-87.

197. Gotora D. DPhil Thesis. Oxford University 2005;Chapter 4:77.

198. J.H Muyonga CGBC, K.G. Duodu. Fourier transform infrared (FTIR) spectroscopic study of acid soluble collagen and gelatin from skins and bones of young and adult Nile perch (LAtes niloticus). Food Chemistry 2004; 86:325-332.

199. Friess W, Lee G. Basic thermoanalytical studies of insoluble collagen matrices. Biomaterials 1996 Dec; 17(23):2289-2294.

200. Wang XH, Li DP, Wang WJ, Feng QL, Cui FZ, Xu YX, et al. Crosslinked collagen/chitosan matrix for artificial livers. Biomaterials 2003 Aug; 24(19):3213-3220.

201. Katsunori Tsunoda MS, Masashi Sonoyama, Hirofumi Yajima, Tadahiro Ishii, Jiro Tniyama, Hiroshi Itoh Characterization of water contribution to excimer laser ablation of collagen. Journal of Photochemistry and Photobiology A: Chemistry 2001; 145:195-200.

202. WAHL D. Collagen-hydroxyapatite scaffolds for tissue engineering. PhD, Department of Materials, University of Oxford 2004.

203. Holder WDGHE, Roland, W.D., Moore, A.L., Culberson, C.R.. Loebsack. A.B., Burg, K.J.L. and Mooney, D.J. Increased vascularization and heterogeneity of vascular structures occurring in polyglycolide matrices containing aortic endothelial cells implanted in the rat. Tissue Engineering 1997; 3:194-160.

204. Perng CK, Wang YJ, Tsi CH, Ma H. In Vivo Angiogenesis Effect of Porous Collagen Scaffold with Hyaluronic Acid Oligosaccharides. The Journal of surgical research 2009 Oct 23.

205. Druecke D, Langer S, Lamme E, Pieper J, Ugarkovic M, Steinau HU, et al. Neovascularization of poly(ether ester) block-copolymer scaffolds in vivo: long-term investigations using intravital fluorescent microscopy. J Biomed Mater Res A 2004 Jan 1; 68(1):10-18.

206. Song YS, Lin RL, Montesano G, Durmus NG, Lee G, Yoo SS, et al. Engineered 3D tissue models for cell-laden microfluidic channels. Analytical and bioanalytical chemistry 2009 Sep; 395(1):185-193.

207. Nazhat SN, Neel EA, Kidane A, Ahmed I, Hope C, Kershaw M, et al. Controlled microchannelling in dense collagen scaffolds by soluble phosphate glass fibers. Biomacromolecules 2007 Feb;8(2):543-551.

208. He Jiankang LD, Liu Yaxiong, Yao Bo, Lu Bingheng and Lian Qin. Fabrication and characterization of chitosan/gelatin porous scaffolds with predefined internal microstructures. Polymer 2007; 48(15):4578-4588.

209. Lazarous DF, Shou M, Scheinowitz M, Hodge E, Thirumurti V, Kitsiou AN, et al. Comparative effects of basic fibroblast growth factor and vascular endothelial growth factor on coronary collateral development and the arterial response to injury. Circulation 1996 Sep 1; 94(5):1074-1082.

210. Thirumurti. V. Shou M, Hodge, E., Goncalves, L., Epstein, S.E., Lazarous, D.F. and Unger, E.F. Lack of efficacy of intravenous basic fibroblast growth factor in promoting myocardial angiogenesis. J Am Coll Cardiol 1998;31(54A).

211. Kristina A. Szabo RJA, Gurmit Singha. Matrix metalloproteinases and the immune response. Clinical and Applied Immunology Reviews 2004; 4:295-319.

212. Williams DF. On the mechanisms of biocompatibility. Biomaterials 2008 Jul; 29(20):2941-2953.

213. Xia Z, Triffitt JT. A review on macrophage responses to biomaterials. Biomedical materials (Bristol, England) 2006 Mar; 1(1):R1-9.

214. Xia Z, Ye H, Choong C, Ferguson DJ, Platt N, Cui Z, et al. Macrophagic response to human mesenchymal stem cell and poly(epsilon-caprolactone) implantation in nonobese diabetic/severe combined immunodeficient mice. Journal of biomedical materials research 2004 Dec 1; 71(3):538-548.

215. Phillips JM, Kao WJ. Macrophage adhesion on gelatin-based interpenetrating networks grafted with PEGylated RGD. Tissue engineering 2005 May-Jun; 11(5-6):964-973.

216. Berton G, Lowell CA. Integrin signalling in neutrophils and macrophages. Cellular signalling 1999 Sep; 11(9):621-635.

217. Martin P. Wound healing--aiming for perfect skin regeneration. Science (New York, NY 1997 Apr 4; 276(5309):75-81.

218. Xia Z, Grover LM, Huang Y, Adamopoulos IE, Gbureck U, Triffitt JT, et al. In vitro biodegradation of three brushite calcium phosphate cements by a macrophage cell-line. Biomaterials 2006 Sep; 27(26):4557-4565.

219. French MF, Bhown A, Van Wart HE. Identification of Clostridium histolyticum collagenase hyperreactive sites in type I, II, and III collagens: lack of correlation with local triple helical stability. Journal of protein chemistry 1992 Feb; 11(1):83-97.

220. van Wachem PB, van Luyn MJ, Olde Damink LH, Dijkstra PJ, Feijen J, Nieuwenhuis P. Biocompatibility and tissue regenerating capacity of crosslinked dermal sheep collagen. J Biomed Mater Res 1994 Mar; 28(3):353-363.

221. Walton RS, Brand DD, Czernuszka JT. Influence of telopeptides, fibrils and crosslinking on physicochemical properties of Type I collagen films. Journal of materials science 2009 Oct 23.

222. Yannas IV, Burke JF, Huang C, Gordon PL. Correlation of in vivo collagen degradation rate with in vitro measurements. J Biomed Mater Res 1975 Nov; 9(6):623-628.

223. Petite H, Frei V, Huc A, Herbage D. Use of diphenylphosphorylazide for cross-linking collagen-based biomaterials. J Biomed Mater Res 1994 Feb; 28(2):159-165.

224. Chevallay B, Abdul-Malak N, Herbage D. Mouse fibroblasts in long-term culture within collagen three-dimensional scaffolds: influence of crosslinking with diphenylphosphorylazide on matrix reorganization, growth, and biosynthetic and proteolytic activities. J Biomed Mater Res 2000 Mar 15; 49(4):448-459.

225. Pek YS, Spector M, Yannas IV, Gibson LJ. Degradation of a collagen-chondroitin-6-sulfate matrix by collagenase and by chondroitinase. Biomaterials 2004 Feb; 25(3):473-482.

226. Anderson JM, Rodriguez A, Chang DT. Foreign body reaction to biomaterials. Seminars in immunology 2008 Apr; 20(2):86-100.

227. Nahrendorf M, Swirski FK, Aikawa E, Stangenberg L, Wurdinger T, Figueiredo JL, et al. The healing myocardium sequentially mobilizes two monocyte subsets with divergent and complementary functions. The Journal of experimental medicine 2007 Nov 26; 204(12):3037-3047.

228. McKegney M, Taggart I, Grant MH. The influence of crosslinking agents and diamines on the pore size, morphology and the biological stability of collagen

sponges and their effect on cell penetration through the sponge matrix. Journal of materials science 2001 Sep; 12(9):833-844.

229. J. Skopinska-Wisniewska AS, A. Kaminska, A. Kaznica, R. Jachimiak and T. Drewa. Surface characterization of collagen/elastin based biomaterials for tissue regeneration. Applied Surface Science 2009; 255(19):8286-8292.

230. Krombach F, Munzing S, Allmeling AM, Gerlach JT, Behr J, Dorger M. Cell size of alveolar macrophages: an interspecies comparison. Environmental health perspectives 1997 Sep; 105 Suppl 5:1261-1263.

231. Webster NL, Crowe SM. Matrix metalloproteinases, their production by monocytes and macrophages and their potential role in HIV-related diseases. Journal of leukocyte biology 2006 Nov; 80(5):1052-1066.

232. Goetzl EJ, Banda MJ, Leppert D. Matrix metalloproteinases in immunity. J Immunol 1996 Jan 1; 156(1):1-4.

233. Shapiro SD, Kobayashi DK, Ley TJ. Cloning and characterization of a unique elastolytic metalloproteinase produced by human alveolar macrophages. J Biol Chem 1993 Nov 15; 268(32):23824-23829.

234. Wesley RB, 2nd, Meng X, Godin D, Galis ZS. Extracellular matrix modulates macrophage functions characteristic to atheroma: collagen type I enhances acquisition of resident macrophage traits by human peripheral blood monocytes in vitro. Arteriosclerosis, thrombosis, and vascular biology 1998 Mar; 18(3):432-440.

235. Rouwkema J, Rivron NC, van Blitterswijk CA. Vascularization in tissue engineering. Trends in biotechnology 2008 Aug; 26(8):434-441.

236. Moldovan NI. Role of monocytes and macrophages in adult angiogenesis: a light at the tunnel's end. Journal of hematotherapy & stem cell research 2002 Apr; 11(2):179-194.

237. Gerhardt LC, Widdows KL, Erol MM, Burch CW, Sanz-Herrera JA, Ochoa I, et al. The pro-angiogenic properties of multi-functional bioactive glass composite scaffolds. Biomaterials 2011 Jun; 32(17):4096-4108.

238. Berse B, Brown LF, Van de Water L, Dvorak HF, Senger DR. Vascular permeability factor (vascular endothelial growth factor) gene is expressed differentially in normal tissues, macrophages, and tumors. Molecular biology of the cell 1992 Feb; 3(2):211-220.

239. Pugh-Humphreys RG. Macrophage-neoplastic cell interactions: implications for neoplastic cell growth. FEMS microbiology immunology 1992 Dec; 5(5-6):289-308.

240. Sunderkotter C, Steinbrink K, Goebeler M, Bhardwaj R, Sorg C. Macrophages and angiogenesis. Journal of leukocyte biology 1994 Mar; 55(3):410-422.

241. Koch AE, Polverini PJ, Kunkel SL, Harlow LA, DiPietro LA, Elner VM, et al. Interleukin-8 as a macrophage-derived mediator of angiogenesis. Science (New York, NY 1992 Dec 11; 258(5089):1798-1801.

242. Fromer CH, Klintworth GK. An evaluation of the role of leukocytes in the pathogenesis of experimentally induced corneal vascularization. II. Studies on the effect of leukocytic elimination on corneal vascularization. The American journal of pathology 1975 Dec; 81(3):531-544.

243. Moldovan NI, Goldschmidt-Clermont PJ, Parker-Thornburg J, Shapiro SD, Kolattukudy PE. Contribution of monocytes/macrophages to compensatory

neovascularization: the drilling of metalloelastase-positive tunnels in ischemic myocardium. Circulation research 2000 Sep 1; 87(5):378-384.

244. Klimetzek V, Sorg C. Lymphokine-induced secretion of plasminogen activator by murine macrophages. European journal of immunology 1977 Mar; 7(3):185-187.

245. Falcone DJ, McCaffrey TA, Haimovitz-Friedman A, Garcia M. Transforming growth factor-beta 1 stimulates macrophage urokinase expression and release of matrix-bound basic fibroblast growth factor. Journal of cellular physiology 1993 Jun; 155(3):595-605.

246. Falcone DJ, McCaffrey TA, Haimovitz-Friedman A, Vergilio JA, Nicholson AC. Macrophage and foam cell release of matrix-bound growth factors. Role of plasminogen activation. The Journal of biological chemistry 1993 Jun 5; 268(16):11951-11958.

247. Dennis JE, Charbord P. Origin and differentiation of human and murine stroma. Stem cells (Dayton, Ohio) 2002; 20(3):205-214.

248. Minguell JJ, Erices A, Conget P. Mesenchymal stem cells. Experimental biology and medicine (Maywood, NJ 2001 Jun; 226(6):507-520.

249. Schumann P, Tavassol F, Lindhorst D, Stuehmer C, Bormann KH, Kampmann A, et al. Consequences of seeded cell type on vascularization of tissue engineering constructs in vivo. Microvascular research 2009 Sep; 78(2):180-190.

250. Unger RE, Ghanaati S, Orth C, Sartoris A, Barbeck M, Halstenberg S, et al. The rapid anastomosis between prevascularized networks on silk fibroin scaffolds generated in vitro with cocultures of human microvascular endothelial and osteoblast cells and the host vasculature. Biomaterials 2010 Sep;31(27):6959-6967.

251. Sahota PS, Burn JL, Heaton M, Freedlander E, Suvarna SK, Brown NJ, et al. Development of a reconstructed human skin model for angiogenesis. Wound Repair Regen 2003 Jul-Aug; 11(4):275-284.